A STUDY OF SYSTEM-INDUCED INSTABILITIES IN FORCED-CONVECTION FLOWS WITH SUBCOOLED BOILING

JOHN S. MAULBETSCH

PETER GRIFFITH

April 15, 1965

Contract AF 49(638)-1468
Report No. 5382-35
Department of Mechanical Engineering
Massachusetts Institute of Technology

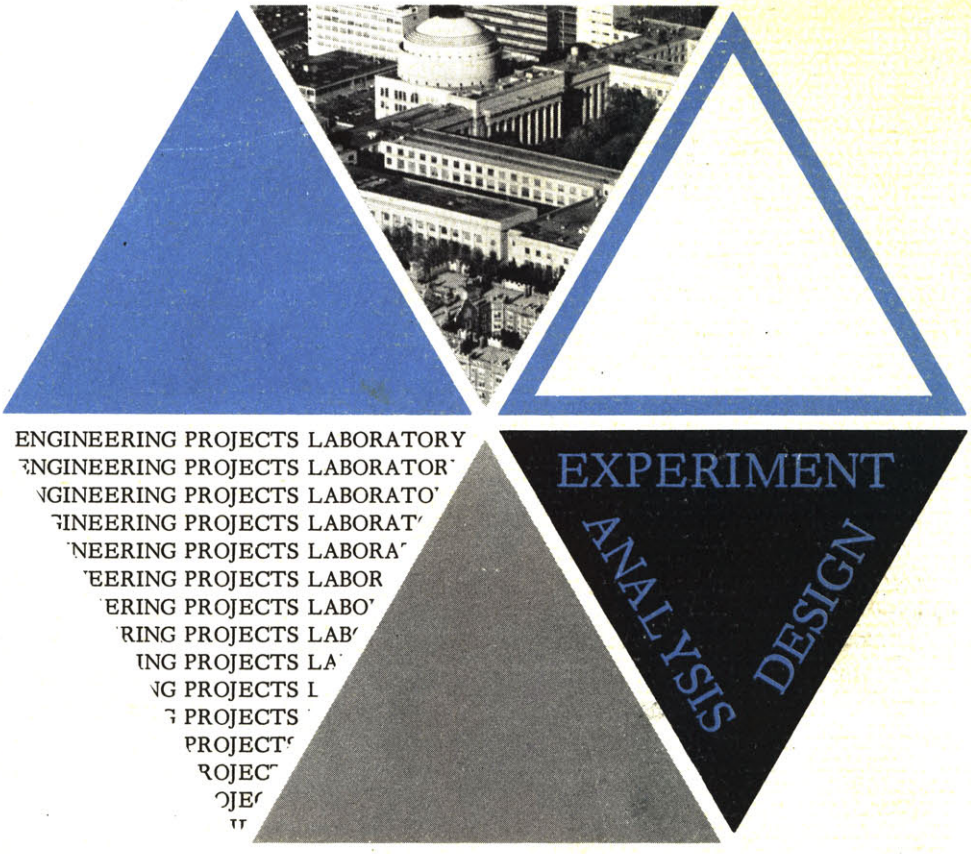

TECHNICAL REPORT No. 5382-35

A STUDY OF SYSTEM-INDUCED INSTABILITIES IN FORCED-CONVECTION FLOWS WITH SUBCOOLED BOILING

by

John S. Maulbetsch
Peter Griffith

for

Massachusetts Institute of Technology
National Magnet Laboratory

Sponsored by the Solid State Sciences Division
Air Force Office of Scientific Research (OAR)
Air Force Contract AF 49(638)-1468
DSR Project No. 5382

April 15, 1965

Department of Mechanical Engineering
Massachusetts Institute of Technology
Cambridge 39, Massachusetts

ABSTRACT

A combined analytical and experimental program was carried out to investigate the problem of hydrodynamic stability of forced-convection flows with boiling. The study was restricted to the flow of water in small channels (<".250 I.D.), high length-to-diameter ratios (25-200), moderate temperature and pressure ($T_i \approx 70^{o}F$; $p_{ex} < 60$ psia), and primarily directed toward subcooled, local boiling ($h_{ex} < h_{sat.liq.}$).

Two types of instability were recognized: The first, a non-recurring excursive instability, and the second, an oscillatory instability in which the operating point varies in a sustained, repetitive way around the original condition.

The excursive behavior was predicted on the basis of a comparison of the slopes of the pressure drop vs. flow rate curve of the heated section and the external system. The criterion for stability was simply that the slope of the external system characteristic be more strongly negative than that of the heated section. This was verified experimentally. This excursion was found to be the limiting condition on the heat flux in a parallel channel system.

The oscillatory instability was investigated analytically through the use of a linearized, lumped parameter model in which steady-state measurements of the pressure drop were assumed to be valid in characterizing the transient characteristics of the heated section. For cases in which the energy storage mechanism was a compressible volume either upstream of, or within, the heated section, a critical slope of the pressure drop vs. flow rate curve in the heated section could be computed, as well as an associated frequency.

The analytical results were verified on a single-tube apparatus with controlled compressibility, and the onset of the instability agreed well with the theoretical predictions.

The criterion was applied to the data of a number of other investigations and gave excellent correlation in all cases where the restriction of subcooled or low quality operation was met. In a few isolated cases, the predicted frequencies could be checked against reported values, and the agreement was good.

ACKNOWLEDGMENT

The study was entirely supported by the National Magnet Laboratory at the Massachusetts Institute of Technology.

Professors Warren M. Rohsenow, S. W. Gouse, Jr., and H. H. Richardson gave generously of their time to discuss various aspects of the program. Special thanks are due to Professor A. E. Bergles who worked very closely with the program throughout. The work of R. S. Daleas in one phase of the experimental program is gratefully acknowledged.

The personnel of the Engineering Projects Laboratory and the Heat Transfer Laboratory assisted in the construction details. The National Magnet Laboratory Staff was helpful throughout the program.

Mrs. Nancy Jones and Miss Lucille Blake typed the final manuscript as well as the interim reports.

We wish to express our thanks to all concerned.

TABLE OF CONTENTS

LIST OF FIGURES

NOMENCLATURE

Symbol	Variable	Units
A	area	ft^2
a,b,c,d	coefficients defined in App. B	
$cp(=(\frac{\partial h}{\partial T})_p)$	specific heat at constant pressure	BTU/lbm-^oF
D	inside tube diameter	ft, in.
f	friction factor	
G	mass velocity	lbm/ft^2-hr
h	enthalpy	BTU/lbm
$I(=\rho L/A_F)$	fluid element inertia	lbm/ft^4
j	imaginary number, $\sqrt{-1}$	
K_c	constant (defined in Eq. 4-2)	
K_{in}	constant (defined in Eq. 4-5)	
L	length	ft, in.
L/D	length-to-diameter ratio	
$\mathcal{L}(y)=\tilde{y}$	denotes LaPlace transform	
p	pressure	lbf/in^2
$Q(=w/\rho)$	volume flow rate	ft^3/hr
q/A	heat flux	BTU/hr-ft^2
s	LaPlace variable	
T	temperature	^oF
$\Delta T_{sat}(=T_w - T_b)$	wall superheat	^oF
t	time	sec,hr.
V	volume	ft^3
$\vec{V}$	velocity	ft/sec
w	mass flow rate	lbm/hr

Subscripts

adb	adiabatic conditions
b	bulk fluid conditions
c.v.	compressible volume
ex	test section exit conditions
exc.	excursive condition
ext.	characterizes external system
F (A_F)	through-flow area
H (A_H)	heated surface area
in	test section inlet conditions
iso	isothermal conditions
o	initial conditions
osc	oscillatory condition
pl	plenum
sat	saturated fluid conditions
t.s.	test section
w	wall conditions
0-1, 1-2, 1-3	defined in App. A

Greek Letters

α	void fraction	
Δ	denotes difference or small change	
μ	dynamic viscosity	lbm/ft-hr
τ	shear stress	lbf/ft^3
ω	frequency	sec^{-1}

CHAPTER I

INTRODUCTION

1.1 Background of Problem

For the past several years, the study of heat exchanger designs utilizing a boiling fluid has been a subject of considerable interest. In particular, situations in which very high heat fluxes are expected, the use of subcooled, or local, surface boiling has appeared to be quite attractive. This is due to the very large increase in the heat transfer coefficient which is obtained in a boiling situation over that expected with purely forced-convection heat transfer. A qualitative boiling curve is shown in Figure 1. The basic curve is drawn for the simplest case of pool boiling in a saturated fluid. At very low wall superheats the heat transfer takes place entirely by natural convection and has the low heat transfer coefficients and slope normally associated with this mechanism. As the wall temperature is increased, local boiling begins at the surface, and the curve swings sharply upward. With further increases in the heater temperature, boiling becomes more violent until fully developed nucleate boiling is achieved. This is characterized, as may be seen, by very high heat transfer rates for modest temperature differences. The additional factors of fluid subcooling and forced convection behave just as would be expected in the non-boiling region, but the effects seem to wash out once fully-developed boiling is established. A detailed discussion of this phase of the problem is given by Bergles.[1]*

* Numbers in parentheses refer to references at end of the report.

However, a brief reference to Figure 1 bears out the contention that a given flow rate, the onset of boiling greatly augments the heat transfer capacity of the cooling channel. To obtain the equivalent heat transfer rate by forced convection alone would require enormously increased flow rates with the associated increase in pressure drop and pumping power. On this basis, the utilization of surface boiling has been chosen in a number of areas where high heat fluxes are encountered as in cooling of rocket nozzles, wave guides, electron tubes, nuclear reactors, and high-performance electromagnets. An extensive investigation has been going on at the M.I.T. Heat Transfer Laboratory for some years with the primary goal of providing quantitative information for the design of cooling systems for high-field electromagnets. Studies have been carried out to investigate the heat transfer coefficient [1] and the associated pressure drops [2] in nucleate boiling situations in small tubes. However, another very important design consideration is that of the maximum, or burnout, heat flux. [3]

1.1.1 Stable Burnout

Again with reference to Figure 1, it is seen that if the heat flux is increased beyond the region of fully-developed nucleate boiling, the curve passes through a local maximum. If an attempt is made to increase the heat flux beyond this maximum value, the heat which cannot be transferred away at that wall temperature goes into raising the internal energy of the heater material. This permits even less heat transfer, and the system proceeds unstably to higher and higher temperatures along the path indicated until a new stable

operating point (E') is reached. Unfortunately in most situations with water as the cooling fluid, this wall temperature is well above the melting point of the heater materials, and the heater surface fails. The identical situation can occur in a forced-convection system. The physical explanation for the occurrence of this local maximum is the following. In the region of fully-developed nucleate boiling, bubbles grow and depart from selected sites on the heater surface, and it is the resultant agitation in addition to the latent heat transport which accounts for the high heat transfer rates. If the heat flux is increased, more and more nucleation sites are activated until they are packed together so closely that an effective vapor blanket covers the surface and serves to insulate it, thus causing a sharp decrease in the attainable heat flux. In the forced-convection case, the cold fluid flowing by the wall aids in tearing the bubbles away, but even in cases where the flow is maintained at a prescribed constant value, the phenomenon does occur. This is what will be referred to as the limit of stable burnout. Although this might be construed as a misnomer since burnout is in fact a type of instability, it occurs at stable conditions with regard to the flow rate. However, it is found that in many situations the system fails at heat flux levels well below those which would be predicted on the basis of this stable burnout. This can often be attributed to sudden and unexpected reductions or changes in the flow rate with a small change in the heat flux. This often, though not always, leads to burnout and is referred to as a hydrodynamic instability.

1.2 Hydrodynamic Stability

The problem of hydrodynamically unstable behavior in flows with heat addition has received a great deal of attention in the last fifteen years. The end result, however, has been a rather confused picture and a number of contradictory conclusions. This is largely due to the fact that there are a great variety of mechanisms which can lead to unstable behavior. This was not always recognized by earlier investigators with the result that analyses or criteria geared to one mechanism were erroneously applied to systems in which an entirely different mode of behavior was dominant. In addition, experimental set-ups designed to investigate a particular type of instability would often go unstable for reasons quite unforeseen by the experimenters. This, coupled with the fact that for many years the number of theories far exceeded the number of data points, led to the rather unsettled state of the art which presently exists. In the following sections, an attempt will be made to categorize the various types of instability which can arise, and to review the approaches taken and results obtained by various investigators in the general area of hydrodynamic instabilities.

1.2.1 Nucleation Instabilities

The first general category is that of nucleation instabilities, sometimes referred to as "flashing" instabilities. The name is derived from the fact that these instabilities are caused physically by sudden vaporization of the liquid phase, with a resultant rapid increase in the specific volume of the mixture.

One example of this type of instability originates in the fact that a finite amount of wall superheat is required to initiate bubble nucleation at the heater surface.[1] This is accompanied by additional superheat in the liquid adjacent to the heated surface. For some conditions, particularly for scrupulously clean, smooth surfaces, this superheat can be quite large (of the order of 50-100°F). Under these conditions, when a bubble does start to grow, it will grow violently and eject liquid from the heated channel. This process will cool the remaining liquid and the heater surface with the result that further nucleation will be snuffed out, until the required degree of superheat is reestablished. Such behavior can be sustained at a frequency associated with the time required for bubble growth, ejection and runback of the liquid, and reestablishment of the superheat. It can thus be expected to depend strongly on the surface characteristics of the heater used, the geometry of the system, and the fluid properties. Such behavior was encountered on the SPERT I-A reactor at the Space Technology Laboratories.[4] In this instance, riveted channels, with a large number of good nucleation sites were found to be much more stable than welded ones where the sites were absent.

A second type of "flashing" instability was investigated by Griffith[5] for the particular geometry of vertical tubes, heated at the bottom, opening into a large reservoir at the top. When a bubble started to grow, the liquid in the channel above it would be displaced into the reservoir. This caused the pressure at the bubble, which was just comprised of the hydrostatic head of the liquid above it, to drop. The reservoir was large enough so that the pressure there

remained constant. Hence, near the bubble, the local saturation temperature would decrease, raising the superheat and causing the bubble to grow faster. The end result would be the violent ejection of the liquid from the tube followed by runback of cold water and the reinitiation of nucleation. This behavior would continue indefinitely at a fairly regular frequency. The system could be stabilized by reducing the reservoir volume to the point where a small amount of liquid leaving the tube would cause a significant increase in the reservoir pressure.

1.2.2 Flow Pattern Instabilities

This type of instability arises from the fact that, when gas and liquid flow together in a channel, there are a variety of possible geometric configurations into which the two phases can arrange themselves. These arrangements are known as flow regimes and are illustrated in Figure 2. The particular flow regime of most interest to this discussion is that of "slug" flow, characterized by an alternating succession of liquid slugs separated by large vapor bubbles with rounded noses and bubbly wakes. For the flow of boiling water at low pressures, this flow pattern is encountered only at very low qualities of the order of 0 to 7%.

If conditions are monitored at any given point, they are characterized by apparent oscillations in pressure, flow, and heat transfer coefficient attributable to the fact that at the point in question, the channel is filled alternately by liquid and gas. The pressure fluctuations are of a magnitude commensurate with the pressure drop

associated with a single slug of liquid[6]. The heat transfer coefficient will vary from the value expected in a liquid-filled channel to that associated with a thin liquid film and a vapor core. The frequency of these oscillations is clearly given by the length of time required for a slug of liquid and a gas bubble to pass a given point. Equally important is the length of time required for the gas bubble alone to pass a given point, for it is during this part of the cycle that the heat transfer coefficient is lowered drastically. This inability to transfer heat to the liquid results in a sharp rise in the heater wall temperature. If this is not reversed by the appearance of a liquid slug, burnout can occur.

The most difficult aspect of dealing with this mode of behavior is that of predicting when slug flow will occur. An empirical flow regime map is proposed by Griffith and Wallis[7] and an annular-slug transition criterion was investigated by Haberstroh[8]. However, these investigations were for two-component flow of air and water. In these cases, the flow rate of each phase can be determined independently. In the case of one component flow with heat addition, however, a use of these maps would require a knowledge of the void fraction. A calculation of the void fraction on the basis of a heat balance is virtually useless since the departures from thermodynamic equilibrium are quite large. As a result, an equilibrium calculation yields void fractions orders of magnitude greater than are actually observed in visual tests. In spite of these difficulties, however, it is fairly well established by Tippetts[9] and others that a slug-flow regime can exist and lead to premature burnout.

1.2.3 Instabilities in Natural Circulation Loops

The class of instabilities which has probably received the most attention is that which occurs in natural circulation loops. Perhaps the most lucid treatment of this phenomenon was that presented by Wallis and Heasley.[10] This approach was based on the use of LaGrangian coordinates which avoids the non-linear differential equations which result from an Eulerian description. Three types of oscillatory mechanisms were investigated.

(a) flow oscillations due to changes in riser density

(b) flow oscillations excited by the heated section

(c) flow oscillations caused by a restriction at the riser exit

A simple description of the physical mechanism can be given with reference to Figure 3. A slight perturbation to a lower flow rate can, at certain conditions, lead to a large increase in the vapor fraction entering the riser. As the riser density decreases, the driving head around the loop will increase and accelerate the flow. An increased flow rate in the heater will produce a decrease in the vapor fraction entering the riser, which will eventually increase the riser density, reduce the driving head, and decelerate the flow. This behavior can be sustained at a regular frequency and amplitude. The period, in general, is of the order of the transit time for a fluid particle in the riser.

A large number of other treatments of the stability problem in a natural circulation loop have appeared in the literature. Among these are treatments by Wissler, Isbin and Amundson[11], Beckjord[12],

Fleck[13], and McGowan and Bodoia[14]. The details of these investigations will not be presented here since they are well outside the scope of this investigation. However, the general conclusions will be listed. The following items normally tend to increase the stability of the system:

1. increasing loop inertia
2. increasing loop throughput velocity
3. decreasing the fraction of the loop pressure drop associated with the two-phase portion of the heated section, particularly the heated section exit
4. increasing system pressure
5. decreasing inlet subcooling.

In general, it may be stated that a prediction of the onset of loop instabilities and a complete description of the unstable behavior in terms of frequency and amplitude cannot be performed satisfactorily at this time. However, the general trends listed above are fairly well established, and can be visualized on a physical basis. Unfortunately, they are often quoted as cure-alls for systems which are not natural circulation loops, thus giving rise to widespread misconceptions about the nature of other stability problems. It should also be noted that a natural circulation loop is also susceptible to the nucleation and flow pattern instabilities discussed in the previous sections.

1.2.4 Instabilities in a Forced-Convection System

The remaining, and perhaps most general, class of instabilities is that associated with flow in forced-convection systems. Whereas it should be noted that such systems are subject to both nucleation

and flow pattern instabilities, it is often the case that these mechanisms are unimportant compared with instabilities which are attributable to the overall system. A forced-convection system differs from the case of natural circulation in that the driving force is imposed upon the heated section externally and is not normally a function of the conditions in the heated section. Exceptional cases in which uncondensed vapor enters the pump and affects the driving force will not be considered.

One of the first treatments of forced-convection flow instabilities was presented by Ledinegg[15] in 1938. Here a system was judged unstable if the two-phase flow pressure drop increased with decreasing flow rate. Under such conditions, operation at more than one point is possible and operation in such a region can lead to sudden decreases in flow rate and burnout. This type of instability will be discussed at some length in Chapter II, but it should be pointed out that this mechanism alone cannot lead to oscillatory behavior but only to sudden changes in the flow rate of an excursive nature. More detailed treatments of this subject were presented by Markels[16] and Chilton[17]. These investigations were identical to Ledinegg's as far as the basic mechanism was concerned, but they contained detailed calculational procedures.

More recently, a number of investigations have been reported which deal with oscillatory behavior. One of the first of these was that of Quandt[18] in 1960 and is a good example of the approaches taken. The analysis begins with the formulation of the basic transient equations of fluid flow: continuity, momentum, energy, and the

equation of state. These equations are then written for small perturbations and certain assumptions are made concerning the spatial form of the flow and enthalpy perturbations. The perturbed equations are then integrated along the channel and LaPlace transforms of the integrated equations are taken. In this case, a constant pressure drop boundary condition is applied, and algebraic manipulation yields a solution for a transfer function between heat flux and inlet flow perturbations which is of second order, and stability criteria may be stated. The basic result is that, in order for sustained oscillatory behavior to occur, $(\frac{\partial \rho}{\partial h})$ must be negative and sufficiently large. It is further stated that oscillatory behavior will occur in regions where the slope of the pressure drop vs. flow rate curve at constant heat flux is positive. These results will be discussed in detail in Chapter IV, but certain comments may be made at this point. The first is that the mathematical manipulation in this treatment becomes so complex that the physical picture is lost. As a result, the stability criterion is a purely analytical one and the actual destabilizing mechanism is not easy to visualize. Furthermore, certain assumptions such as the linearization of the flow and enthalpy perturbation profiles, although well justified for the particular case, are clearly inappropriate for general application. Finally, the form chosen for the equation of state, $\rho = \rho(h)$, where the density is computed as a function only of the local bulk enthalpy is demonstrably incorrect, particularly for the case of subcooled, surface boiling. This is not to degrade the quality of the effort, for a very difficult problem was pushed through to a solution and the agreement with experiment for

the specific apparatus was excellent. Rather, this is intended to illustrate the pitfalls of applying any particular analysis to an arbitrary system when the physical mechanism is not clearly presented.

A similar treatment was presented by Meyer and Rose[19]. In this case, a computerized difference-equation method of solution is applied to a so-called "momentum integral" model. Here the approach is not limited to small perturbations since it was devised to study more general transients. The essential restriction on the model is that all fluid properties are evaluated at a single reference pressure. Hence, any situation where the plenum-to-plenum pressure drop is large is not covered by the analysis. More pertinent, however, is that the two-phase flow treatments of such quantities as slip ratio, density, fraction factor and void fraction seem too crude to justify the quite involved and expensive calculational procedures which follow. There appears to be no hope of obtaining any design criteria from this procedure. Extension and refinements of this work have been presented by Meyer[20] and Meyer and Reinhardt[21].

Another approach is that of Jones[22] which involves a point-by-point computer solution along the heated channel. Although the effects of subcooled boiling are neglected, considerable attention is given to all of the other two-phase flow calculations, and the analysis appears to be the most precise yet presented. Again, however, the physical picture is obscured in the mathematics and general application of the results seems impossible. One interesting aspect of the analysis deals with the number of calculation points or grid size required for an

accurate solution. In this case, a single node corresponds to Quandt's[18] linear enthalpy profile, and this is shown to be unsatisfactory in general.

An earlier treatment was that by Bick[23] in 1959. This consisted of a purely mathematical approach to the stability of the distribution of flow in a multi-channel matrix where the total flow is assumed constant. No mention is made, however, of the methods of calculating the two-phase flow quantities introduced in the analysis. One other method of approach was presented by Anderson et al.[24] in which a very large analog computer simulation was attempted. Here a somewhat better physical understanding of the mechanism was obtained, but the formulation of quantitative design criteria was difficult.

Two purely experimental investigations have appeared in the literature and are worthy of note. The first of these was by Lowdermilk et al.[25] in 1958 and dealt with stable and unstable burnouts at low pressures in small diameter tubes. The effects of upstream compressibility and upstream throttling were extensively investigated and considerable data was obtained. The second was by Aladiev et al.[26] in 1961. Here the region of interest was that of high pressures and temperatures in somewhat larger tubes than those of Lowdermilk. The effects of a variety of upstream compressible volumes were documented experimentally. In both cases, the state of the art at the time was not well enough developed to permit the results to be fully interpreted. The investigations were significant, however, in that they isolated a well-defined energy storage mechanism for the sustaining of oscillatory

behavior. The results of both investigations will be dealt with in detail in Chapter IV.

More recent investigations by Gouse and Andrysiak[27] and also Stenning and Veziroglu[28] have attempted to clarify the total picture through the use of Freon-11 as the cooling fluid. In these cases, the heat fluxes required to investigate the instabilities were low enough so that the test sections were not destroyed by the unstable behavior. In particular, Stenning and Veziroglu[28] have isolated three distinct types of oscillatory behavior. These are called "density wave," "pressure drop," and thermal" oscillations. A further treatment of this investigation will be given in Chapter IV.

1.3 Summary

In summary, it can be stated that while a great deal of work has been carried out in the general area of boiling stability, the picture is not yet clear. This is largely due to the large variety of mechanisms which can lead to unstable behavior. In this study, attention will be concentrated on instabilities occurring in forced-convection systems and primarily concerned with subcooled boiling in small tubes. A particular mechanism will be selected to the exclusion of all others. Whereas this will not provide a complete solution to the boiling stability problem, it is felt that the limits of applicability can be sufficiently well-defined so that useful design information can be provided for application to enough systems to be of general interest. The relationship between the results of this investigation and the previous studies described here will be established in a later chapter.

CHAPTER II

ANALYTICAL CONSIDERATIONS

2.1 General Approach

In order to deal with the problem of predicting the onset of various instabilities theoretically, it was decided to make use of a linearized, lumped-parameter mode of analysis. In its simplest form, this consists of viewing the heated section as a single element with associated inertia, capacitance, and friction determined from steady-state measurements and investigating its behavior when subjected to various boundary conditions which are sufficient to characterize the external system as encountered in a real situation. The limitation on this approach will be discussed in a later section, but it is intended that the degree of complexity will be limited to that sufficient to describe the essential elements of the observed behavior.

Attempts by other investigators to describe the internal details of the transient flow, as described in Chapter I, have been seen to result in such complexity that it is nearly impossible to glean any useful design information from the final results.

2.2 Excursive Instability

The simplest type of hydrodynamic instability is that referred to as an excursive instability in which the operating point of the system shifts from one flow rate to another (usually to a lower flow) in a non-recurring manner. The system will remain at the new operating point from then on, if the new point is compatible with other restraints on the system, such as stable burnout. This non-recurring behavior is amenable

to a simpler analytical treatment than that which will be necessary to deal with oscillatory behavior. This is due to the fact that no mechanism for energy storage is required for an excursive instability.

The details of the analysis are given in Appendix A. The final result of the basic analysis is given by Equation (2-1), which states that for the instability to take place (see Fig. A-1; App. A)

$$\left\{ \frac{\partial(\Delta P_{ext.})}{\partial Q} - \frac{\partial}{\partial Q}\left[\Delta P_{0-1} + \Delta P_{1-2} + \Delta P_{2-3} \right] \right\} \geq 0 \qquad (2\text{-}1)$$

where $Q \equiv w/\rho$

Physically, this is interpreted as meaning that if the slope of the pressure drop vs. flow rate is more negative than that of the external supply system an excursive instability will occur. Such a conclusion is to be expected from previous works,[15],[16] but the implications of this result will be discussed here in some detail for the purpose of clarity.

2.2.1 Effect of Supply System

Figure 4 presents a typical plot of an overall pressure drop vs. mass flow rate curve for a heated section. The pressure drop includes contributions due to arbitrary inlet and outlet configurations as well as the constant area heated section itself. Superimposed upon this are four distinct external system characteristics, (A),(B),(C) and (D).

(a) Constant Pressure-Drop Supply System:

The first condition under consideration is that of the constant pressure drop supply system. This is the boundary condition which most closely approximates the situation as seen by an individual cooling

passage in an axial-flow electromagnet. As described previously, the geometry of these magnets is that of a large number of small coolant channels arranged in parallel passages between large common headers, an arrangement commonly encountered in heat exchanger design. If, prior to the onset of unstable behavior in any of the tubes, the total flow rate is distributed uniformly among "n" tubes, an individual tube will carry 1/n th of the total flow. If one tube should become totally blocked, each of the remaining tubes would now carry $\frac{1}{n-1}$ th of the total flow. For large n, $\frac{1}{n} \approx \frac{1}{n-1}$ and the pressure drop across the array is nearly unchanged. Hence, it is argued that the pressure drop across any individual channel is independent of the flow within it. This type of arrangement effectively uncouples the heated section from the pumping apparatus. Such a condition is indicated by (A) in Figure 4.

If operation at points (1) and (3) is considered, Equation (2-1) indicates that

$$\left\{ \frac{\partial(\Delta P_{ext.})}{\partial Q} - \frac{\partial(\Delta P_{ov.})}{\partial Q} \right\}_{(1),(3)} < 0.$$

and the operating point is expected to be stable. If, on the other hand, operation at point (2) is examined, Equation (2-1) yields

$$\left\{ \frac{\partial(\Delta P_{ext.})}{\partial Q} - \frac{\partial(\Delta P_{ov.})}{\partial Q} \right\}_{(2)} > 0.$$

and unstable operation is predicted. Physically, if the flow rate at point (2) increased slightly along (A), it is seen that the external system is supplying more pressure drop than that which is required to maintain the flow, and the flow rate will increase until a new operating

point (point (1)) is reached. By the same token, if the flow rate should decrease slightly, more pressure drop is required to sustain the new flow rate than is being provided by the external system. Hence, the flow will continue to decrease until point (3) is reached.

In any real system, point (2) could never be attained in the first place. As the power to the magnet is increased, a situation such as described by (B) would be encountered. Point (4) by the foregoing arguments is stable to small increases in flow but unstable with regard to small decreases. An attempt to operate at point (4) will result in an excursion to point (5). The flow rate associated with point (5) is often below the critical flow rate at which stable burnout occurs, and the system will usually fail. It can be argued that this modelling procedure is only valid for one heated tube in parallel with a large number of unheated tubes, since if all the channels were to reach point (4) simultaneously, the concept of one tube acting independently of the others would be unsatisfactory. However, even in well-designed systems where all the channels are expected to take the same heat load, it seems very reasonable to expect that one tube would always reach an unstable point slightly in advance of the others. In the case of an electromagnet, the failure of just one, or at most a very few, of the coolant channels is sufficient to disable the entire unit. Within this framework, this analysis yields a pertinent design criterion.

(b) Constant Flow Rate Delivery System

The other extreme case which may be considered is that of a constant flow rate delivery system. This is indicated in Figure 4 by the system

characteristic labelled (C). Such a condition may be encountered physically in a single-channel geometry either through the use of a positive-displacement pump with a nearly vertical characteristic or through the insertion of a throttle valve just upstream of the heated section. In the latter case, nearly all of the resistance to flow in the overall loop is due to the presence of the throttle valve, and small changes in the resistance of the heated section produce a negligible effect on the flow rate. By the very nature of the system, no flow excursions are possible. In terms of Equation (2-1) at point (6)

$$\frac{\partial(\Delta P_{ext.})}{\partial Q} = -\infty$$

Therefore,

$$\left\{ \frac{\partial(\Delta P_{ext.})}{\partial Q} - \frac{\partial(\Delta P_{ov.})}{\partial Q} \right\}_{(6)} < 0.$$

and the system is always stable. Hence, such an arrangement can be used to investigate single tube behavior in all regions of the curve.

(c) Generalized System Characteristics

In reality, of course, no supply system corresponds exactly to either of the extreme cases just described. A possible real characteristic is shown in Figure 4 as (D). Through the use of arguments exactly the same as those used to deal with the constant pressure drop situations, it is seen that points (7) and (9) are stable, whereas point (8) is not. Again it should be noted that it would be impossible to establish operation at point (8), but it is often possible to operate well into the negative sloping region without fear of an excursive instability, as at point (9).

2.3 Oscillatory Instability

Before going on to deal with the character and individual components of the heat exchanger pressure drop, a more complex variety of hydrodynamic instability will be treated; that of an oscillatory instability. To produce higher order, oscillatory behavior, some sort of energy storage mechanism is required. This could be accounted for in a variety of ways such as by superheated liquid or by the heat capacity of the heated surface. However, perhaps the simplest sort of energy storage mechanism, and one which is always present in a real system, is that of a compressible volume located just upstream of, or within, the heated length. This type of mechanism was chosen for the analysis to the exclusion of all others, and while this will produce useful stability criteria for a large variety of systems, it must be kept in mind that a system which is predicted to be stable on this basis is not necessarily unconditionally stable since other, destabilizing mechanisms may be present. A description of the model and the details of the analysis are presented in Appendix B.

The final result as given by Equations (2-2) and (2-3) yields a critical slope of the pressure-drop flow curve at which marginal stability will occur (see Fig. B-1; App. B)

$$\left[\frac{\partial(\Delta P_1)}{\partial Q}\right]_{crit.} = \frac{\frac{\partial}{\partial Q}(P_{IN})\ [I_1+I_2] + \sqrt{\left[\frac{\partial}{\partial Q}(P_{IN})\ (I_1+I_2)\right]^2 + 4I_1^2 I_2 \left(dP/dV\right)_o}}{2I_2} \qquad (2\text{-}2)$$

where $Q \equiv W/\rho$; $I \equiv \rho L/A$

and an expression for the frequency of these oscillations.

$$\omega^2 = \frac{-\left(\frac{\partial(P_{IN})}{\partial Q}\right)(I_1+I_2) - \left(\frac{\partial(P_{IN})}{\partial Q}\right)\sqrt{\left(\frac{\partial(P_{IN})}{\partial Q}\right)^2(I_1+I_2)^2 + 4I_1^2 I_2\left(dP/dV\right)_o} - 2I_1 I_2\left(dP/dV\right)_o}{2I_1 I_2^2} \qquad (2\text{-}3)$$

In the case of the oscillatory instability, it is more difficult to describe the mechanism in physical terms. However, briefly, the situation is the following. If a slight perturbation to a lower flow occurs, the supply pressure to the heated section will increase (if g' is negative as it is in all normal systems). This will drive flow into the compressible volume, diverting it from the heated section. The pressure will continue to increase until it increases at a faster rate than the resistance of the heated section is increasing. At this point the flow to the heated section will increase, removing fluid from the compressible volume until the original operating point is reached. Then the inertia of the flow from the compressible volume will cause an overcorrection with a resultant pressure reduction at the heated section inlet. This pressure will continue to drop until the flow to the test section can no longer be maintained and the cycle will be repeated. A possible locus of operating points is indicated in Figure 5. As noted previously, the steady-state characteristics of the test section may not specify the correct, instantaneous resistance during the transient, but the adequacy of the assumption will be evaluated experimentally.

The trends predicted by the analysis may now be examined and their physical significance discussed. The first of these is the characteristic of the external system.

2.3.1 Effect of External System

The characteristics of the external system are included in the analysis in the term $\frac{\partial(P_{IN})}{\partial Q}$ which represents the slope of the pressure drop vs. flow rate curve of the supply system. This can vary from $-\infty$ in the case of a constant flow delivery system to 0 in the other extreme of a constant upstream pressure supply. In the case of a constant flow delivery system with $\partial(P_{IN})/\partial Q = -\infty$; a limit investigation of the equations yields

$$\left(\frac{\partial \Delta P_1}{\partial Q}\right)_{crit.} = 0 \qquad (2\text{-}4)$$

and

$$\omega^2 = \frac{(dp/dV)_0}{(I_1 + I_2)} \qquad (2\text{-}5)$$

This, in a sense, represents the least stable condition since instabilities will occur as soon as the pressure drop-mass flow rate curve reaches a minimum. As the characteristic of the supply system becomes less steep, the critical slope required for incipient instability becomes more negative. This is understood physically by consideration of the fact that in order for a small perturbation to grow, the supply pressure must increase steeply with decreasing flow in order for flow to be forced into the compressible volume. The change in frequency is in the direction of higher frequencies as shown in Figure 6. If the extreme case of $\partial(P_{IN})/\partial Q = 0$, representing a constant pressure supply, is examined, it is seen from Figure B-1 (Appendix B) that the oscillatory instability can no longer exist. If the inlet pressure is constrained to remain constant, no flow can ever enter or leave the

compressible volume. Hence, the situation degenerates to that of the zero-frequency, excursive instability discussed in a previous section. In a similar way, another type of excursive instability may be envisioned. If $(\partial p_{IN})/\partial Q$ is quite small, it is possible that the heat exchanger slope will become more negative than the slope of the supply system, before the critical slope necessary for oscillatory behavior as given by Equation (2-2) is reached. This will give rise to an excursive behavior and, although there will be some flow into the compressible volume, an oscillatory condition will not be sustained. The locus of the operating points encountered in the situation is indicted in Figure 7.

2.3.2 Effect of System Stiffness

Another trend indicated by the oscillatory instability criterion which may be interpreted physically is that of system stiffness. The quantity $(dp/dV)_o$ is a measure of the compressibility of the energy storage medium. If $(dp/dV)_o$ is very large, the system is said to be "stiff." If, on the other hand, $(dp/dV)_o$ is quite small, the result is a so-called "squishy" system.

An examination of Equation (2-2) shows that for a "squishy" system where

$$\left[\frac{\partial p_{IN}}{\partial Q}(I_1 + I_2)\right]^2 >> 4 I_1^2 I_2 (dp/dV)_o$$

the critical slope is simply

$$\left(\frac{\partial \Delta p_1}{\partial Q}\right)_{crit.} = 0$$

By the same token, the frequency is a minimum. Since, in this case, the instability will occur right at the location of the minimum in the pressure drop-flow rate cuve, this is the most unstable situation. On the other hand, as $(dp/dV)_o$ increases, (or as the system becomes stiffer), the slope required for instability becomes more negative, and the frequency increases. This corresponds to a more stable system. It should be noted that as $(dp/dV)_o$ becomes quite large, (very stiff system), the critical slope required for instability can attain such a large negative value that stable burnout will be encountered prior to the onset of oscillatory instability. This represents an upper limit beyond which it is not possible to improve the system performance and hence represents what, for practical purposes, is an infinitely stiff system. The variations in the critical slope and the associated frequency are indicated qualitatively in Figure 8.

CHAPTER III

EXPERIMENTAL PROGRAM

3.1 Purpose of Experimental Program

The second phase of the overall investigation consisted of an experimental program designed to verify the results of the analytical portion. In general, it can be stated that the experimental work was divided into two major sections. Since the results of the analysis indicated that both the excursive and oscillatory modes of instability depended on the slope of the pressure drop vs. mass flow rate curve, the first goal was to determine this curve experimentally for a wide range of system parameters, in a stable system under steady-state conditions. The second phase of the program attempted to simulate the external system conditions which were postulated in the analytical models and to verify the onset of the predicted instabilities. The following discussion of the experimental work will consist of two parts: a description of the experimental apparatus and a description of the tests performed.

3.2 Description of Apparatus

The following section contains a description of the experimental facility which was used in this investigation. This was divided into three categories: the hydraulic system, the power supply, and the associated instrumentation. Although detailed descriptions of the apparatus are available in other reports,[1],[2] they are repeated here for the convenience of the reader. The basic apparatus had been designed and constructed on a previous study by Bergles.[1]

3.2.1 Hydraulic System

A schematic of the flow loop is shown in Figure 9. The pipings and fittings, all of brass and stainless steel for corrosion resistance, are erected around a test bench constructed of Dexion slotted angles and plywood. Rayon reinforced rubber hose was used where flexible connections were required. Flow circulation is provided by a Fairbanks Morse two-stage regenerative pump (260 psi at 3.6 gal/min) driven through a flexible coupling by a 3 HP Allis Chalmers induction motor. To avoid contamination of the system water, the pump was fitted with special seals of teflon-impregnated asbestos. A relief valve set for 300 psi protected the pump casing from overpressure, and a bypass maintained sufficient flow.

The main flow loop consists merely of a Jamesbury ball valve to control the overall pressure drop. The test section line, installed in parallel with the main loop can be isolated by means of two more Jamesbury ball valves. The downstream valve is used to control the pressure level in the test section. The test section flow rate is controlled by means of a Hoke metering valve of 20 turns from closed to open, set just upstream of the test section itself. The test section line also contains two basic Fischer-Porter flowmeters with the appropriate isolating valves. Four Chromalox heaters of approximately 6 kw. each are also provided to control the test section inlet temperature. Three of these are controlled simply with "off-on" switches while the fourth can provide a continuous range from 0 to 6 kw. by means of a bank of two variacs mounted on the test bench. Pressure fluctuations at the outlet of the pump are damped out by means of a 2.5 gallon

Greer accumulator charged with nitrogen to an initial pressure of 40 psi. This accumulator contains a flexible bladder-type separator which prevents the nitrogen from being absorbed by the system water. A Jamesbury ball valve isolates the accumulator from the loop at shut-down.

Since the system is closed loop, the heat added to the system water is rejected to a shell-and-tube heat exchanger connected to a city water line. Due to seasonal temperature variations, the minimum operating temperature varies from approximately $50^{o}F$ in the winter to $75^{o}F$ for summer operation. Continuous deionization and deoxygenation is provided in a parallel loop containing four resin beds, two of which provide deionization and the other two, deoxygenation. The conductivity of the loop water may be maintained at less than .1 ppm as read on a conductivity meter made by Industrial Instruments, Inc. In order to insure a minimum of dissolved air in the system, a 5 gallon degassing tank was provided with five electrical heaters (3-220 VAC and 2-110 VAC). This tank was also used to provide make-up water to the system. A storage tank for filling the system and degassing tank was mounted above the degassing tank and could be filled with distilled water from standard 5 gallon bottles with a small Hypro pump. Both the storage tank and the degassing tank were equipped with glass sight gages so that the proper levels could be maintained.

3.2.2 Power Supply

Power was supplied to the test section by means of two 36 kw. Chandrysson externally excited generators, each capable of delivering 3000 amperes at 12 volts. The generators are driven by 440 volt-3 phase-600 rpm synchronous motors.

The power could be regulated from zero to maximum power as desired through a portable control console. The generator outputs were connected in series and the output from one was added to or subtracted from the output of the other. Water-cooled shunts, installed in parallel with the test section, eliminated the shock of a sudden open circuit caused by a test section burnout.

An existing buss-bar system was used, with the addition of water-cooled copper braided cables just at the test section. The use of these flexible cables permitted considerable flexibility in the size of the test section which could be accomodated. At the upstream end of the test section, the cable assembly is clamped to a copper plate to which a rigid brass test section holder is attached. At the downstream side, the connection to the test section holder is accomplished by a flexible braided conductor to permit thermal expansion of the test section. The test section holders were made of brass plate in two segments which, when bolted together, clamped to the test section bushing. The inner surfaces were lined with high-temperature soft solder to provide good electrical contact between the test-section bushings and the holders. The downstream end of the test section was connected to the piping with rubber hose to provide electrical insulation and increased flexibility.

3.2.3 Instrumentation

Instrumentation was provided to monitor the steady-state and transient conditions throughout the system. Pressure gages on the main loop, as indicated in Figure 9, aid in adjusting the pressure level in the test section and in insuring system stability. A thermocouple was installed in the degassing tank to monitor the water

temperature during degassing operations. Another at the discharge of the pump insured that the water temperatures in the deionizing beds never exceeded 140°F. A variety of metering tubes and floats which could be installed interchangeably in the basic Fischer-Porter flowmeter housing provided measurement of the test section flows from 1.5 to 4000 lbm./hr. Calibration curves for these flowmeters are given in Figures 10 and 11. The results were calibrated at installation and checked periodically against the initial calibration.

The test section itself was instrumented with thermocouples to record inlet and outlet water temperatures. In both cases, the thermocouples were located at positions where the flow was well-mixed. At the downstream end, the thermocouple was located far enough from the exit of the heated section so that it could be safely assumed that the vapor fraction is completely condensed. In cases where several outlet thermocouples were provided, sufficient agreement was obtained to give confidence that the true mixed mean temperature was being recorded. Fiberglass insulation was wrapped around the piping between the heated section and the upstream and downstream thermocouples to minimize errors due to heat transfer from the surroundings.

Test section pressures, both upstream and downstream were monitored on 8½-inch Helicoid gages with a specified accuracy of ¼% of full scale. A 200 psi gage was used upstream with either a 100 psi or 60 psi gage on the downstream end. Each gage was checked on a dead weight tester and adjusted to an accuracy of approximately .1 psi over the entire range. They were checked against one another periodically at various static pressure levels under zero flow conditions.

Porous-plug snubbers were provided to protect the gages from severe momentary overpressure.

Thermocouples were constructed from Leeds and Northrup 30-gage duplex copper-constantan wire. Calibrations were performed and deviations from N.B.S. standard tables were found to be so slight that no corrections were necessary. All of the thermocouples were connected to a common ice junction through a twelve position Leeds and Northrup thermocouple switch. The output could be read on either a potentiometer or a recorder.

The recorder is a pen-type, single channel instrument manufactured by Minneapolis-Honeywell Brown. There are five manually selected ranges for 0-6, 5-11, 10-16, 15-21, and 20-26 millivolts. Occasional calibration against the potentiometer insured the accuracy of the recorder to within .01 millivolts.

Test section pressure drops were measured by means of a manometer system shown schematically in Figure 12. Basically it consists of two 60-in. U-tube Merriam manometers, manifolds and valves, and rubber hose connecting lines. The system could read up to 10 pressure differences from one or two reference points on either manometer. One manometer contained mercury and had a maximum range of about 25 psi, while the other, containing a manometer oil with a specific gravity of 2.00, had a range of about 2 psi. An approximate check on the pressure drop could be obtained from the pressure gages. The line could be freed of trapped air through appropriate vents, and the system was assumed to be operating correctly when, under isothermal conditions, pressure level alone had no effect on the pressure drop.

The heat input to the test section was computed from measurements of the voltage drop across the heated length and the current to the section. The voltage drop was read on a Weston, multirange d.c. voltmeter with a specified accuracy of $\pm\frac{1}{2}\%$ of full scale. The current was inferred from the voltage drop across an air-cooled N.B.S. shunt with a calibrated conductance of 60.17 amps/m.v.

3.3 Experimental Procedure

3.3.1 General Loop Operation

Many aspects of the experimental procedure, particularly the installation of test sections and final preparation of the loop for operation were common to all types of runs. Distilled water was pumped into the storage tank from the standard five gallon bottles. The system and degassing tank were filled by gravity. Vents on the flowmeter, preheaters, test section, exit plenum, and the deionization tank were opened to allow the displaced air to escape. The degassing tank vent was open at all times. The other vents were closed when no further bubbles were seen. The pump was then turned on and all valves opened and closed several times to dislodge any remaining air pockets. The vents were then opened and closed again in turn until air-free water was obtained at each vent. Visual observation of the flow through the glass flowmeter tube aided in determining when the system was free of air.

At this point, all the degassing tank heaters were turned on, and water was circulated through the system. The temperature of the degassing tank water was monitored on the recorder, and all but one of the heaters turned off as the boiling point was approached. If this

was not done, the degassing tank was found to boil too vigorously with the result that considerable overpressure built up in the tank and a large amount of water was forced out through the vent. When boiling occurred, water from the loop was bypassed into the degassing tank. The amount of flow was regulated so that a small but continuous flow of steam issued from the vent hose. The system water was effectively degassed by being dumped into the boiling water at the top of the degassing tank. This was continued until the temperature in the loop rose to approximately 180°F. Care was taken to shut off flow to the deionization tank before the loop temperature exceeded 140°F. The entire procedure took about 30 minutes. A standard Winkler analysis, described in Reference (1), indicated that this method of degassing reduced the air content to less than .5 cc air/liter. Upon completion of the process, the remaining tank heaters were shut off, and the heat exchanger turned on. The flow of system water to the degassing tank was turned off as soon as steam stopped coming out the vent. The system was then ready for operation. This process was repeated at the beginning of each day of operation, or whenever gassy makeup water had to be added from the storage tank. The daily degassing was necessary since the degassing tank is vented to the atmosphere, and the water in the tank would eventually become saturated with air (~18 cc/liter).

The system was then operated for at least 15 minutes at zero power before taking measurements. At the end of this time the system water was completely cool and had been thoroughly circulated through the deionizers. This time was also used to allow the generators to

warm up. If the generators were used immediately after starting, fluctuations in the power level were much larger and harder to control. If a particularly low resistance test section was in place, it was necessary to disconnect one of the power leads until the generators had come up to speed. If this was not done, high voltage drops could result from the fact that the two generators did not speed up in unison and on occasion could lead to unwanted burnouts.

At shutdown, it was necessary to isolate the accumulator from the loop. Otherwise, the water would be forced out of the accumulator, into the loop, and eventually out through the degassing tank vent. The pump and generator were connected together electrically so that the generators would be shut off if the pump should be turned off accidentally or due to a power failure. However, the generators could be shut off independently by means of a switch on the control console. Turning off the generators or the pump also interrupted the power to the preheaters. This was a safety precaution to prevent burning out the heater elements should they be left on with no flow.

3.3.2 Pressure Drop vs. Flow Rate Data

The bulk of data taken consisted of tracing out heated section pressure drop vs. mass flow rate. The data for a given geometry was obtained at constant exit pressure, inlet temperature, and heat flux while varying the flow rate. At the beginning of each run, the manometer system was checked in the following way. The pressure drop for a variety of flow rates was measured at a given exit pressure, inlet temperature, and under isothermal conditions. These runs were then repeated at two different pressure levels. Since, in the isothermal

case, the pressure drop should be independent of the pressure level, any variation was attributed to air trapped in the manometer lines. If this were the case, the lines were bled and the runs repeated until the maximum variation was less than ½% of the total pressure drop.

When the manometers were felt to be reading satisfactorily, the flow rate was established at a high value (well above where incipient boiling would be encountered at the particular heat flux) and the exit pressure and inlet temperature were set to the desired levels by manipulation of the various pressure control valves, and the preheaters. The desired heat flux was delivered to the test section and then data taking could begin. Inlet and outlet pressures were read from the gages as well as the pressure drop from the manometers. The inlet and outlet water temperatures were also read on the recorder, and the reading on the flowmeter was recorded. A new, lower flow rate was then established. The preheaters and system pressure then had to be adjusted to maintain the values of inlet temperature and exit pressure. In addition, a lower flow rate at the same heat flux resulted in an increased test section wall temperature. This, in turn, led to a change in the overall electrical resistance of the test section so that the power output of the generators had to be adjusted to keep the heat flux constant. The most difficult part of the procedure, however, was in maintaining a constant inlet temperature. This is due to the very slow response, particularly at low flows, of the water temperature to any adjustment in the power to the preheater. As a result, a variation of $\pm 1^{\circ}F$ was permitted in the inlet temperature. The flow rate was further decreased in moderate steps until a further decrease in the flow rate resulted in an increase in the

heated section pressure drop. Since this minimum was the point of primary interest, a number of points were taken at flows close to this minimum. In most cases, a few points were taken at flows well below this minimum, on the negatively sloping portion of the curve. However, since it was desired to avoid burnout, the flow rate was always kept well above the expected critical value. Although this effort was not always successful, it was found that if care was taken in the construction of a new test section to reproduce the old dimensions of heated length and distance between the pressure taps that the agreement between two nominally identical test sections was sufficiently good to permit a meaningful comparison. This is discussed in greater detail in Section 4.2.

When burnout did occur, the generators, preheaters, and pump were turned off, and the test section line isolated from the main loop. Before tightening the inlet and outlet fittings on a new test section, water was allowed to leak out in both directions to minimize the amount of air entrapped in the system. The manometers were normally isolated during start-up and shut-down to prevent their being blown by momentary pressure surges. A single "set" of data, consisting of a pressure drop-flow rate trace for four or five distinct heat fluxes at a given set of isolated exit conditions, could be taken in about one hour. A typical data sheet is, with the attendant calculations, shown in Appendix C.

3.3.3 Simulation of Constant Pressure Drop Condition

The second phase of the experimental program consisted of simulating conditions which were thought to lead to unstable behavior and

attempting to verify this behavior as predicted by the analysis. The first of these conditions was that of a constant pressure drop across the test section. This was accomplished through the installation of a large bypass around the test section as sketched in Figure 13. With only about 5% of the total flow passing through the test section, the pressure drop was set primarily by the flow in the bypass and hence virtually independent of the test section flow. This was checked in the following way. With the bypass shut off, the test section pressure drop could be measured, under isothermal conditions, at various flow rates measured on the flowmeter. The bypass was then opened and the resistance of the test section line could be varied by means of a small valve installed just upstream. The flow to the test section could be inferred from a measurement of the pressure drop and the previous calibration. In addition, the overall pressure drop was measured. The results are shown in Figure 14, where it is seen that, with the bypass installed, a wide variation in the test section flow rate produces a change in the overall pressure drop of a very few percent.

During actual operation with heat addition, the test section flow rate was calculated from a heat balance as in Equation (3-1).

$$W_1 = \frac{4(L/D)(g/A)(\pi D^2/4)}{c_p(T_{ex.} - T_{in.})} \qquad (3\text{-}1)$$

As before, the test section flow rate was set at a relatively high value, and the exit pressure, inlet temperature, and heat flux were adjusted to the desired levels. All measurements were recorded, and then the test section flow rate was reduced by opening the valve on

the bypass. This was repeated, reducing the flow rate in small increments until an instability occurred. The onset of this instability was detected by the destruction of the test section. This occurs so rapidly that the instrumentation is unable to record any of the transient behavior. However, the significance of this burnout and what it means in terms of the predicted instability will be discussed in a later section.

3.3.4 Simulation of Compressible-Volume Oscillatory Instability

The other external system condition of interest was that of a compressible volume upstream of the test section. The data taken on this loop applicable to this condition was obtained by R. S. Daleas[29] under the supervision of Professor A. E. Bergles. The detailed description of his apparatus and experimental procedure may be found in Reference (29), but is reviewed briefly here. The experiments were performed on the basic loop described previously. The data were all taken on single tube geometries similar to the pressure drop test sections described here. The single exception was the presence of a compressible volume located just upstream of the test section and downstream of the flow control valve. Three distinct compressible volumes were used. Two of these were large brass tubes, mounted between ¼" brass end plates, and inserted directly in the test section line. They were filled at all times with water at the test section inlet temperature. The dimensions of these volumes are given in Table 3-1:

	C.V. I	C.V. II
Length (in.)	15.6	11.5
Inner Diameter (in.)	1.375	3.22
Volume ($in.^3$)	23.2	93.4

TABLE 3-1

The test section was fitted to the exit end plate by a Conax adapter. The flow control valve, connected directly to the upstream end plate, isolated the system from any additional compressibility further upstream. These compressible volumes were instrumented for measurements of temperature and pressure, and were also equipped with a vent for eliminating any trapped air pockets.

The third compressible volume was simply a 1/8" brass tee which was set in the line between the flow control valve and the test section and arranged so that the perpendicular leg would trap a small volume of air. This produced an equivalent compressibility equal to a rather large volume of subcooled water.

The data was taken at constant flow rate and increasing power until an instability occurred. Again this was detected by the destruction of the test section. For purposes of comparison, a number of tubes were burned out at similar conditions but without the compressible volumes present. A Dynisco strain-gage type pressure transducer was connected to the large compressible volume to see if any disturbances could be detected prior to burnout, but this proved to be unsuccessful. A sketch of the compressible volumes and the associated instrumentation is given in Figure 15.

CHAPTER IV

DISCUSSION OF RESULTS

The primary difficulty in any investigation of flow stability in boiling systems lies in the proper interpretation of the results once they are obtained. As noted in the discussion at the beginning of Chapter II which dealt with the choice of an analytical model, considerable care must be exercised in the application of information obtained on a particular system to the design and operation of other systems. This is due to the large number of mechanisms which can lead to instabilities in a boiling situation. In the following sections, the experimental and analytical results will be examined and compared. In addition, results of other investigators will be considered to see how they relate to the particular mechanism treated in this study. This will aid in determining the limitations on the usefulness of this investigation, since a knowledge of when the results are applicable to a particular situation is fully as necessary to the designer as the results themselves. In this light, the range of variables covered in the experimental program will be presented at the outset.

4.1 Range of Experimental Parameters

Insofar as the original motivation of the program was to provide information which might be applied to the design of cooling systems for high-performance electromagnets, the general range of interest was set, to a large degree, by magnet design considerations. The primary limitation, from this standpoint, was that of channel size. Since the production of a uniform field is a primary requirement, magnetic circuit considerations dictated the use of a large number of small passages

rather than fewer, but larger, ones. Therefore, the investigation is restricted to circular channels with a diameter less than ¼". Typical ranges for other variables are presented in Table 4-1.

1.	Coolant	Water
2.	Cooling Passages	Circular; $D_i < .25"$; $\frac{L}{D} \sim 25\text{-}250$
3.	Pressure Level	$p_{ex} < 80$ psia
4.	Inlet Temperature	$T_i \approx 70^{\circ}F$
5.	Velocity	$V_{in} = 5\text{-}50$ ft/sec
6.	Heat Flux	$(q/A) = .5\text{-}5 \times 10^6$ Btu/hr-ft^2
7.	Exit Conditions	$h_{ex} < h_{sat.liq.}$

TABLE 4-1

RANGE OF EXPERIMENTAL PARAMETERS

Within this range, the experimental program is further limited by the choice of tubing available from which to construct test sections and by the capacity of the power supply. The tubes chosen to cover the required range of diameters are given in Table 4-2.

I.D.	O.D.	Material	Resistance (Ω) per ft.
.0465	.0645	Type 304-Stainless steel	23.8×10^{-2}
.062	.120	"	4.42×10^{-2}
.094	.120	"	8.67×10^{-2}
.120	.250	"	1.18×10^{-2}
.1805	.2105	'A' Nickel	$.76 \times 10^{-2}$

TABLE 4-2

DIMENSIONS AND PROPERTIES OF TEST-SECTION TUBING

As the generators are limited to a maximum output of either 24 volts or 3000 amperes, a maximum heat flux can be computed for each tube diameter as a function of its length. This information is presented in tabular form in Table 4-3.

D ↓ / $\frac{L}{D}$ →	25	50	100	150	200
.047	5.5×10^6	13.8×10^6	3.45×10^6	1.53×10^6	$.86 \times 10^6$
.062	$70. \times 10^6$	44.7×10^6	11.17×10^6	4.96×10^6	2.79×10^6
.094	$25. \times 10^6$	6.30×10^6	1.58×10^6	$.70 \times 10^6$	$.40 \times 10^6$
.120	9.53×10^6	9.51×10^6	6.55×10^6	2.91×10^6	1.65×10^6
.180	4.22×10^6	4.21×10^6	2.90×10^6	1.29×10^6	$.72 \times 10^6$

TABLE 4-3

MAXIMUM HEAT FLUX - BTU/hr-ft^2

In order to keep the total amount of data taken from becoming too unwieldy, a representative range was selected on the basis of the power supply capacity. A geometry of ".094 I.D. and $\frac{L}{D}$ = 50 was chosen as a representative geometry to investigate the effect of varying thermodynamic parameters. (T_{in} = 70, 91.5, 113, and 134.5°F; p_{ex} = 15, 28 and 45 psig). Geometry effects were covered by testing tubes of ".062 I.D. for a range of $\frac{L}{D}$ = 25-200, while tubes of $\frac{L}{D}$ = 50 were tested at diameters of ".0465, ".062, ".094, ".120, and ".1805.

Of these, only selected cases were chosen to check the onset of instability in a constant pressure drop situation. The compressible volume tests were run primarily on short tubes ($\frac{L}{D} < 100$) and small diamters (D = ".0465 and ".094).

4.2 Pressure Drop vs. Mass Flow Rate

The results for the heated section pressure drop vs. mass flow rate are presented in Figures 16 through 33. An extensive investigation of pressure drop with surface boiling in small diameter tubes was recently completed on this project by Thomas Dormer, Jr.,[2] in which he found that a reasonable correlation of a large amount of data could be obtained by plotting the results in the manner shown in Figure 34. The parameters chosen were $\Delta p/\Delta p_{ADB}$, the ratio of the measured pressure drop to the pressure drop obtained in a similar tube under isothermal conditions at the same velocity and inlet temperature, and (q/A)/(q/A)sat., the ratio of the actual heat flux to that which would be required to produce a saturated exit condition. The use of these parameters eliminated all effects except geometry. The diameter is seen to have a small, but measurable, effect, whereas the length-to-diameter ratio is of prime importance. The correlation was found to be suspect when the velocities and heat fluxes covered by Dormer were greatly exceeded. It should also be noted that, in general, this data was taken at constant flow rate while varying heat flux. Cross-plotting of the data to obtain a Δp vs. w curve could not provide sufficiently detailed information in the vicinity of the minimum.

The salient features of the pressure drop vs. flow rate curves in Figures 16 through 33 are the following. At high flow rates, where the situation is one of pure forced-convection, the pressure drop falls below that of the isothermal case, due to variation in fluid properties, primarily viscosity, with temperature. A correlation for this range, in terms of a friction factor correction as suggested by Dormer[2],

is of the form

$$f/f_{iso} = (\mu_w/\mu_b)^{.35} \qquad (4\text{-}1)$$

As the flow rate is decreased, surface boiling commences, and a further decrease in the flow rate results in the curve's passing through a minimum pressure drop. It shall be noted that this minimum occurs at exit conditions which are well subcooled; typically of the order of $(T_{SAT} - T_b) = 50^{\circ}F$. At such a subcooling, visual studies have indicated that there is virtually no non-equilibrium void fraction present. Hence, the increase in pressure drop can not be attributed to a Bernoulli-type acceleration, but must be the result of increased wall friction caused by agitation at the wall where bubbles are growing and collapsing very rapidly. Curves of a similar nature have been obtained by Weiss[31] and others[32],[33].

A comparison of the measured results with those calculated through the aid of Dormer's correlation (Figure 34) are presented in most cases. It is seen that whereas precise determination of the minimum location is not possible by this means, the agreement is sufficiently good that this correlation may be used with a reasonable degree of confidence over most of the range. It will be employed extensively in a later section when the predicting of the onset of oscillatory instability will require the computation of the slope of the pressure drop vs. flow rate curve in the negatively sloping region.

An indication of the reproducibility of these data is given in Figure 35. Three separate runs are presented; two taken on the same test section and the same day, and a third taken on a different, though nominally identical, test section at another time. The maximum deviation is seen to be of the order of $\pm 3\%$ with most of the data falling nearer

to ±1%. This is considered to be sufficiently good agreement, so that distinctions between data taken on different test sections are unnecessary. The same test section was normally used, however, to obtain all of the data for a given geometry, unless burnout forced its replacement.

4.3 Onset of Excursive Instability

As derived in Appendix A, an excursive instability will occur when the slope of the heat exchanger pressure drop vs. flow rate curve becomes more negative than that of the external system. In the case investigated, an external system with a constant pressure drop (zero slope) characteristic was simulated as described in Section 3.3.3. Hence, the onset of an excursive instability is to be expected when the heat exchanger pressure drop vs. flow rate curve passes through a minimum. As has been seen, the heated section pressure drop does in fact possess such a minimum. However, the overall pressure drop seen by the external system is made up not only of the heated section pressure drop but two additional components: a sudden contraction entrance loss and a sudden expansion exit pressure change.

The first of these, the sudden contraction pressure drop, may be dealt with quite simply. At the entrance to the test section the flow is always single phase and means for computing the pressure drop may be found in any standard text. Rohsenow and Choi[30] gives the following expression:

$$\Delta P_{cont.} = \frac{\rho V^2_{in}}{2}(1 + K_c) \qquad (4\text{-}2)$$

where K_c for turbulent flow is a function only of the area ratio across the contraction. For the very small values ($A_{t.s.}/A_p < .05$) encountered

in this study a nominal value of $K_c = .5$ will be assumed, and the quantity of interest, the slope of the pressure drop vs. flow rate curve is

$$\frac{\partial (\Delta P_{cont})}{\partial Q} = \frac{1.5\rho Q}{A_F^2} \qquad (4\text{-}3)$$

The sudden expansion pressure change is far more complicated. Several investigators [34],[35],[36] have attempted to deal with this problem and have met with little success. A typical expression for the pressure rise across a sudden expansion in terms of the void fraction is given by Romie[37] as

$$\Delta P_{exp.} = \frac{-V_{ex}^2}{2} \left(\frac{A_F}{A_{PL.}}\right)\left(\frac{2}{1-\alpha}\right) \qquad (4\text{-}4)$$

For a typical geometry encountered in this study at a mass flow rate of $400 \frac{lbm}{hr.}$ ($V \approx 40$ ft./sec. for D = ".094") a void fraction of 50% would lead to a pressure rise of .92 psi. Measurements were attempted to verify this expression, and very bad scatter was obtained. The data presented in the literature[34] exhibits the same scatter. However, it was clear that for even the highest void fractions encountered in this program, the pressure change across the sudden expansion was always quite small (< 1 psi). In particular, at the high subcoolings present in the vicinity of the minimum, the sudden expansion contribution to the overall pressure drops was considered to be negligible. Therefore, the onset of an excursive instability in the constant pressure drop situation was compared to the location of the minimum of a pressure drop vs. mass flow rate curve made up of the sudden contraction pressure drop calculated from Equation (4-2) and the heated length pressure drop measured and presented in Figures 16

through 33. These comparisons are presented in Figures 36 through 38. The onset of the instability as mentioned previously was indicated by the destruction of the system. As may be seen, the agreement is excellent. This, of course, is not surprising since this particular mode of instability has long been recognized. It is of interest to note, however, that in all cases, it was possible to operate right down to the minimum. In other words, no other type of instability intervenes and causes a burnout in the positive sloping region to the right of the minimum.

In a few cases, stable burnout points obtained in a constant flow delivery system by Bergles[1] are superimposed on the curves showing the critical condition in a constant pressure drop system. It is seen that an excursion, and its attendant burnout, will often occur at heat fluxes equal to only 50% of those which might be expected from stable burnout predictions.

4.4 Onset of Compressible-Volume, Oscillatory Instability

As derived in Appendix B, an oscillatory instability will occur in a system with sufficient upstream compressibility if the slope of the pressure drop vs. flow rate curve reaches a certain critical negative value given in Equation 2-2. As described in Section 3.3.4, data was taken on the basic heat transfer loop in which a measurable amount of compressibility was introduced into the system in the form of a large volume of subcooled water just upstream of the heated section. The bulk of the data was taken with the largest compressible volume, a brass tank containing approximately 93 cubic inches of water. A comparison of the critical heat fluxes for identical situations with and without

the compressible volume present is shown for a variety of cases in Figures 39 through 45.

4.4.1 Data of Daleas[29]

A numerical evaluation of the critical slope required for an oscillatory instability as given by Equation 2-2, (see Appendix D) indicates that for the geometries and conditions investigated by Daleas[29], the 93 $in.^3$ compressible volume has essentially zero stiffness. As a result, the critical slope is equal to zero within the accuracy of the calculations. Figures 39 through 45 present scatter plots which compare the onset of the instability with the heat flux required to produce the predicted critical slope.

4.4.2 Method of Comparison of Measured and Predicted Results

The method used to predict the onset of an oscillatory instability is a combined numerical and graphical comparison of slopes and will be explained in some detail. A numerical example is given in Appendix D. The pertinent data taken and reported by Daleas[29] was the following:

1. inlet temperature
2. exit pressure
3. pressure in the compressible volume (steady-state)
4. mass velocity
5. critical heat flux
6. heated section length
7. tube diameter.

The difference between the pressure in the compressible volume and the exit pressure gave the overall pressure drop. A knowledge of the inlet temperature, exit pressure, mass velocity, geometry and heat flux combined with Dormer's correlation (Figure 34) was sufficient to

calculate the pressure drop in the heated section. The comparison between pressure drops in Figures 16 through 33 indicates that sufficient accuracy can be obtained in this way. The difference between the reported overall pressure drop and the calculated heated-length pressure drop was attributed to inlet losses. These losses were assumed to follow a "square law" resistance of the form

$$\Delta P_{in} = K_{in} Q^2 \tag{4-5}$$

and the constant, K, was evaluated at the reported flow rate and pressure drop. Heated section pressure drops were then calculated for flows slightly different from the actual, at the same exit pressure, inlet temperature, and heat flux. The slope of the resultant curve at the reported conditions was evaluated graphically. This slope, usually negative, was then added to the positive sloping contribution of the inlet fittings given by

$$\frac{\partial (\Delta P_{in})}{\partial Q} = 2K_{in} Q$$

If the sum of these slopes was equal to zero, representing a minimum in the overall pressure drop vs. flow rate curve, this was said to be the predicted onset of oscillatory instability. If the slope was not zero, then heat flux was changed slightly and the procedure repeated until the minimum corresponded to the reported flow rate.

In some cases, certain difficulties were encountered. Points at which the instability occurred near the saturation point or slightly above, were not always within the range of Dormer's correlation, and the heated-length pressure drop could not be evaluated. However, a wide representative sample of Daleas' reported points were tested,

and the comparison between the predicted onset of instability and the reported burnout is indicated in Figures 39 through 45. This particular method of presenting the comparison by means of scatter plots was chosen for the following reason. If the comparison were indicated as, for example, in Figure 39, there would be a great temptation to connect the points in a smooth curve and assume that this was a generally applicable correlation for the onset of oscillatory instability. However, as may been seen from the calculational procedure described in Appendix D, the location of the point of instability depends very strongly on the inlet fitting losses. Since identical heated section conditions could be attained for a number of inlet pressure losses, the predicted points have meaning only as related to a particular data point, and any curve fitting would be erroneous. It is only because all of the data were taken on the same apparatus, with the same inlet configuration, that the points appear to lie on a smooth curve.

On the basis of Figures 39 through 45, it may be stated that the correspondence between the predicted instability and the observed burnout is within calculational and experimental error. It should be noted that the experimental evidence of the instability was, in all cases, a sudden failure of the tube. A comparison between a typical frequency of oscillation and the thermal time constant of the tube indicates that failure might be expected on the first cycle. Certain differences in the appearance of the burned out test sections between the two cases of constant pressure-drop excursive burnout and the compressible volume oscillatory burnout indicate that the mechanisms were

quite different. In the excursive case, the tubes, after burnout, were quite ragged and showed evidence of overheating along most of their length. This is typical of burnouts caused by sudden flow starvation. The tubes which failed due to the presence of a compressible volume, on the other hand, exhibited a very clean break, with no evidence of overheating outside of a very narrow region on either side of the burnout location. In this respect they were similar to the ordinary, stable burnout tests.

The range of variables covered in this comparison includes mass velocities of $G = 2\text{-}10 \times 10^6 \frac{lbm}{hr\text{-}ft^2}$, $T_{in} = 75\text{-}180^oF$; $p_{ex} = 30\text{-}80$psia; $\frac{L}{D} = 25\text{-}100$; and $D = ".049\text{-}".246$. The agreement appears to be uniformly good with the exception of some of the lower flow rates. At $G = 2.23 \times 10^6 \frac{lbm}{hr\text{-}ft^2}$, the difference between the reported overall pressure drop and the calculated heated-length pressure drop was so small as to make the computation of the inlet losses quite inaccurate. In some cases, as shown in Figures 45 and 46 there was no measurable difference between the critical heat fluxes with and without the presence of the compressible volumes. A comparison of the slopes in these cases indicates that operation all the way down to burnout is stable, and the results are as expected.

Included in the data are runs taken with the brass tee described in Section 3.3.4 serving as the compressible volume. In this case as well, the compressibility is sufficiently great, (system soft enough) so that the critical slope is essentially zero. In the case of the small compressible volumes, however, the system has sufficient stiffness to require a negative slope of the overall pressure drop curve to

initiate the instability. This is evidenced by the fact that, as shown in Figure 39, the critical heat fluxes, although still well below those for stable burnout, are well above those for the case of the larger volume of the air-filled brass tee. A comparison of the critical slopes required to initiate oscillatory behavior in the two cases, is given in Figure 47. For the case of the smaller compressible volumes, a direct numerical comparison was not possible since the data lay outside the range in which the heated section pressure drop could be calculated accurately.

Direct verification of the foregoing conclusions was attempted for four particular cases at varying conditions. This was done by rerunning test sections identical to those which had been burned out in the absence of the compressible volume. The critical heat flux, flow rate, and thermodynamic conditions were reestablished and then, with all else held constant, the mass flow rate was varied while the overall pressure drop was measured. In each case, as shown in Figure 43, the critical conditions corresponded to the minimum in the pressure drop vs. flow rate curve to well within experimental error. The very close agreement in these cases lends further confidence to the results obtained with Dormer's[2] correlating procedure.

4.4.3 Data of Lowdermilk et al.[25]

In 1958, Lowdermilk, Lanzo and Siegel[25] reported results from low pressure burnout tests in which system stability was investigated. In particular, two sets of data are of interest to this discussion. The first of these was a comparison of burnout data taken in a stiff, well-throttled system with no compressible volume between the control valve and the heated section with data taken on the same system with

a highly compressible surge tank installed just upstream of the test section. A sketch of the configuration is shown in Figure 49, and a comparison of the two sets of data is displayed in Figure 50. A detailed sketch of the test section construction indicated that the only pressure drop downstream of the compressible volume other than the heated section was a simple, sudden contraction at the test section inlet. This was accounted for in the manner described in Section 4.3, and a prediction of the onset of compressible volume oscillations was made on the basis of requiring zero slope of the pressure drop vs. flow rate curve. This prediction is indicated in Figure 50 and a sample of the graphical comparison of slopes is shown in Figure 51 . The agreement is seen to be substantial. Again, at the very low flow rates, an accurate calculation of the pressure drops was impossible due to the inability to extrapolate the pressure drop correlation into the region of exit quality.

The second set of data dealt with the variations in the amount of pressure drop which had to be taken across the flow control valve in order to stabilize the system. Although in this particular set of runs, there was no deliberate attempt to insert a compressible volume in the system, the very nature of a blow-down system, along with the upstream piping and instrumentation, is sufficient to provide considerable compressibility. Figure 52 indicates that as the pressure drop across the throttle valve was increased, the critical heat flux also increased until a maximum value corresponding to stable burnout was attained. After this further throttling had no effect. The critical heat fluxes observed correspond to the predicted onset of instability in every

case for which a comparison was possible. As the heat flux increased at constant flow rate, exit quality was reached quite soon and no comparison could be made. An attempt to utilize the Martinelli-Nelson correlation[38] for cases with quality exit led to the prediction of heated length pressure drops which exceeded the reported overall pressure drop. This is apparently due to the small diameter tubes, since the Martinelli-Nelson correlation was based on data taken in large channels where the void fraction picture might be expected to be quite different. The occurrence of a minimum throttle-valve pressure drop required to completely stabilize the system is consistent with the picture presented here. As the slope of the valve pressure drop vs. flow rate curve becomes more and more steeply positive, a large negative slope is required in the heated section to produce a minimum in the overall pressure drop vs. flow rate curve. When this required negative slope exceeds that which can be obtained at stable burnout, the system is unconditionally stable in the sense that stable burnout will intervene before an oscillatory instability can be initiated.

4.4.4 Data of Aladiev et al.[26]

In 1960, data similar to that of Lowdermilk[25] was taken by a team of Russian investigators.[26] The range of variables was quite different in that they worked at very high pressure and temperature (p = 100atm, $T_{IN} \approx 350^{\circ}F$) and with larger diameter tubes (8mm I.D.). Here again, comparisons were made between critical heat fluxes with and without a compressible volume upstream of the test section. In all, three compressible volumes were tested.

The first of these consisted of a tank filled with water at 210°F, well below the corresponding saturation temperature and constituting a virtually incompressible medium. The second was also filled with water but at the saturation temperature. This resulted in about a twelve-fold increase in compressibility. In the third case, the expander was filled with highly compressible superheated steam or nitrogen. The results are shown in Figures 53 and 54, along with the predicted points of marginal stability based on a zero slope criterion. For comparisons at points when the fluid at exit was well subcooled, Dormer's correlation was used to evaluate the pressure drop. For points with quality at the exit, the Martinelli-Nelson[38] correlation was used. In this case, the tubes were of large enough diameter to permit the application of this method. It should be noted, as on Figure 55, that the slope of the pressure drop vs. flow rate curve was nearly zero for a wide range of flow rates in the vicinity of the tested flow. This made an accurate location of the minimum point quite difficult. As a result, considering the rather large scatter exhibited by the data anyway, a detailed calculation of each point was not attempted. Only a few representative points are indicated, but the agreement seems to be reasonable within these limitations. Whereas the correlation was intended primarily for subcooled boiling situations, in this particular case, with the high test pressures and the low flow rates and heat fluxes, only a very small degree of wall superheat is to be expected. This would, in all probability, rule out the occurrence of nucleation instabilities and leave the compressible volume instabilities as the dominant mechanism.

It is seen that in this investigation, a volume of subcooled water did not provide sufficient compressibility to initiate oscillatory behavior. This is at variance with the results of Daleas but is explainable in the following way. With the particular heated section geometry chosen by Aladiev, the inertias of the test sections are much lower than for Daleas' tubes. Hence, for an equivalent compressibility a steeper negative slope is required for instability. As pointed out before, the slope of the pressure drop vs. flow rate curve for Aladiev's conditions, although negative, is always very small, all the way down to stable burnout. Hence, in this case, the critical slope was never reached, and the tube burned out stably. For the other compressible volumes investigated, however, sufficient squishiness was present for the zero slope criterion to be applied.

4.4.5 Data of Todreas[39]

An investigation is currently underway in the M.I.T. Heat Transfer Laboratory to study high-quality burnout in vertical tubes with non-uniform heat flow. In the early stages, some uniform heat flux tubes were tested in order to check out the system. At some conditions, the tubes burned out at heat fluxes well below what was expected. Although no compressibility was deliberately inserted in the system between the control valve and the heated section, it was felt that enough compressibility was present upstream of the control valve in the form of preheaters and accumulators to initiate an instability should the slope of the overall pressure drop, including the control valve and the heated section, vs. flow rate curve go to zero. The suspect points were checked on this basis and this was found to be the

case. A comparison of the unstable points with the stable ones and the zero slope location is shown in Figure 56. A sample graphical comparison of the heated section pressure drop characteristic with that of the control valve is given in Figure 57. Similar calculations along with some experimental measurement were made on the points which were believed to be valid and the overall slope was established as positive. In all future tests, sufficient throttling was maintained to eliminate the possibility of unstable behavior.

4.4.6 Data of Andoh[40]

In a thesis recently concluded by Hiroshi Andoh[40], the problem of oscillatory instabilities in a very long (L/D = 600) heated tube was investigated. In this instance, the heat fluxes required for unstable behavior were sufficiently low that the tube did not fail at burnout; i.e., film boiling could be tolerated. This permitted measurement of the oscillatory frequency as well as the location of the point of marginal stability. A typical stability map is reproduced in Figure 58. If the flow rate is reduced at constant heat flux, it is seen that the onset of oscillatory behavior corresponds very closely to the point of minimum pressure drop. It was intended that the flow control valve be set immediately upstream of the heated section in order that the only compressibility present in the system would be that which is inherent in the heated length due to the formation of vapor, and in fact a great deal of the data was taken in this way. However, for the runs in which careful frequency measurements were recorded, an open-end manometer had been installed downstream of the control valve. With the system in this condition the compressibility inherent in the heated

length was entirely negligible compared to that of the manometer. Predictions of the frequency based on the compressibility of the manometer agree reasonably well with the experimental results as indicated in Figure 59.

It should be noted that when the flow rate was reduced to the point where the pressure drop vs. flow rate curve passed through its maximum and reentered a region of positive slope, the oscillations did not die out as would be predicted by the analysis. One possible explanation of this is related to the fact that although the tube as a whole is in a region of positive slope on the pressure drop vs. flow rate curve, there are portions of the tube near the upstream end which are still operating in a negatively sloping region. This gives rise to the possibility of one section's oscillating and driving the remainder of the tube. In this case, however, the single node lumped parameter approach is not sufficient to deal with the problem.

This point was not pursued further, however, since the main objective of this investigation was the prediction of the onset of unstable behavior. In any high heat flux system, these additional complexities would be precluded by tube failure at the minimum.

One salient feature of Andoh's work, however, is the conclusion that for sufficiently long test sections, the inherent compressibility of the vapor fraction is sufficient to produce compressible volume oscillations. This conclusion is strengthened by reference to Daleas' data in Figure 43 where a comparison of critical heat fluxes with and without the compressible volume present is shown plotted against length-to-diameter ratio. It is seen that for large L/D, the so-called

stable points occur at lower and lower heat fluxes and extrapolation by eye of the two curves would seem to indicate that they could merge at some given length.

4.4.7 Data of Stenning and Veziroglu[28]

A recent report by Stenning and Veziroglu[28] describes an experimental program in which three distinct types of oscillatory behavior are identified. These are referred to as "density wave," "pressure-drop," and "thermal" oscillations. Of interest to this investigation are the "pressure drop" oscillations in which a surge tank upstream of the heated section provides the mechanism for energy storage. These oscillations occur in a region of negative slope on the overall pressure drop vs. flow rate curve. The use of Freon-11 permitted the investigators to operate in the unstable region without destroying the test section. Figure 60 is reproduced from Figure 2 of their report. It is seen that the oscillations occur only over a certain portion of the negative sloping region. This is consistent with the requirement of a finite negative slope for the initiation of oscillations. Attempts to stabilize the system through the use of a throttle valve indicated that after stability was attained, some negative slope remained. Calculations indicate that the remaining negative slope was not sufficiently large to initiate instabilities. Estimates of the predicted period agree reasonably well with the reported values.

A discussion of the other modes of instability is outside the scope of this study, but it should be noted that the so-called "density wave" oscillations occur at flow rates just below those at which

pressure drop oscillations were encountered. In this particular case, the frequencies of the two phenomena were quite different and as a result it was easy to distinguish between them. However, one can easily imagine a situation, in a somewhat stiffer system, in which the two types of oscillations exhibit nearly the same frequency, and it would be difficult to differentiate between them by visual observations.

This comparison with the results of Stenning and Veziroglu[28] is perhaps the most significant of those presented here. In the other comparisons, the only verification of the analysis was the fact that burnout occurred when the slope of the pressure drop vs. flow rate curve became negative. It is possible to imagine that this prediction would result from a variety of physical models. However, the ability of this model to predict the oscillatory frequency with reasonable accuracy as well as the existence of stable behavior in certain negative sloping regions lends confidence to the modelling procedure.

4.4.8 Results of Quandt[18]

The results of this investigation are somewhat at variance with the conclusions presented by Quandt[18]. In his report, it is specifically stated that oscillatory instabilities will take place only in regions where the slope of the pressure drop vs. flow rate curve is positive. In an experimental program which simulated a constant pressure drop boundary condition, oscillatory behavior was found to take place to the right of the minimum. This was clearly the case, for if the minimum had been reached, the test section would have been

susceptible to excursive instability and burnout would have occurred. However, in this investigation, it was possible in all cases to operate right up to the minimum in a constant pressure drop situation without the onset of oscillatory behavior.

This apparent discrepancy is clearly due to the fact that entirely different mechanisms are involved. The oscillatory behavior observed by Quandt was apparently due either to nucleation instabilities in which energy was stored in superheated liquid or else due to rapid changes in flow resistance characteristics of the test section exit with quality which would correspond to the "density wave" phenomenon discussed by Stenning and Veziroglu[28]. This is consistent with the predictions of Quandt's[18] analysis which yields that $(\frac{\partial \rho}{\partial h})$ must be strongly negative for instability. For the range of temperatures and pressures involved, this condition arises well before the occurrence of the minimum in the pressure drop vs. flow rate curve. As a result, the type of instability dealt with in this study is not the dominant mechanism even when sufficient compressibility is present. However, for situations involving subcooled boiling and high heat fluxes, the minimum in the pressure drop vs. flow rate curve occurs at very high values of subcooling when $(\frac{\partial \rho}{\partial h})$, though negative, is nearly zero.

4.4.9 Results of Pulling and Collier[41]

Pulling and Collier in some preliminary experiments to investigate two-phase flow instabilities obtained results which are much the same as those of Quandt[18]. That is, oscillatory behavior occurs in regions where the slope of the pressure drop vs. flow rate curve is positive. Very nearly the same comments as made in connection with

Quandt's investigation apply here. The onset of "density wave" instabilities would preclude the occurrence of a compressible volume type of oscillation even if sufficient compressibility were available. Here it was found that if net quality was maintained at the inlet to the test section, stable conditions were obtained. This would appear to be consistent with Quandt's prediction since $(\frac{\partial \rho}{\partial h})$ would be most negative if a transition from subcooled conditions to bulk boiling were to take place in the heated section itself. Although it is to be expected that, in the absence of these density wave oscillations, the compressible volume phenomenon would again be the dominant mechanism, the conditions of the test were such that a negative sloping region of the pressure drop vs. flow rate curve was never reached. Hence, no definite conclusion can be drawn.

4.4.10 Results of Bertoletti et al.[42]

Some qualitative comments can be made concerning some data on the effect of inlet orificing taken by Bertoletti et al.[42] at CISE. In this case, certain points were found to burn out at unexpectedly low heat fluxes. This condition was eliminated by the use of inlet orificing. Since these points occurred at exit qualities of 2-4%, this effect was attributed to a flow pattern instability or slug flow. However, the inlet fluid was well subcooled, and it is not clear how additional inlet orificing would prevent slug flow if this were in fact the problem. It seems more likely that additional orificing served to eliminate a negative sloping portion of the pressure drop vs. flow rate curve. Unfortunately, there is not sufficient information presented in the report to either confirm or reject this contention.

4.5 Choked Flow Considerations

In a two-phase flow the sonic velocity can be quite low, as demonstrated by Gouse and Brown[43]. Hence, the question always arises in investigations of this kind as to whether or not the flow was choked. This could clearly give rise to additional stability problems. A recent paper by Fauske[44] gives criteria for the onset of choking based on a known exit quality under conditions of thermodynamic equilibrium. Although it is not possible to perform such a calculation for the case of subcooled boiling, one method of presenting his result in terms of a critical pressure ratio vs. length-to-diameter ratio is shown in Figure 62. It was possible to measure these quantities experimentally in the vicinity of the minimum, and, as indicated in Figure 62, the flow was never choked.

CHAPTER V

SUMMARY OF CONCLUSIONS

5.1 Conclusions

The conclusions of this investigation may be summarized as follows:

1. An important class of unstable behavior in forced-convection boiling systems can be dealt with by a linearized, lumped-parameter analysis with an upstream compressible volume as the energy storage element.

2. Steady-state measurements of the pressure drop vs. flow rate curve may be used to describe the unsteady behavior with sufficient accuracy to draw meaningful conclusions concerning system stability.

3. In a parallel channel system where the plenum-to-plenum pressure drop seen by an individual channel is constant, the excursive instability is the dominant mechanism at subcooled or low-quality conditions. The instability will occur at the minimum in the overall pressure drop vs. mass flow rate curve.

4. In a single tube system, for a known supply system characteristic, and for a known amount of compressibility upstream of the heated section, a critical slope of the overall pressure drop vs. mass flow rate curve can be computed for the initiation of oscillatory instability. The associated frequency may also be calculated.

5. For certain geometries such as very small heated sections operating at high heat flux levels, the amount of compressibility required

for unstable behavior is surprisingly small (of the order of a few cubic inches of cold water is sufficient).

6. When the compressible volume is external to the test section, this instability can always be eliminated by sufficient throttling between the compressible volume and the heated section.

7. In cases of very long test sections ($L/D > 150$), there can be sufficient compressibility inherent in the test section itself due to vapor generation to initiate this type of instability. In this case, no amount of external throttling will be of any value.

8. The criterion is primarily intended for use with subcooled or very low quality conditions. In high quality situations, the compressible volume oscillation is very likely to be precluded by "density-wave" instabilities. Hence, even a design which satisfies the stability requirements for the compressible volume mechanism cannot be termed unconditionally stable.

APPENDIX A

Derivation of Excursive Instability

In this section, the details of the derivation of the mechanism of an excursive instability are presented. The heated section, chosen to conform generally with the geometry encountered in a typical, axial-flow electromagnet, is shown schematically in Figure A-1. The overall pressure drop is seen

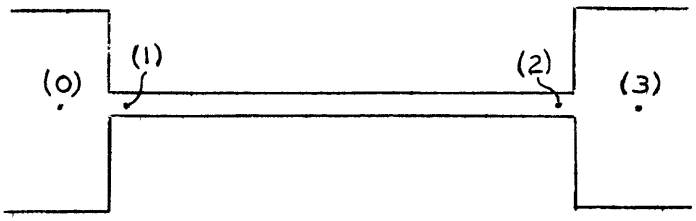

Schematic of Heated Section
Figure A-1

to be made up of three components:

1. a single-phase, sudden contraction (Δp_{0-1})
2. the heated section pressure drop (Δp_{1-2})
3. a two-phase, sudden expansion (Δp_{2-3}).

Imposed upon this heated section is some flow-delivery system which can be characterized by an imposed pressure drop given as some function (Δp_{ext}) of the volume flow rate.

If the inertia of the heated length is included, a force balance across the test section is given by

$$\Delta p_{ext}(Q) = \Delta p_{0-1}(Q) + \Delta p_{1-2}(Q) + \Delta p_{2-3}(Q) + \left(\frac{\rho L}{A}\right)_{1-2} \frac{dQ}{dt} \qquad \text{(A-1)}$$

where $Q \equiv w/\rho$

A small perturbation analysis may be performed by looking at a flow rate slightly different from the equilibrium, steady flow condition as follows:

$$Q = Q_o + \Delta Q \tag{A-2}$$

The resulting equation, to first order terms, is given by

$$\Delta p_{ext}(Q_o) + \frac{\partial(\Delta p_{ext})}{\partial Q}\Delta Q = \Delta p_{o-1}(Q_o) + \Delta p_{1-2}(Q_o) + \Delta p_{2-3}(Q_o) + \frac{\partial}{\partial Q}(\Delta p_{o-1} + \Delta p_{1-2} + \Delta p_{2-3})\Delta Q + \tag{A-3}$$

$$(\rho L/A)_{1-2}\frac{d}{dt}(Q_o + \Delta Q)$$

Subtracting out the steady-state terms yields

$$\frac{\partial(\Delta p_{ext})}{\partial Q}\Delta Q = \frac{\partial}{\partial Q}(\Delta p_{o-1} + \Delta p_{1-2} + \Delta p_{2-3})\Delta Q + \left(\frac{\rho L}{A}\right)_{1-2}\frac{d\Delta Q}{dt} \tag{A-4}$$

Performing a LaPlace transform in t, with the following definitions

$$\widetilde{\Delta Q} \equiv \mathcal{L}(\Delta Q) \equiv \int_0^\infty e^{-st}\,dt \tag{A-5}$$

yields

$$\frac{\partial(\Delta p_{ext})}{\partial Q}\widetilde{\Delta Q} = \frac{\partial}{\partial Q}(\Delta p_{o-1} + \Delta p_{1-2} + \Delta p_{2-3})\widetilde{\Delta Q} + \left(\frac{\rho L}{A}\right)_{1-2} s\,\widetilde{\Delta Q} \tag{A-6}$$

or

$$s = \frac{1}{(\rho L/A)_{1-2}}\left[\frac{\partial(\Delta p_{ext})}{\partial Q} - \frac{\partial}{\partial Q}(\Delta p_{o-1} + \Delta p_{1-2} + \Delta p_{2-3})\right] \tag{A-7}$$

The requirement for stability is that "s" be negative, or that

$$\left[\frac{\partial(\Delta p_{ext})}{\partial Q} - \frac{\partial}{\partial Q}(\Delta p_{o-1} + \Delta p_{1-2} + \Delta p_{2-3})\right] \leq 0 \tag{A-8}$$

APPENDIX B

Derivation of Oscillatory Instability

In this section, a description of the model formulated to analyze the case of an oscillatory instability will be given and the mathematical details of this analysis presented. As in the case of the excursive instability, a lumped parameter model will be utilized. A schematic of the model of the flow loop is shown in Figure B-1.

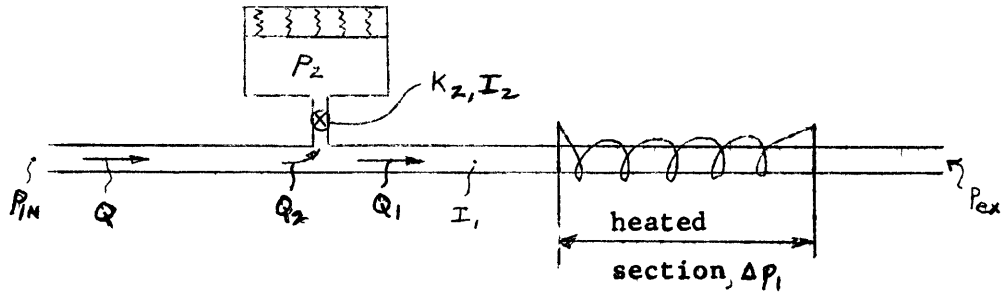

Schematic of Model for Analysis of
Oscillatory Instabilities

Figure B-1

The essential elements of the modelling procedure are the following.

1. The external system is characterized by the inlet and exit pressures seen by the heat exchanger. The exit pressure is considered to be constant, while the inlet pressure varies as an arbitrary function of the total flow rate; i.e., $p_{in} = p_{in}(Q)$. (For example, a constant flow delivery system is characterized by $\frac{\partial p_{IN}}{\partial Q} = -\infty$; a constant pressure drop system by $\frac{\partial p_{IN}}{\partial Q} = 0$.

2. The energy storage mechanism is assumed to be that of a compressible volume upstream of the test section.

3. The pressure drop across the heat exchanger section, $\Delta p_1(Q)$, includes, as in Appendix A, all of the steady-state pressure drops between the compressible volume and the downstream, constant pressure plenum; i.e., the heated section as well as any valves, pipes, sudden contractions and expansions, etc. It is assumed in doing this that $\Delta p_1(Q)$ may be determined from steady-state measurements.

4. The model includes the effects of inertia in the test section and in the fluid entering the compressible volume.

5. The flow resistance between the entrance plenum and the compressible volume is characterized by a "square-law" resistance. ($\Delta p = KQ^2$).

Within this framework, the equations of motions are applied to the model in the following way:

1. <u>Flow through the Test Section</u> (Q_1)

The flow through the test section is given by

$$P_{in} - P_{ex} = \Delta P_1(Q_1) + \left(\frac{\rho L}{A_F}\right)\frac{dQ_1}{dt} \qquad \text{(B-1)}$$

Since p_{in} is a function of the total flow to the heat exchanger, this may be written as

$$P_{in}(Q) - P_{ex} = \Delta P_1(Q_1) + I_1\frac{dQ_1}{dt} \qquad \text{(B-2)}$$

2. <u>Flow to the Compressible Volume</u>

The flow to the compressible volume is given by

$$P_{in}(Q) - P_2 = K_2 Q_2^2 + I_2\frac{dQ_2}{dt} \qquad \text{(B-3)}$$

3. Definition of Inertia

The inertia terms are evaluated in the following way. If Newton's Second Law is applied to a control volume around a fluid flowing in a pipe, as sketched in Figure B-2,

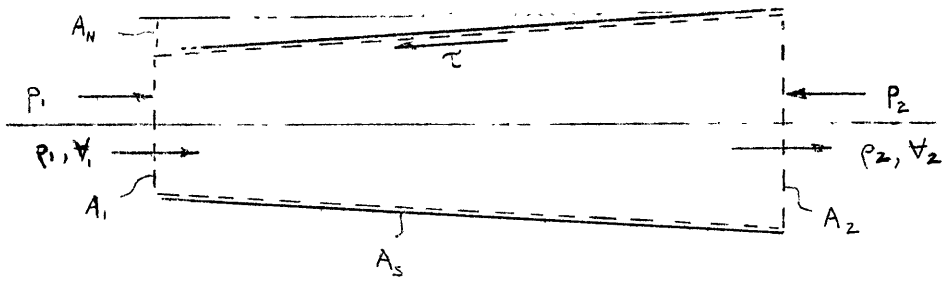

Control Volume for Definition of Inertia

Figure B-2

the resultant equation is

$$P_1 A_1 - P_2 A_2 - \int_0^L p\,dA_n - \tau A_s = \iiint \frac{\partial}{\partial t}(\rho \forall)\,dV + (\rho \forall A)_2 - (\rho \forall A)_1 \qquad \text{(B-4)}$$

For a constant area pipe, $A_1 = A_2$ and $A_N = 0$. Therefore, Equation (B-4) reduces to

$$P_1 - P_2 = \left[\frac{\tau A_s}{A_1} + P_2 \forall_2 - P_1 \forall_1\right] + \frac{1}{A_1}\iiint \frac{\partial}{\partial t}(\rho \forall)\,dV \qquad \text{(B-5)}$$

For nearly incompressible flow, ρ = constant and $\forall_1 \simeq \forall_2$. Hence,

$$P_1 - P_2 = \frac{\tau A_s}{A_1} + \frac{\rho}{A_1}\frac{\partial}{\partial t}(\forall A_1 L) \qquad \text{(B-6)}$$

Defining $Q = \forall A$

$$P_1 - P_2 = \frac{\tau A_s}{A_1} + \frac{\rho L}{A_1}\frac{\partial Q}{\partial t} \qquad \text{(B-7)}$$

In the steady state $\left(\frac{\tau A_s}{A_1}\right)$ may be characterized as $\Delta p(Q)$ and

$$I \equiv (\rho L / A)$$

4. Pressure in Compressible Volume

As previously stated, the energy storage mechanism is characterized by a compressible volume upstream of the test section. Therefore, if the initial pressure and volume are given by p_o and V_o, the pressure at any time may be expressed as

$$P_2 = P_o + \left(\frac{dP}{dV}\right)_o \Delta V \tag{B-8}$$

The instantaneous volume may be computed by integrating the volume flow into the compressible volume over time; thus

$$\Delta V = -\int_o^t Q_2\, dt \tag{B-9}$$

Combining (B-8) and (B-9) gives an expression for the pressure in the compressible volume at any time t.

$$P_2 = P_o - \left(\frac{dP}{dV}\right)_o \int_o^t Q_2\, dt \tag{B-10}$$

5. Continuity Considerations

The continuity equation for the system, assuming an incompressible fluid is given simply by

$$Q = Q_1 + Q_2 \tag{B-11}$$

6. Steady-State

The equations describing the steady-state behavior of the system are:

$$\begin{aligned} P_{IN}(Q) - P_{ex} &= \Delta P_1(Q_1) \\ P_{IN}(Q) - P_2 &= K_2 Q_2^2 \\ Q_2 = 0;\quad Q = Q_1;\quad P_2 &= P_o \end{aligned} \tag{B-12}$$

Manipulation of the preceding equations yields the following description of the system

$$P_{in}(Q) - P_{ex} = \Delta P_1(Q_1) + I_1 \frac{dQ_1}{dt} \tag{B-13}$$

$$P_{in}(Q) - P_o + \left(\frac{dP}{dV}\right)_o \int_o^t Q_2 dt = K_2 Q_2^2 + I_2 \frac{dQ_2}{dt} \tag{B-14}$$

Small Perturbation Solution

The equations may now be written for small perturbations around a steady-state flow.

$$\begin{aligned} Q &= Q_o + \Delta Q \\ Q_1 &= Q_o + \Delta Q_1 \end{aligned} \tag{B-15}$$

From Equation (B-11)

$$Q_2 = \Delta Q - \Delta Q_1 \tag{B-16}$$

In conjunction with the small perturbation assumption, Equation (B-10) may be written as

$$P_2 = P_o - \left(\frac{dP}{dV}\right)_o \int_o^t (\Delta Q - \Delta Q_1)\, dt \tag{B-17}$$

Equations (B-13) and (B-14) now become

$$P_{in}(Q_o) + \frac{\partial (P_{in})}{\partial Q} \Delta Q - P_{ex} = \Delta P_1(Q_o) + \frac{\partial (\Delta P_1)}{\partial Q} \Delta Q_1 + I_1 \frac{d}{dt}(Q_o + \Delta Q_1) \tag{B-18}$$

$$P_{in}(Q_o) + \frac{\partial (P_{in})}{\partial Q} \Delta Q - P_o + \left(\frac{dP}{dV}\right)_o \int_o^t Q_2 dt = K_2 Q_2^2 + I_2 \frac{dQ_2}{dt} \tag{B-19}$$

Subtracting out the steady-state terms and retaining only the first power terms in ΔQ, ΔQ_1 and Q_2 yields,

$$\frac{\partial(P_{IN})}{\partial Q}\Delta Q = \frac{\partial(\Delta P_1)}{\partial Q}\Delta Q_1 + I_1 \frac{d}{dt}\Delta Q_1 \tag{B-20}$$

$$\frac{\partial(P_{IN})}{\partial Q}\Delta Q + \left(\frac{dP}{dV}\right)_o \int_o^t (\Delta Q - \Delta Q_1)\, dt = I_2 \frac{dQ_2}{dt} \tag{B-21}$$

Eliminating Q_2 through the use of Equation (B-16) gives

$$\frac{\partial(P_{IN})}{\partial Q}\Delta Q = \frac{\partial(\Delta P_1)}{\partial Q}\Delta Q_1 + I_1 \frac{d}{dt}\Delta Q_1 \tag{B-22}$$

$$\frac{\partial(P_{IN})}{\partial Q}\Delta Q + \left(\frac{dP}{dV}\right)_o \left[\int_0^t \Delta Q\, dt - \int_o^t \Delta Q_1\, dt\right] = I_2\left[\frac{d}{dt}\Delta Q - \frac{d}{dt}\Delta Q_1\right] \tag{B-23}$$

Performing a LaPlace transform on this system of equations where

$$\widetilde{\Delta Q} \equiv \mathcal{L}(\Delta Q) \equiv \int_o^\infty e^{-st}\Delta Q\, dt$$

and

$$\widetilde{\Delta Q}_1 \equiv \mathcal{L}(\Delta Q_1) \equiv \int_o^\infty e^{-st}\Delta Q_1\, dt$$

the following set of transformed equations is obtained.

$$\frac{\partial(P_{IN})}{\partial Q}\widetilde{\Delta Q} = \frac{\partial(\Delta P_1)}{\partial Q}\widetilde{\Delta Q}_1 + I_1 s\,\widetilde{\Delta Q}_1 \tag{B-24}$$

$$\frac{\partial(P_{IN})}{\partial Q}\widetilde{\Delta Q} + \left(\frac{dP}{dV}\right)_o \frac{1}{s}\left[\widetilde{\Delta Q} - \widetilde{\Delta Q}_1\right] = I_2 s\left[\widetilde{\Delta Q} - \widetilde{\Delta Q}_1\right] \tag{B-25}$$

Eliminating $\widetilde{\Delta Q}$ leads to the following characteristic, polynomial equation in the LaPlace variable, s.

$$\frac{\partial(P_{IN})}{\partial Q}\left[\frac{\frac{\partial(\Delta P_1)}{\partial Q} + sI_1}{\frac{\partial(P_{IN})}{\partial Q}}\right] + \left(\frac{dP}{dV}\right)_o \frac{1}{s}\left[\frac{\frac{\partial(\Delta P_1)}{\partial Q} + sI_1}{\frac{\partial(P_{IN})}{\partial Q}} - 1\right] = I_2 s\left[\frac{\frac{\partial(\Delta P_1)}{\partial Q} + sI_1}{\frac{\partial(P_{IN})}{\partial Q}} - 1\right] \tag{B-26}$$

Rearranging yields

$$s^3\left[\frac{I_1 I_2}{\frac{\partial(P_{IN})}{\partial Q}}\right] + s^2\left[I_2\left(\frac{\frac{\partial(\Delta P_1)}{\partial Q}}{\frac{\partial P_{IN}}{\partial Q}} - 1\right) - I_2\right] + s\left[-\frac{\partial(\Delta P_1)}{\partial Q} - \left(\frac{dP}{dV}\right)_o \frac{I_1}{\frac{\partial P_{IN}}{\partial Q}}\right] + \left[-\left(\frac{dP}{dV}\right)_o\left(\frac{\frac{\partial(\Delta P_1)}{\partial Q}}{\frac{\partial(P_{IN})}{\partial Q}} - 1\right)\right] = 0 \tag{B-27}$$

The case for marginal stability may be investigated in the following way. For a third order expression of the form

$$as^3 + bs^2 + cs + d = 0$$

marginal stability will result when $s = j\omega$. This yields

$$-aj\omega^3 - b\omega^2 + cj\omega + d = 0$$

and implies the conditions that

$$\omega^2 = \frac{d}{b} \quad ; \quad \frac{c}{a} = \frac{d}{b}$$

Setting $\frac{c}{a} = \frac{d}{b}$ determines the value of $\frac{\partial(\Delta P_1)}{\partial Q}$ which will result in a marginally stable system for any arbitrary external characteristic, $\frac{\partial(P_{1N})}{\partial Q}$. Performing this operation results in,

$$\frac{\partial(\Delta P_1)}{\partial Q} = \frac{\frac{\partial(P_{1N})}{\partial Q}(I_1 + I_2) \pm \sqrt{\left(\frac{\partial P_{1N}}{\partial Q}\right)^2 (I_1 + I_2)^2 + 4I_1^2 I_2 (dP/dV)_o}}{2I_2} \qquad \text{(B-28)}$$

Of the two solutions, only the + sign solution is of interest, since it will always occur first in any real system. With this result, the frequency is given by

$$\omega^2 = \frac{d}{b} = \frac{c}{a} = \frac{-\left(\frac{\partial(P_{1N})}{\partial Q}\right)\left(\frac{\partial(\Delta P_1)}{\partial Q}\right) - (dP/dV)_o I_1}{I_1 I_2} \qquad \text{(B-29)}$$

Substituting the expression for $\frac{\partial(\Delta P_1)}{\partial Q}$ from Equation (B-28) gives

$$\omega^2 = \frac{-\left(\frac{\partial(P_{1N})}{\partial Q}\right)^2 (I_1 + I_2) - \left(\frac{\partial P_{1N}}{\partial Q}\right)\sqrt{\left(\frac{\partial(P_{1N})}{\partial Q}\right)^2 (I_1 + I_2)^2 + 4I_1^2 I_2 \left(\frac{dP}{dV}\right)_o} - 2I_1 I_2 (dP/dV)_o}{2I_1 I_2^2} \qquad \text{(B-30)}$$

APPENDIX C - SAMPLE DATA SHEET

D = ".094" $A_F = 4.82 \times 10^{-5}$ ft^2 Heated Length = 50 D = 4.70" $A_H = 9.65 \times 10^{-3}$ft^2 Distance between pressure taps: $L_{\Delta p}$ = 4.80"

RUN NO	1 D (in.)	2 L/D —	3 Scale —	4 W (lbm/hr)	5 V (ft/sec)	6 P_{in} (psig)	7 P_{ex} (psig)	8 ΔP (psi) (6-7)	9 MAN. (scale read.)	10 ΔP (in. Hg)	11 ΔP (psi)	12 T_{in} (mv.)	13 T_{ex} (mv.)	14 T_{in} (°F)	15 T_{ex} (°F)	16 ΔT (°F) (15-14)	17 q ($\frac{BTU}{hr}$) (16 x 4)	18 $V_{T.S.}$ (volts)	19 $V_{SH.}$ (mv)	20 I (amps) (19x(60.17)	21 q ($\frac{BTU}{hr}$)	22 (q/A) ($\frac{BTU}{hr\text{-}ft^2}$)
2-6-64 - 2 - A	.094	50	79.0	323.	29.8	21.0	15.0	6.0	6.02/6.26	12.30	5.60	.47	1.81	53.5	113.0	59.5	19,200	14.05	6.55	394.	18,900	2.0×10^6
- B			58.5	240.	22.2	18.9	15.0	3.9	3.94/4.16	8.10	3.69	.47	2.31	53.5	134.0	80.5	19,250	14.10	6.53	393.	18,900	2.0
- C			49.0	201.	18.6	19.0	15.0	4.0	3.70/3.90	7.60	3.46	.47	2.66	53.5	148.0	94.5	19,000	14.15	6.51	391.	18,900	2.0
- D			39.3	160.	14.8	17.8	15.0	2.8	2.63/2.77	5.40	2.46	.47	3.25	53.5	172.0	118.5	18,950	14.15	6.51	391.	18,900	2.0
- E			34.0	138.	12.8	17.8	15.0	2.8	2.35/2.51	4.86	2.21	.47	3.67	52.5	188.5	135.0	18,650	14.15	6.51	391.	18,900	2.0
- F			33.0	134.	12.4	17.8	15.0	2.8	2.60/2.70	5.30	2.41	.47	3.84	53.5	195.0	141.5	18,950	14.15	6.51	391.	18,900	2.0
2-6-64 - 3 - A	.094	50	58.5	240.	22.2	24.4	15.0	5.4	5.60/5.88	11.48	5.23	.53	3.38	56.5	177.0	120.5	28,900	12.60	7.90	484	29,050	3.0×10^6
- B			55.0	225.	20.9	20.9	15.0	5.9	5.82/6.10	11.92	5.43	.53	3.55	56.5	184.0	127.5	28,700	12.60	7.90	484	29,050	3.0
- C			49.8	204.	18.9	22.0	15.0	7.0	7.08/7.40	14.48	6.89	.53	3.89	56.5	197.0	140.5	28,700	12.60	7.90	484	29,050	3.0
- D			67.0	275.	25.5	21.0	15.0	6.0	5.85/6.13	11.98	5.46	.53	2.99	56.5	161.0	104.5	28,750	12.55	7.91	485	29,050	3.0
- E			61.0	251.	23.3	20.2	15.0	5.2	5.60/5.85	11.45	5.22	.53	3.05	56.5	172.0	115.5	29,000	12.60	7.90	484	29,050	3.0
- F			59.5	245.	22.7	20.2	15.0	5.2	5.55/5.78	11.33	5.16	.53	3.33	56.5	175.0	118.5	29,050	12.60	7.90	484	29,050	3.0

APPENDIX D

Sample of Calculational Procedure

In the following section, a sample calculation is presented which will serve to clarify the procedure used to predict the onset of an oscillatory instability.

The particular point selected for purposes of illustration is Run 2-9 from Daleas.[29] The data reported was the following:

$D = ".047$

$L/D = 24.7$

$G = 4.47 \times 10^6 \frac{lbm}{ft^2\text{-}hr}$

$(q/A)\ crit. = 2.84 \times 10^6 \frac{BTU}{ft^2\text{-}hr}$

$\Delta p_1 = 9.8\ psi$

$p_{ex} = 29.9\ psia$

$T_{in} = 155^oF$

Heated Section Pressure Drop

The first step involves the calculation of the heated section pressure drop for a number of flow rates in the vicinity of the reported flow rate.

$$\Delta p = \Delta p_{ADB}\left(\frac{\Delta p}{\Delta p_{ADB}}\right) \qquad \text{(D-1)}$$

where

$$\left(\frac{\Delta p}{\Delta p_{ADB}}\right) = f\left(\frac{(g/A)}{(g/A)_{sat.}}\right)$$

from Figure 34.

$$\Delta p_{ADB} = 4f\frac{L}{D}\frac{\rho V^2}{2} \qquad \text{(D-2)}$$

where

$$f = f(Rey)$$

$$Rey \equiv \frac{\rho \forall_D}{\mu} \qquad (D\text{-}3)$$

Numerically for $G = 4.47 \times 10^6 \frac{lbm}{ft^2\text{-}hr}$; $\mu = 1.0 \frac{lbm}{ft\text{-}hr}$ @ 155^oF

$$Rey = \frac{(4.47 \times 10^6)(.047)}{(12)(1.0)} = 17,500$$

$$f = .0069 \qquad \text{(Fig. 4-1; Ref. 30)}$$

$$\Delta P_{ADB} = \frac{4(.0064)(24.7)(4.47 \times 10^6)^2}{2(62.4)(32.2)(3600)^2(144)} = 1.82 \text{ psi}$$

$$(q/A)_{sat.} = \frac{G c_p (T_{sat.}^{ex.} - T_{in})}{4(L/D)} \qquad (D\text{-}4)$$

Numerically

$$(q/A)_{sat.} = \frac{(4.47 \times 10^6)(1.0)(250-155)}{4(24.7)} = 4.30 \times 10^6 \frac{BTU}{hr\text{-}ft^2}$$

$$(q/A)/(q/A)_{sat.} = \frac{2.84 \times 10^6}{4.30 \times 10^6} = .66$$

From Fig. 34

$$(\Delta p/\Delta P_{ADB}) = 2.9$$

$$\Delta p = (1.32)(2.4) = 5.3 \text{ psi}$$

For other flow rates.

G	ΔP_{ADB}	$(q/A)/(q/A)_{sat.}$	$\Delta p/\Delta P_{ADB}$	Δp
4.47×10^6	1.82	.66	2.9	5.3
4.0×10^6	1.46	.74	4.7	6.9
5.0×10^6	2.28	.58	2.1	4.8

The difference between the calculated and reported values of the overall pressure drop is attributed to the inlet fittings.

$$\Delta P_{IN} = 9.8 - 5.3 = 4.5 \text{ psi}$$

This is assumed to be a "square-law" resistance, and

$$\Delta P_{IN} = K_{IN} G^2 \tag{D-5}$$

$$\frac{\partial \Delta P_{IN}}{\partial G} = 2 K_{IN} G = \frac{2(\Delta P_{IN})}{G} \tag{D-6}$$

Numerically

$$\frac{\partial \Delta P_{IN}}{\partial G} = \frac{2(4.5)}{4.47 \times 10^6} = 2.02 \times 10^{-6} \frac{\text{psi}}{\text{lbm/ft}^2\text{-hr}}$$

This slope is then compared graphically to that of the heated section

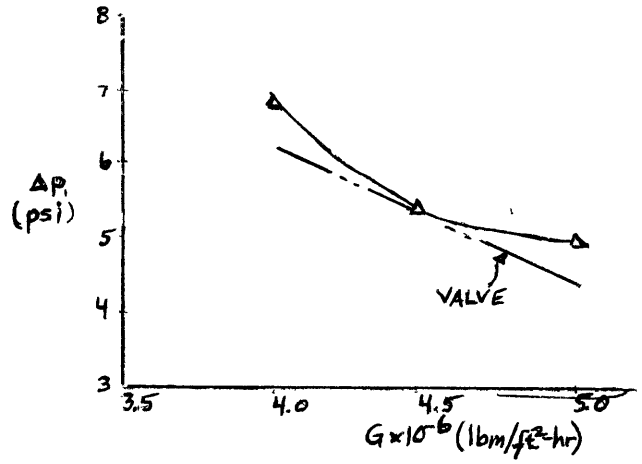

FIGURE D-1

Comparison of Slopes

and, since they are seen to be equal and opposite, this corresponds to the point where

$$\frac{\partial(\Delta P)}{\partial Q} = 0$$

It remains to insure that the critical slope required for the onset of an oscillatory instability is nearly zero.

From equation (B-28)

$$\frac{\partial(\Delta p_1)}{\partial Q} = \frac{\left(\frac{\partial p_{IN}}{\partial Q}\right)(I_1+I_2) + \sqrt{\left(\frac{\partial p_{IN}}{\partial Q}\right)^2 (I_1+I_2)^2 + 4I_1^2 I_2 (dp/dV)_o}}{2I_2}$$

For this case

$$I_1 >> I_2$$

and the external system characteristic is effectively set by the control valve just upstream of the compressible volume. Therefore

$$\frac{\partial p_{IN}}{\partial Q} = -2K_{vp}Q_o$$

$$\frac{\partial(\Delta p_1)}{\partial Q} = \frac{-(2K_{vp}Q_o)I_1 + (2K_{vp}Q_o)I_1\sqrt{1 + \frac{4I_1^2 I_2 (dp/dV)_o}{(2K_{vp}Q_o)^2 I_1^2}}}{2I_2}$$

It can be shown that

$$\frac{4I_2(dp/dV)_o}{(2K_{vp}Q_o)^2 I_1^2} << 1$$

so

$$\left.\frac{\partial(\Delta p_1)}{\partial Q}\right|_{crit.} = \frac{I_1(dp/dV)_o}{(2K_{vp}Q_o)}$$

By definition

$$I_1 = \left(\frac{\rho L}{A_F}\right)_1 = 5.26 \times 10^5 \ \frac{lbm}{ft^4}$$

$$Q_o = \frac{GA_F}{\rho} = .862 \ ft^3/hr.$$

$(dp/dV)_o$ may be evaluated from the compressed liquid tables and

$$(dp/dV)_o = -6.0 \times 10^6 \ \frac{psi}{ft^3}$$

$(2K_{up}Q_0)$ is evaluated by assuming the control valve to obey a square law resistance

$$\Delta p_{up} = K_{up} Q_o^2$$

$$\frac{\partial \Delta p_{up}}{\partial Q_o} = 2 K_{up} Q_o = \frac{2 \Delta p_{up}}{Q_o}$$

The reported value of Δp_{up} = 155 psi, so

$$(2 K_{up} Q_o) = \frac{2(155)}{.862} = 3.6 \times 10^2 \ \frac{psi}{ft^3/hr}$$

$$\left.\frac{\partial(\Delta p_1)}{\partial Q}\right|_{crit.} = \frac{(5.26 \times 10^5)(6 \times 10^6)}{(3.60 \times 10^2)(32.2)(144)(3600)^2} = .146 \ \frac{psi}{ft^3/hr} = 2.35 \times 10^{-3} \ \frac{psi}{lbm/hr}$$

Hence for $A_F = 1.2 \times 10^{-5} ft^2$, and for $\Delta G = 10^6$ lbm/ft^{2}hr

$$\Delta(\Delta p_1) = .028 \text{ psi} \approx 0.$$

BIBLIOGRAPHY

1. Bergles, A. E. and Rohsenow, W. M., "Forced-Convection Surface-Boiling Heat Transfer and Burnout in Tubes of Small Diameter," Report No. 8767-21, Dept. of Mech. Eng., Mass. Inst. of Tech., May 25, 1962.

2. Dormer, T. Jr., and Bergles, A. E.. "Pressure Drop with Surface Boiling in Small-Diameter Tubes," Report No. 8767-31, Dept. of Mech. Eng., Mass. Inst. of Tech., Sept. 1, 1964.

3. Bergles, A. E.. "Subcooled Burnout in Tubes of Small Diameter," ASME Paper No. 63-WA-182, 1963.

4. "Kinetic Studies of Heterogeneous Water Reactors," RWD-RL-190, Annual Summary Report for Ramo-Woolridge, Space Technology Laboratories, Inc., Los Angeles, Dec. 30, 1960.

5. Griffith, P.. "Geysering in Liquid Filled Lines," ASME Paper No. 62-HT-39, 1962.

6. Moissis, R. and Griffith, P.. "Entrance Effects in a Two-Phase Slug Flow," J. Heat Transfer, Trans. ASME, Series C, 84, 1962.

7. Griffith, P. and Wallis, G. B.. "Two-Phase Slug Flow," J. Heat Transfer, Trans. ASME, Series C, 84, 1961.

8. Haberstroh, R. D. and Griffith, P.. "The Transition from the Annular to the Slug Flow Regime in Two-Phase Flow," Report No. 5003-28, Dept. of Mech. Eng., Mass. Inst. of Tech., June 1964.

9. Tippetts, F.E.. "Critical Heat Fluxes and Flow Patterns in High Pressure Boiling Water Flows," ASME Paper No. 62-WA-162, Nov. 1962.

10. Wallis, G. B. and Heasley, J. H.. "Oscillations in Two-Phase Flow Systems," J. Heat Transfer, Trans. ASME, Series C, 83, 1961.

11. Wissler, E. H., Isbin, H. S., and Amundson, N. R.. "Oscillatory Behavior of a Two-Phase Natural-Circulation Loop," J. AIChE, 2, #2, 1956.

12. Beckjord, E. S.. "Dynamic Analysis of Natural Circulation Boiling Water Power Reactors," ANL-5799, March, 1958.

13. Fleck, J. A., Jr.. "The Dynamic Behavior of Boiling Water Reactors," J. Nucl. Energy, Part A, 11, 1960.

14. McGowan, E. J. and Bodoia, J. R.. "An Investigation of Stability in a Glass Model Steam Generator," Bettis Technical Review, Dec. 1962.

15. Ledinegg, M.. "Instability of Flow During Natural and Forced Circulation," Die Wärme, 61, # 8, 1938; AEC-tr-1861, 1954.

16. Markels, M.. "Effects of Coolant Flow Orificing and Monitoring on Safe Pile Power," Chem. Eng. Progress, Symp. Ser., 19, 73, 1956.

17. Chilton, H.. "A Theoretical Study of Stability in Water Flow through Heated Passages," J. Nucl. Energy, 5, 1947.

18. Quandt, E. R.. "Analysis and Measurement of Flow Oscillations," Preprint #27, Presented at the Fourth National Heat Transfer Conf., Buffalo, 1960.

19. Meyer, J. E. and Rose, R. P.. "Application of a Momentum Integral Model to the Study of Parallel Channel Boiling Flow Oscillations," ASME Paper No. 62-HT-14.

20. Meyer, J. E.. "Hydrodynamic Models for the Treatment of Reactor Thermal Transients," Nucl. Sci. Eng., 10, 1961.

21. Meyer, J. E. and Reinhardt, E. A.. "A Small Perturbation Approach to the Study of Parallel Channel Boiling Flow Oscillations," WAPD-TM-342, 1963.

22. Jones, A. B.. "Hydrodynamic Stability of a Boiling Channel," KAPL-2170, Oct. 1961.

23. Bick, J. H.. "A New Method for Determining the Stability of Two-Phase Flows in Parallel Heated Channels with Application to Nuclear Reactors," WAPD-TM-210, Dec. 1959.

24. Anderson, R. P. et al.. "An Analogue Simulation of the Transient Behavior of Two-Phase Natural Circulation Systems," Chemical Engineering Progress, Symposium Series, 41, Vol. 59, (Houston) 1963.

25. Lowdermilk, W. H., Lanzo, C. D., and Siegel, B. L.. "Investigation of Boiling Burnout and Flow Stability in Tubes," NACA-TM-4382, Sept. 1958.

26. Aladiev, I. T., Miropolsky, Z. L., Doroschuk, V. E., and Styrikovich, M. A.. "Boiling Crisis in Tubes," Int. Heat Transfer Conf., Publ. by ASME, 1961.

27. Gouse, S. W., Jr., and Andrysiak, C. D.. "Flow Oscillations in a Closed Loop with Transparent, Vertical Heated Channels," Report No. 8973-2, Dept. of Mech. Eng., Mass. Inst. of Tech., June, 1963.

28. Stenning, A. H., and Veziroglu, T. N.. "Flow Oscillation Modes in Forced-Convection Boiling," NASA Grant NSG-424, Report No. 6, Dept. of Mech. Eng., Univ. of Miami, Jan. 1965.

29. Daleas, R. S.. "Effect of an Upstream Compressibility on Subcooled Burnout in Tubes of Small Diameter," Nuclear Engineer Thesis, Dept. of Nuclear Engineering, Mass. Inst. of Tech., Sept. 1964.

30. Rohsenow, W. M., and Choi, H.. "Heat, Mass and Momentum Transfer, Englewood Cliffs, New Jersey: Prentice-Hall Inc., 1961.

31. Weiss, D. H.. "Pressure Drop in Two-Phase Flow," ANL-4916, Oct. 1952.

32. Kennel, W. E. "Local Boiling of Water and Superheating of High Pressure Steam in Annuli," Sc.D. Thesis, Dept. of Chemical Engineering, Mass. Inst. of Tech., 1948.

33. Jens, W. H. and Lottes, P. A.. "Analysis of Heat Transfer, Burnout, Pressure Drop, and Density Data for High Pressure Water," ANL-4627, May 1, 1951.

34. Straub, L. B., and Silberman, E.. "Air-Water Mixture Flow Through Orifices, Bends, and Other Fittings in a Horizontal Pipe," St. Anthony Falls Hydraulic Laboratory, Univ. of Minnesota, Proj. Rep. No. 63, Sept. 1963.

35. Richardson, B. L.. "Some Problems in Horizontal Two-Phase, Two-Component Flow," ANL-5949, Dec. 1958.

36. Lottes, P. A.. "Expansion Losses in Two-Phase Flow," Nucl. Sci. and Eng.: 9, 1961.

37. Described in: Lottes, P.A.. "Expansion Losses in Two-Phase Flow," Nucl. Sci. and Eng., 9, 26-31, 1961.

38. Martinelli, R. C., and Nelson, D. B.. "Prediction of Pressure Drop During Forced-Circulation Boiling of Water," Trans. ASME, 70, 1948.

39. Todreas, N. E.. "The Effect of Non-Uniform, Axial Heat Flux Distributions on High-Quality Burnout," ScD. Thesis, Dept. of Nuclear Engineering, Mass. Inst. of Tech., (in progress; to be completed Sept. 1965).

40. Andoh, H.. "Discharge Flow Oscillations in a Long Heated Tube," S. M. Thesis, Dept. of Mech. Engineering, Mass. Inst. of Tech., August 1964.

41. Pulling, D. J., and Collier, J. G.. "Instabilities in Two-Phase Flow: Preliminary Experiments," AERE-M-1105, Atomic Energy Research Establishment, Harwell, England, 1963.

42. Bertoletti, S., et al.. "Heat Transfer Crisis in Steam-Water Mixtures," Report No. R-90, CISE, Milan, June 1964.

43. Gouse, S. W., Jr., and Brown, G. A.. "A Summary on the Velocity of Sound in Two-Phase Mixtures," ASME Paper No. 64-WA/FE-35.

44. Fauske, H.K. "Two-Phase Critical Flow," Notes from Special Summer Program on Two-Phase Gas-Liquid Flow, Mass. Inst. of Tech., July 1964.

FIGURES

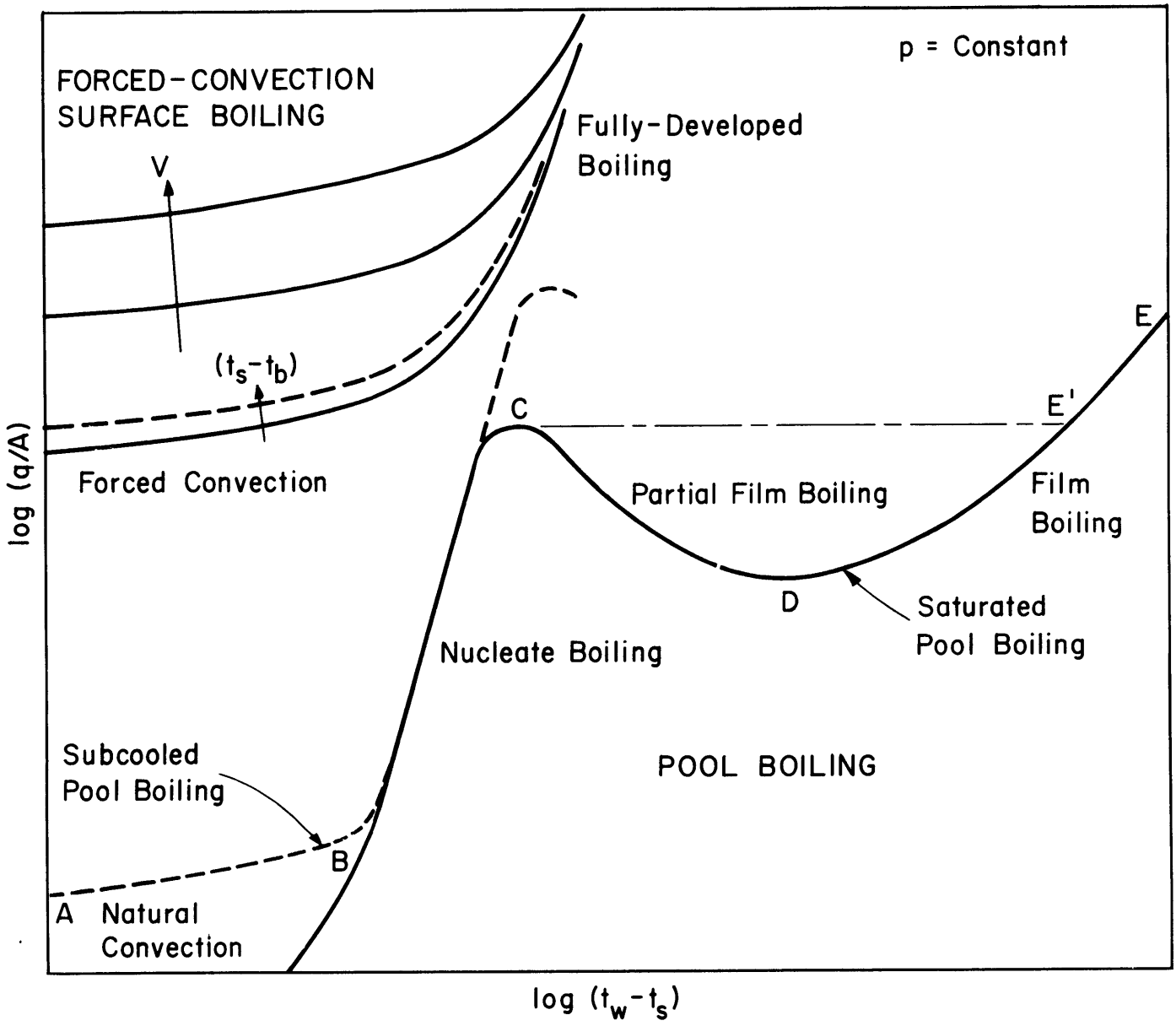

FIGURE 1: REGIMES IN BOILING HEAT TRANSFER

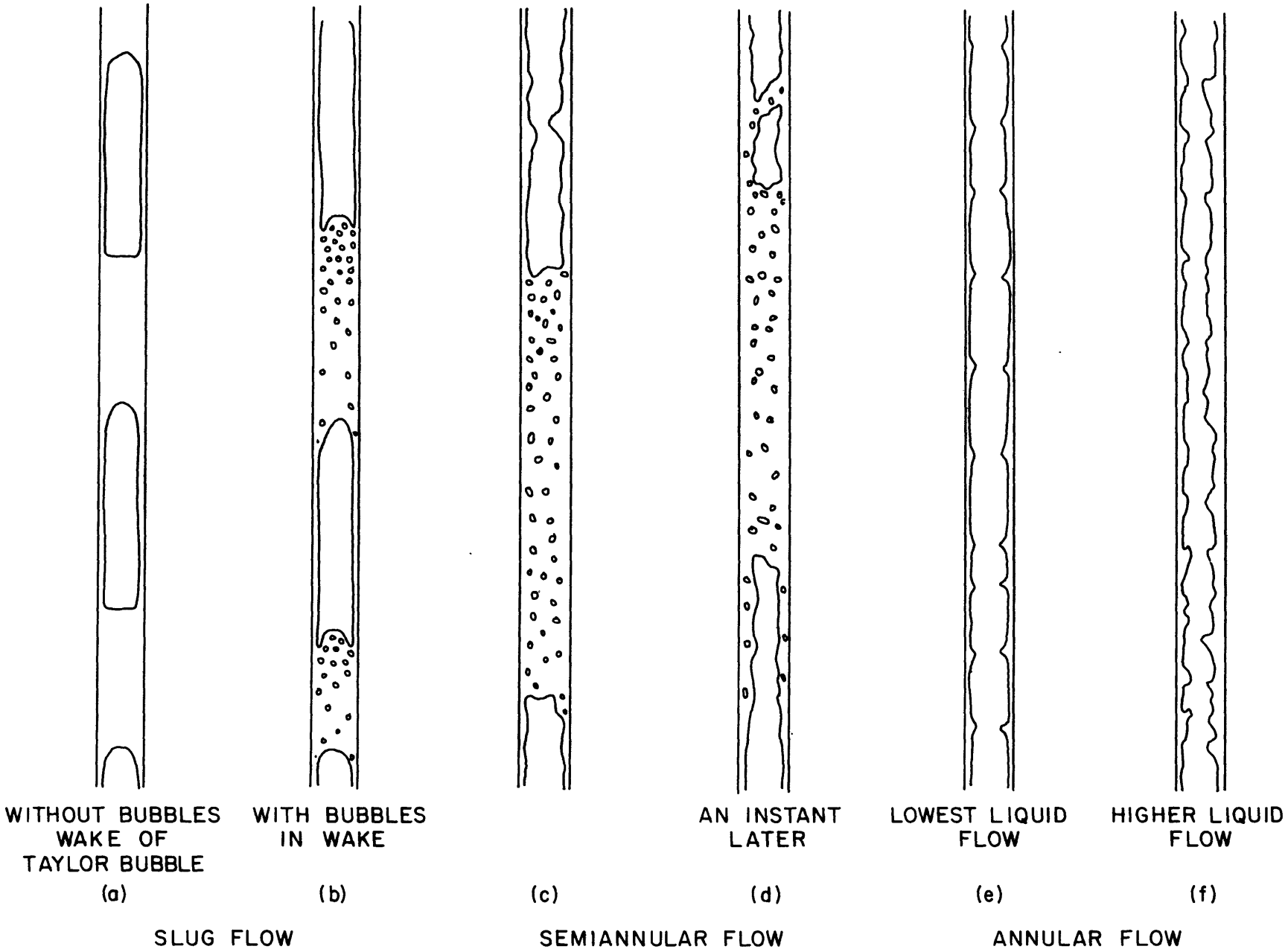

FIGURE 2: SKETCHES OF VARIOUS FLOW-REGIME GEOMETRIES

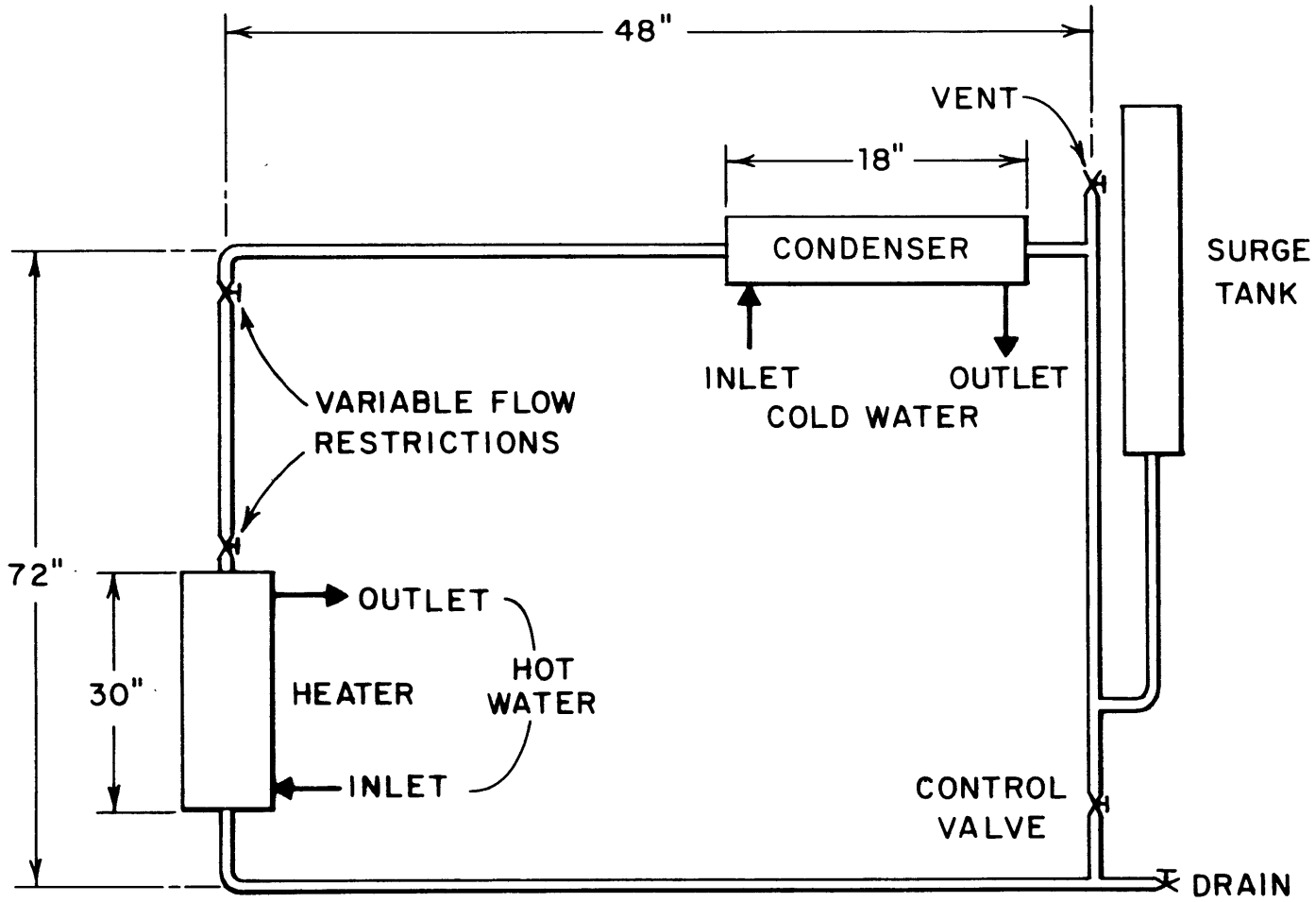

FIGURE 3: SKETCH OF NATURAL CIRCULATION LOOP (FROM WALLIS & HEASLEY[10])

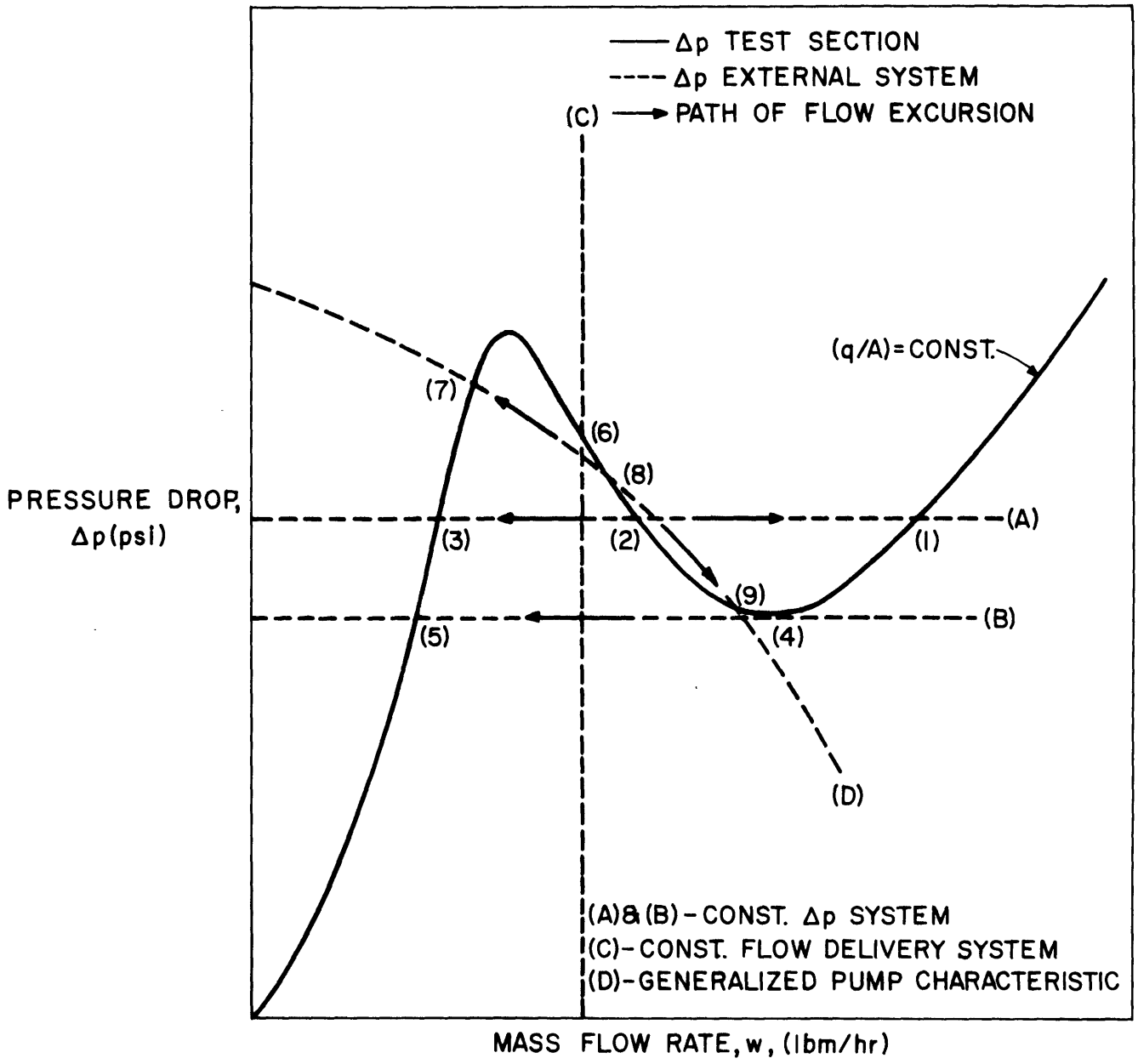

FIGURE 4: GRAPHICAL INTERPRETATION OF EXCURSIVE INSTABILITY

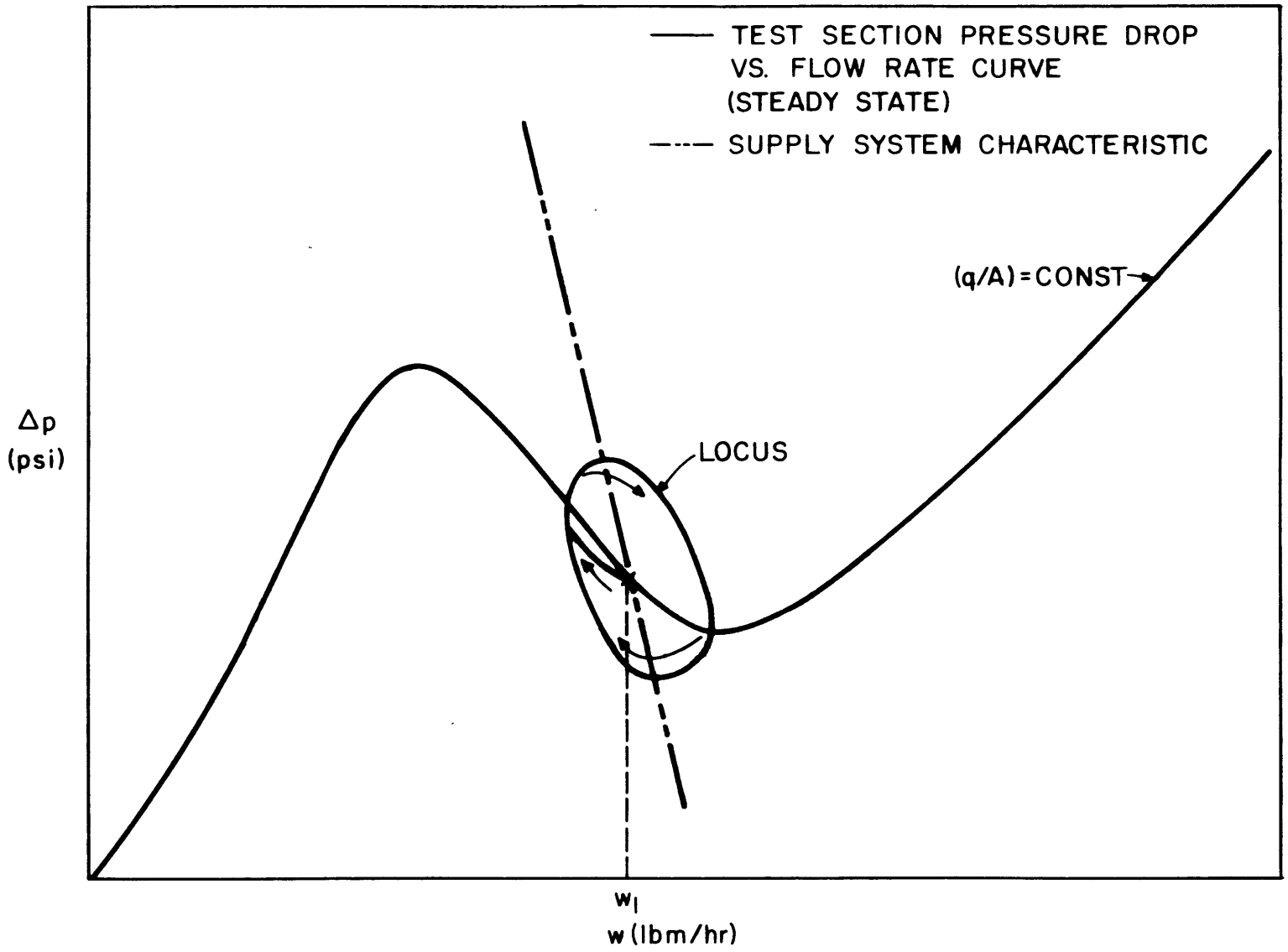

FIGURE 5: LOCUS OF OPERATING POINTS IN OSCILLATORY MODE

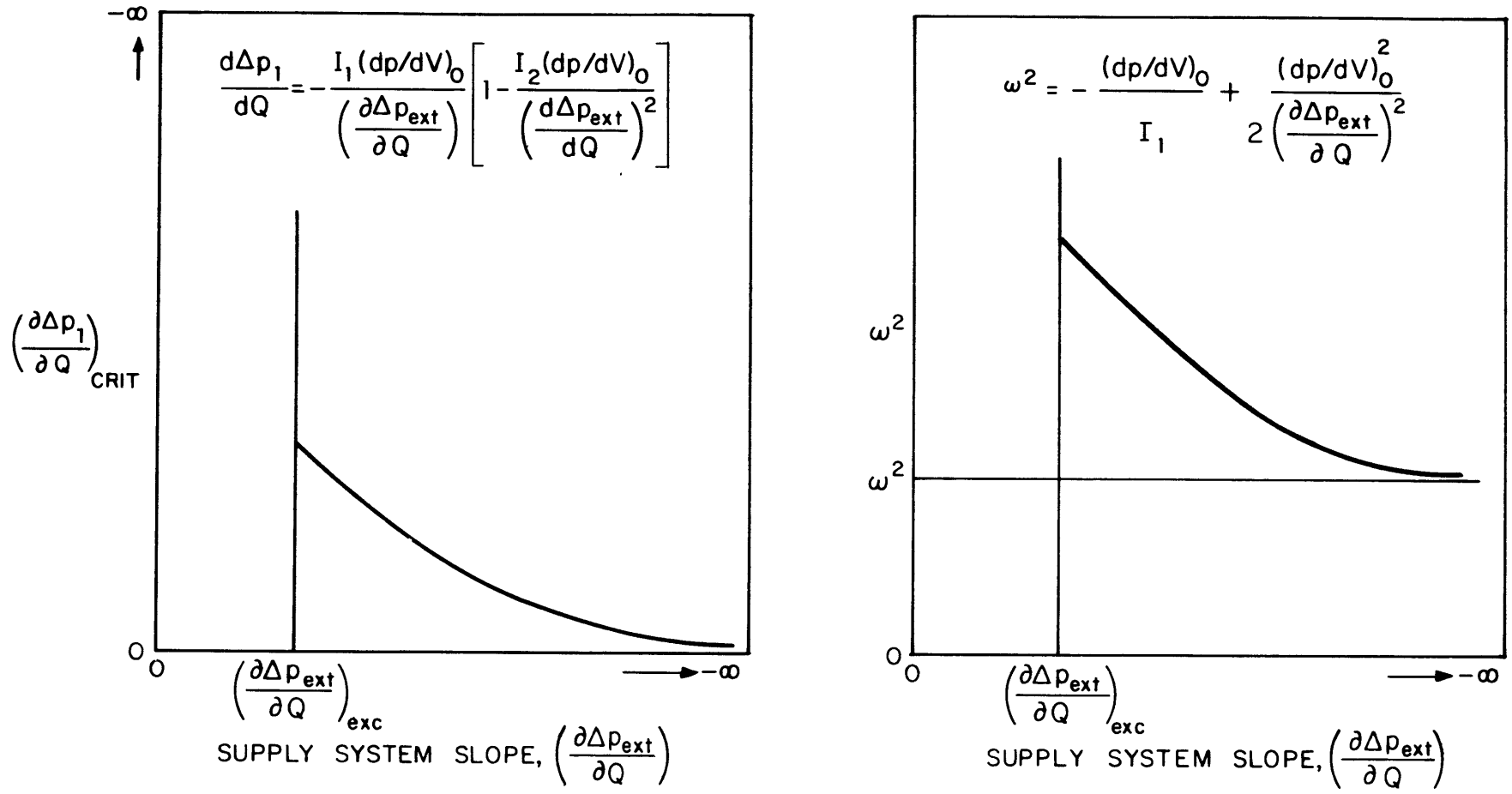

FIGURE 6: VARIATIONS IN CRITICAL SLOPE AND FREQUENCY WITH CHARACTERISTIC OF SUPPLY SYSTEM

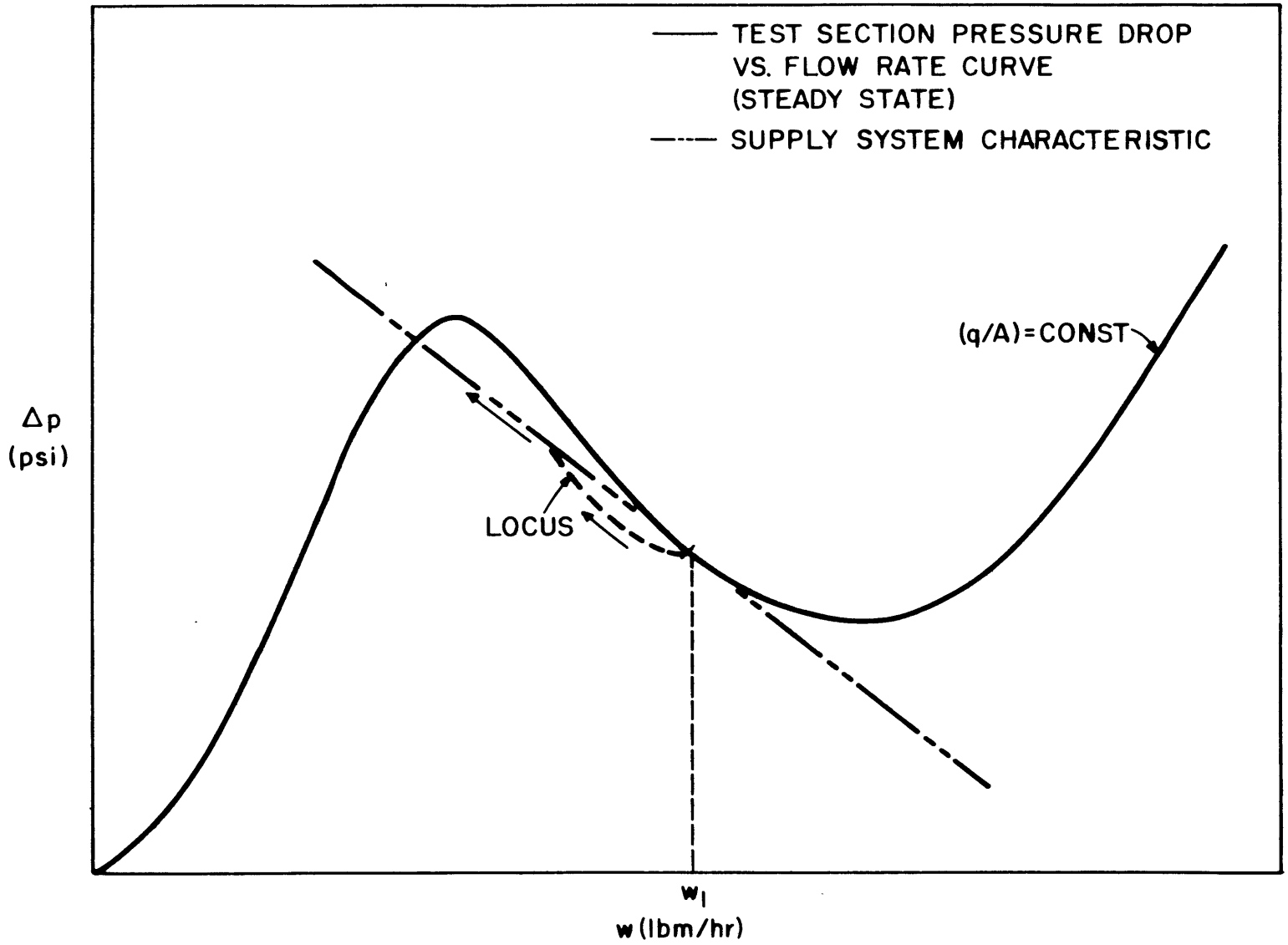

FIGURE 7: LOCUS OF EXCURSION WITH COMPRESSIBLE VOLUME

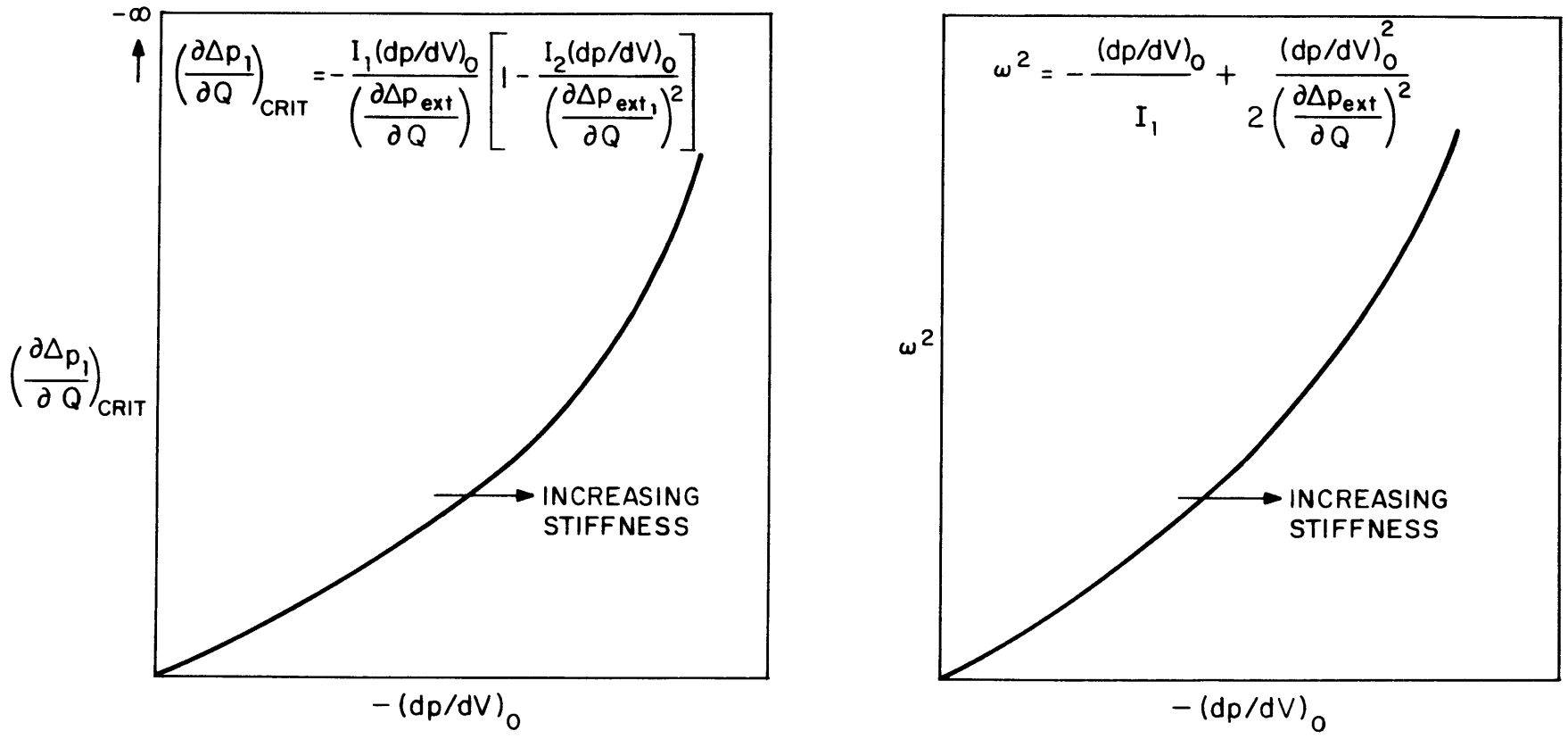

FIGURE 8: VARIATIONS IN CRITICAL SLOPE AND FREQUENCY WITH STIFFNESS OF COMPRESSIBLE VOLUME

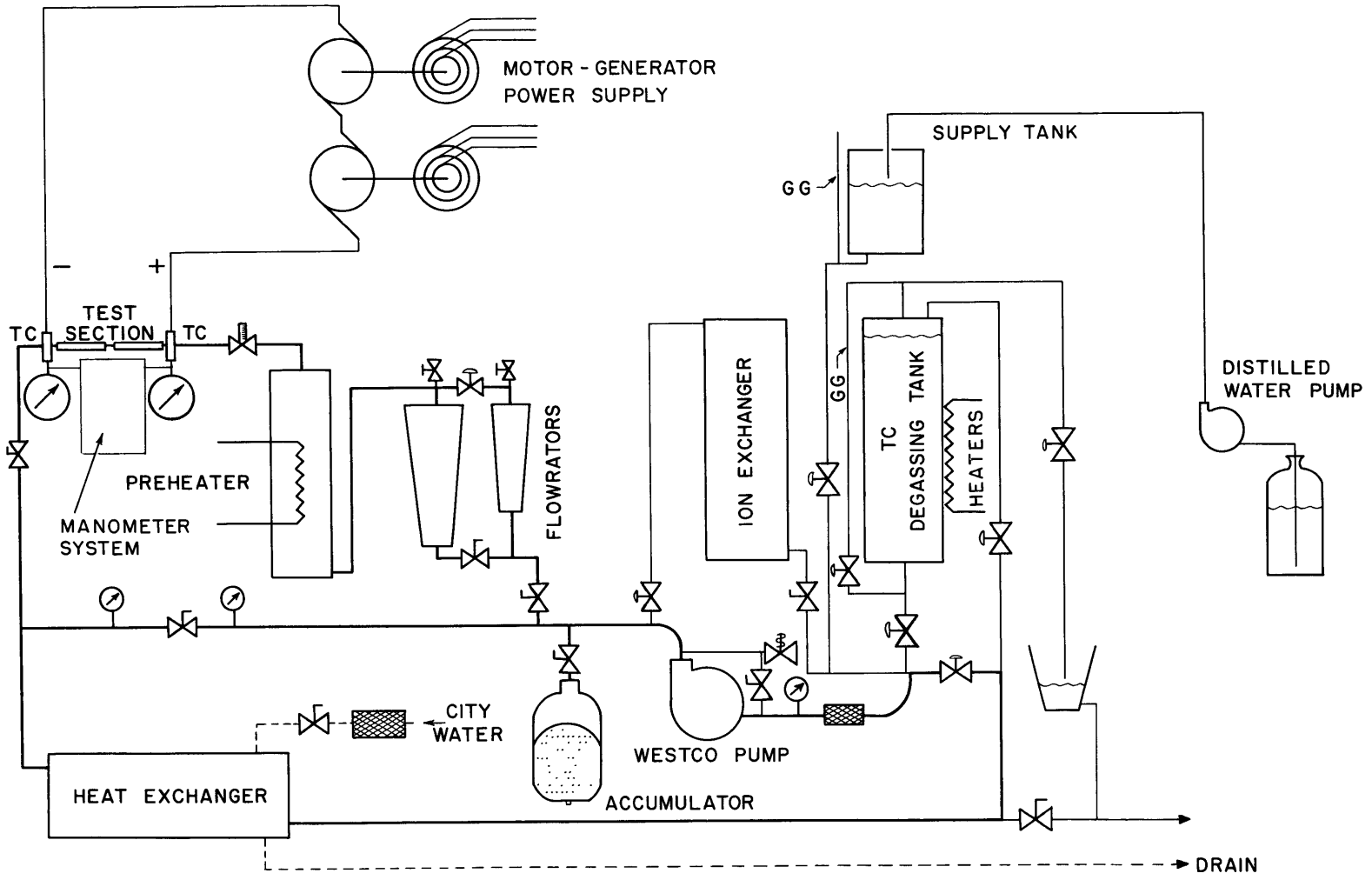

FIGURE 9: SCHEMATIC LAYOUT OF EXPERIMENTAL FACILITY

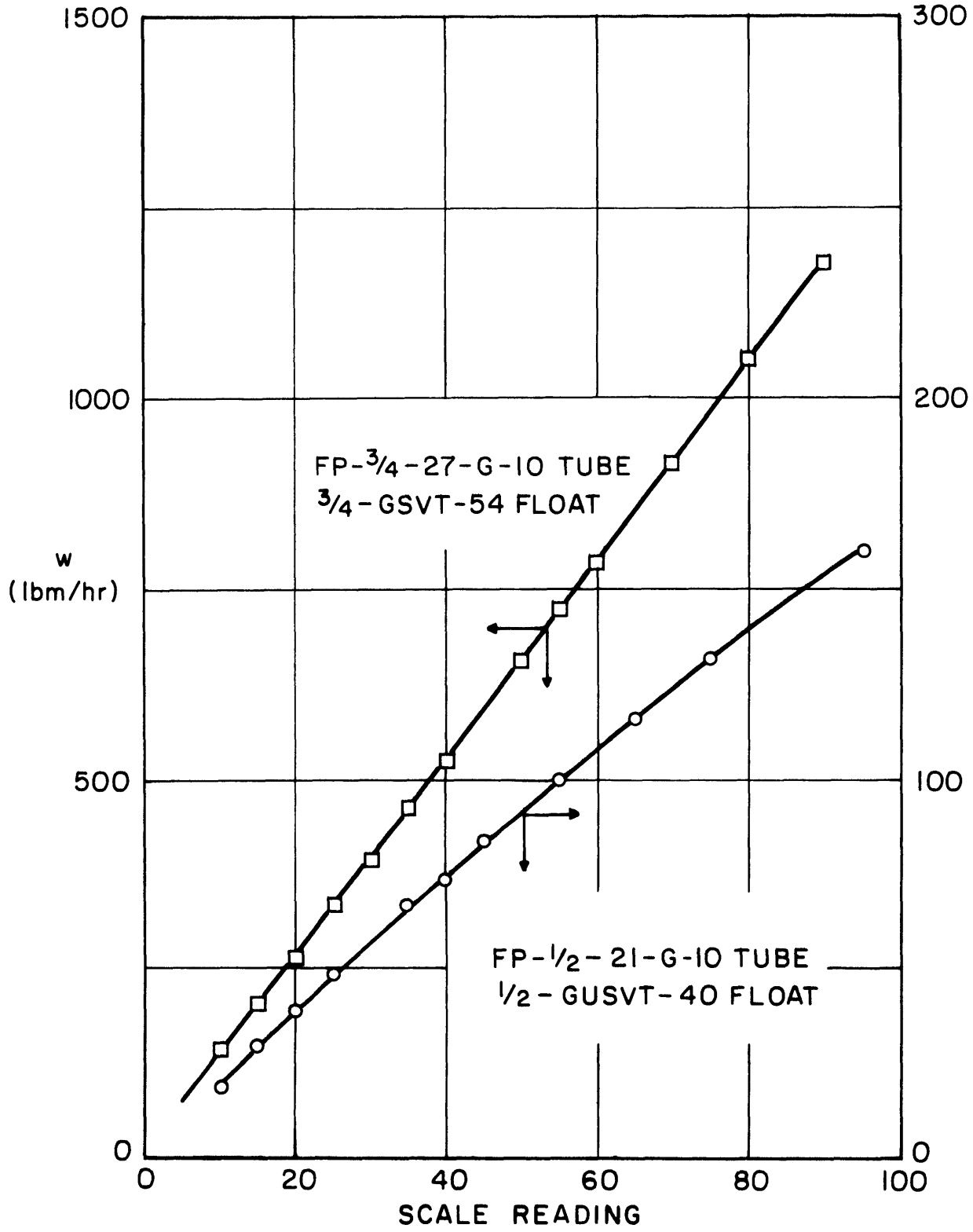

FIGURE 10: ROTAMETER CALIBRATION CURVE

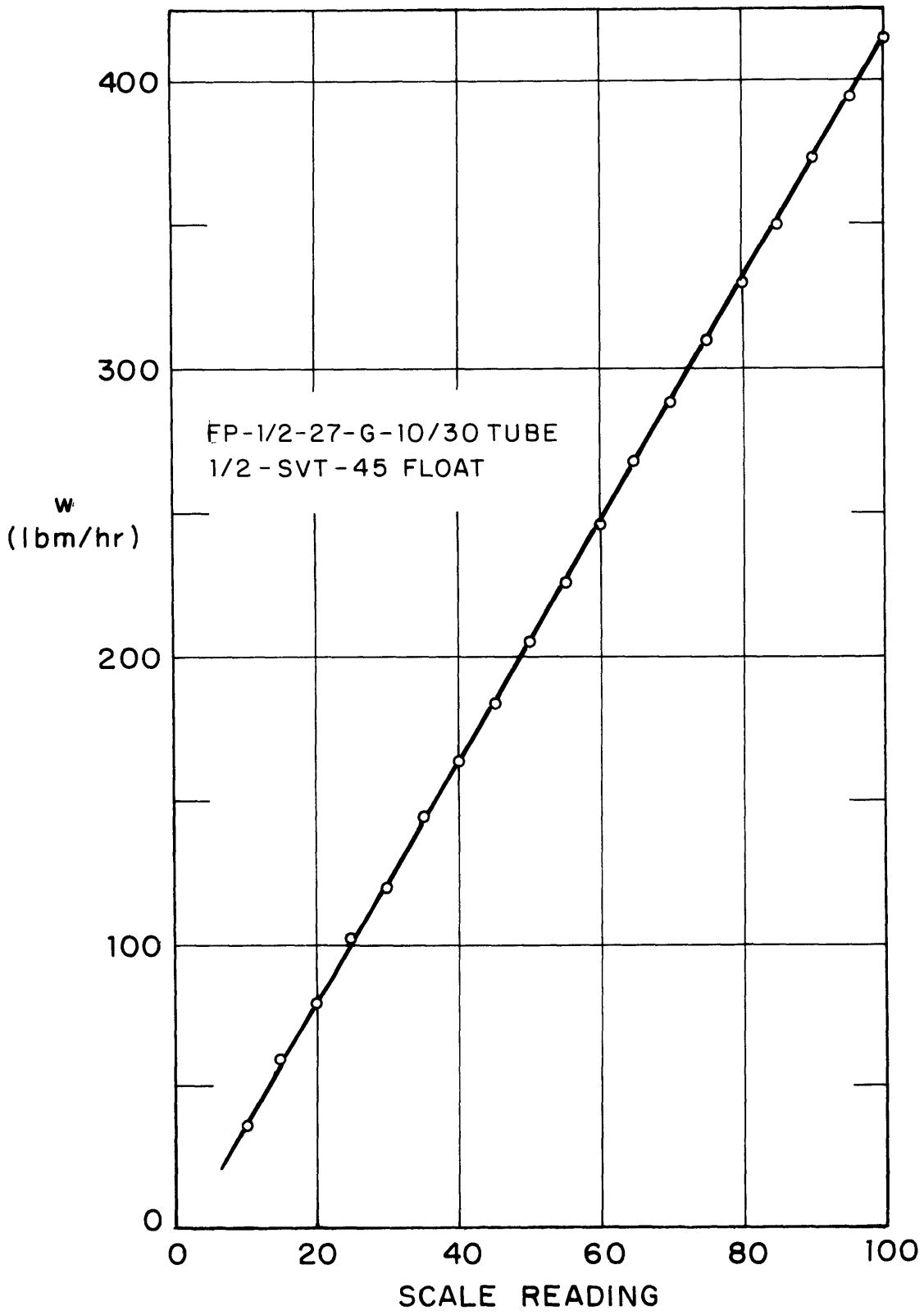

FIGURE 11 : ROTAMETER CALIBRATION CURVE

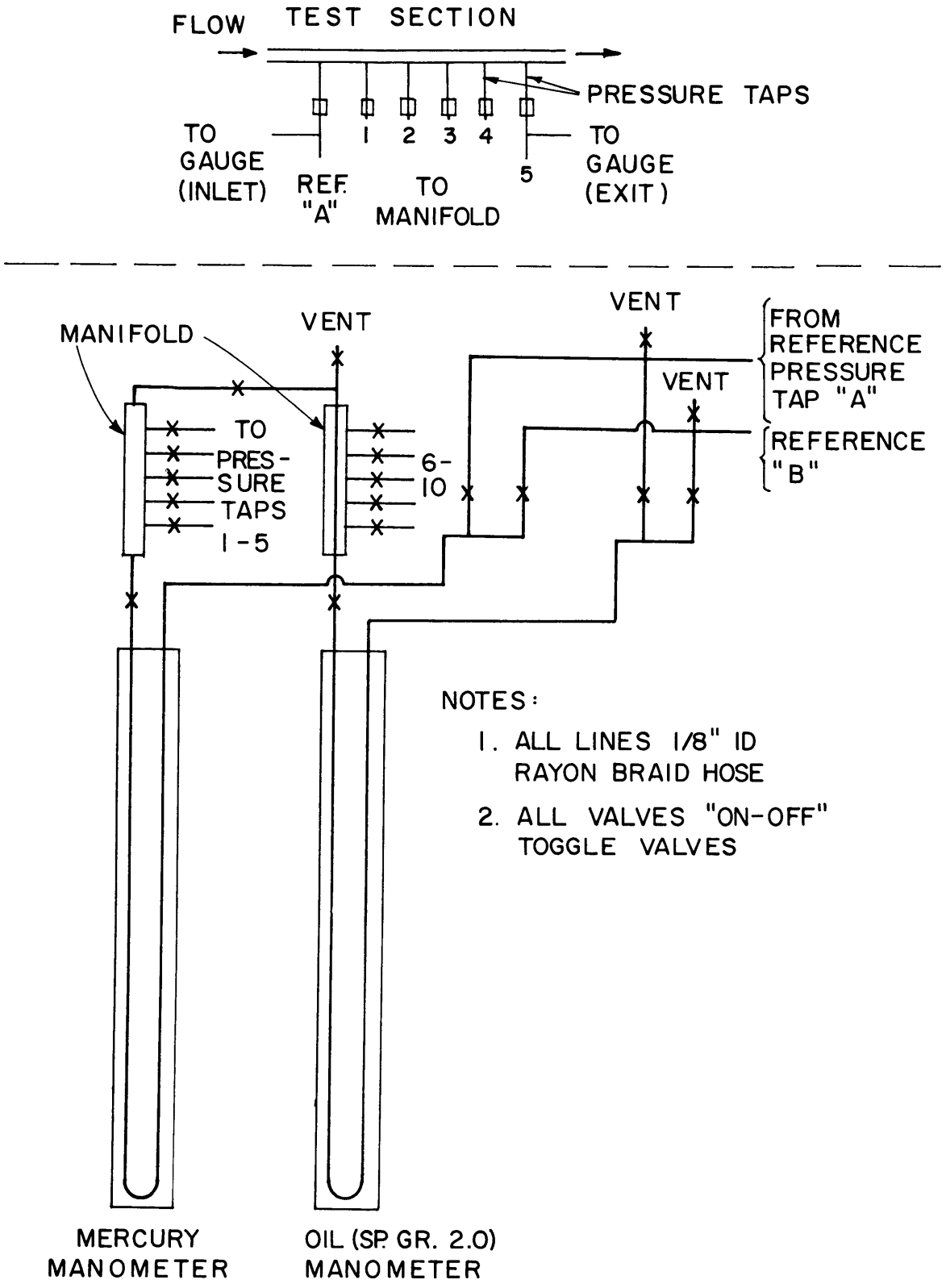

FIGURE 12: SCHEMATIC OF MANOMETER SYSTEM

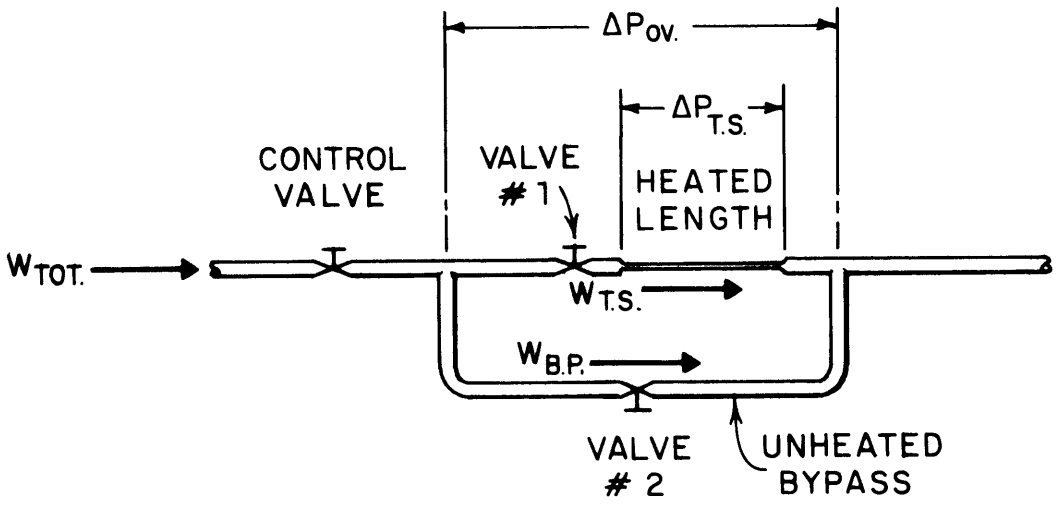

FIGURE 13: SKETCH OF BYPASS FOR SIMULATION OF CONSTANT PRESSURE DROP CONDITION

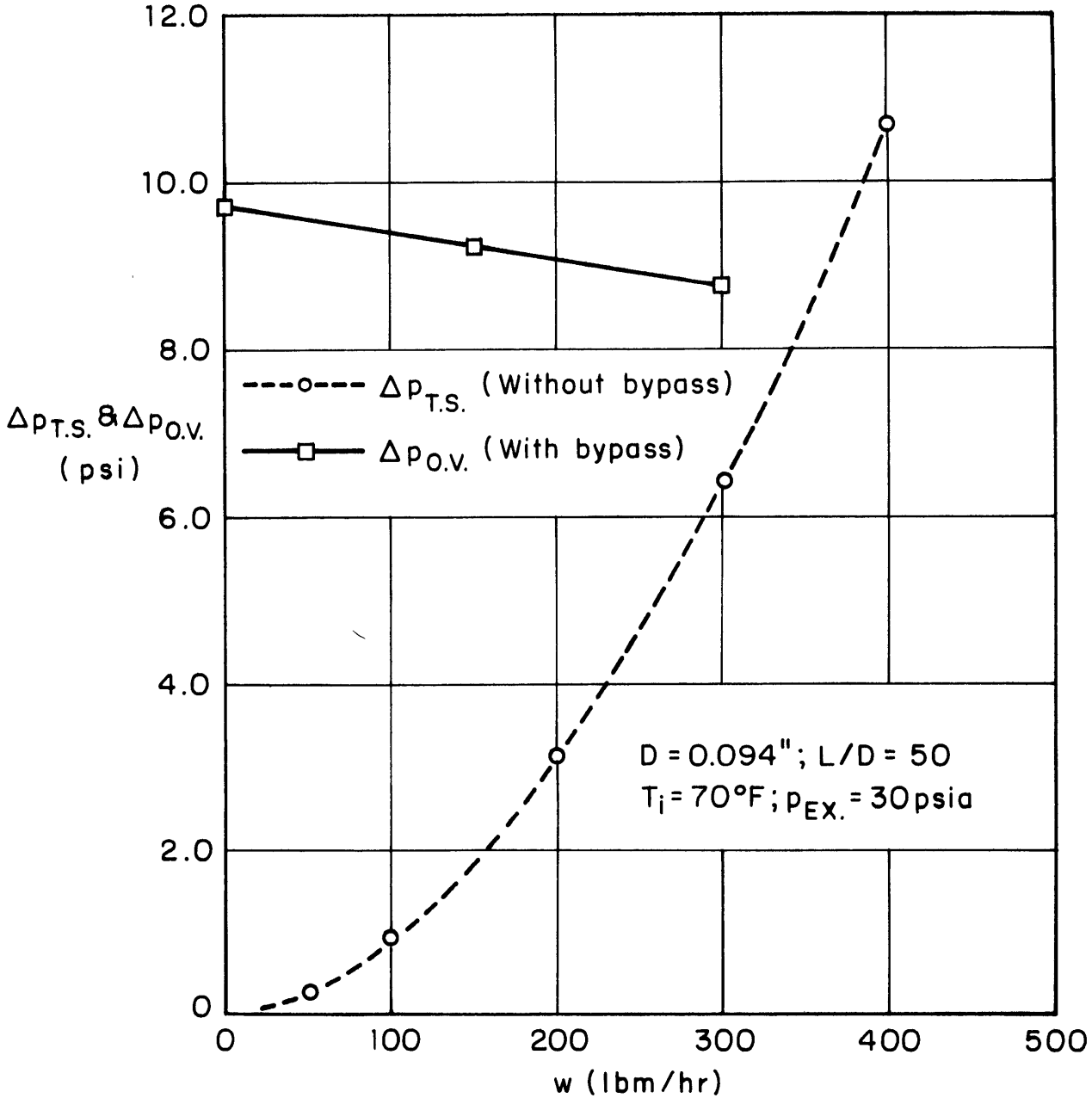

FIGURE 14: EXPERIMENTAL VERIFICATION OF CONSTANT PRESSURE DROP SIMULATION

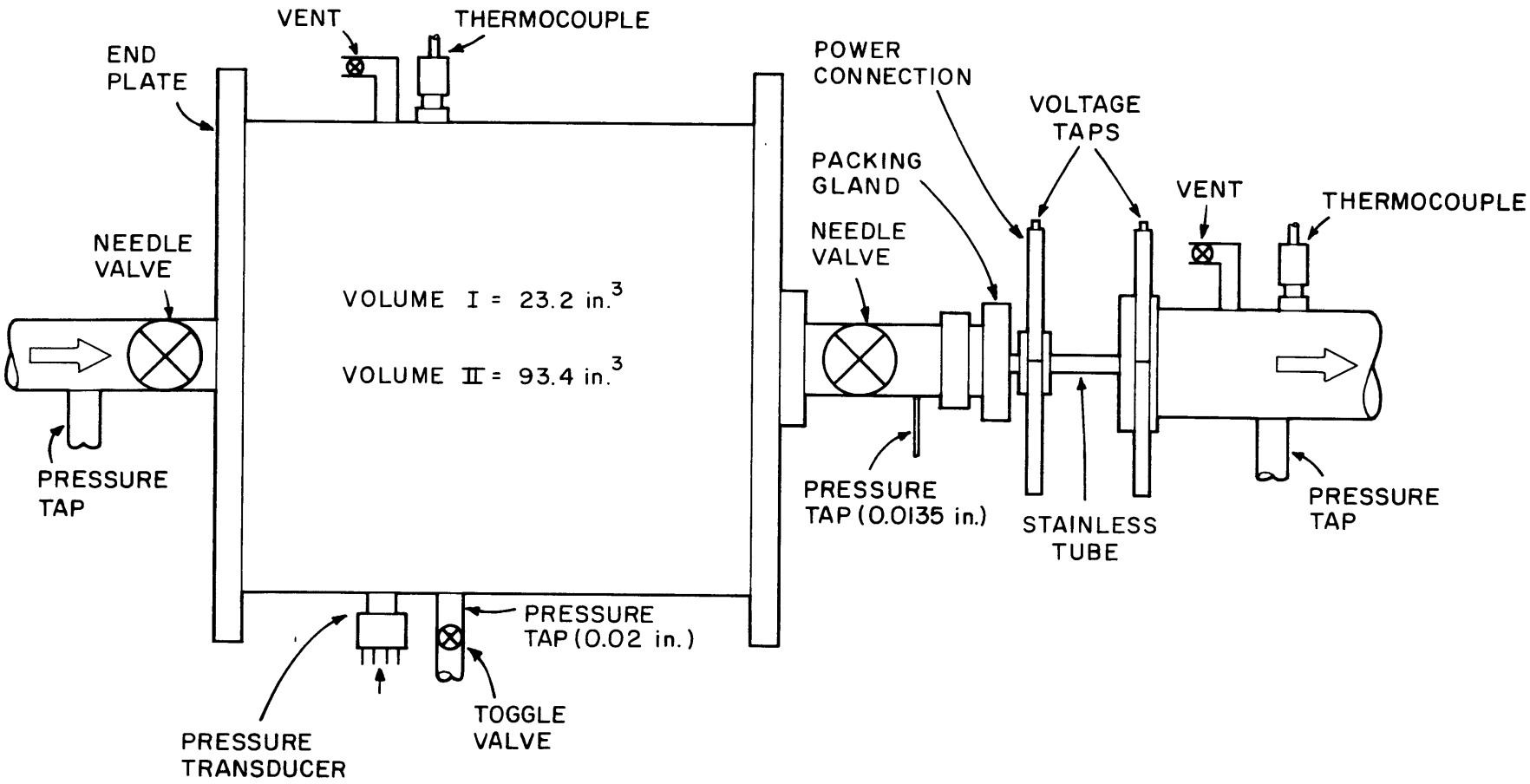

FIGURE 15: SKETCH OF DALEAS' COMPRESSIBLE VOLUME[29]

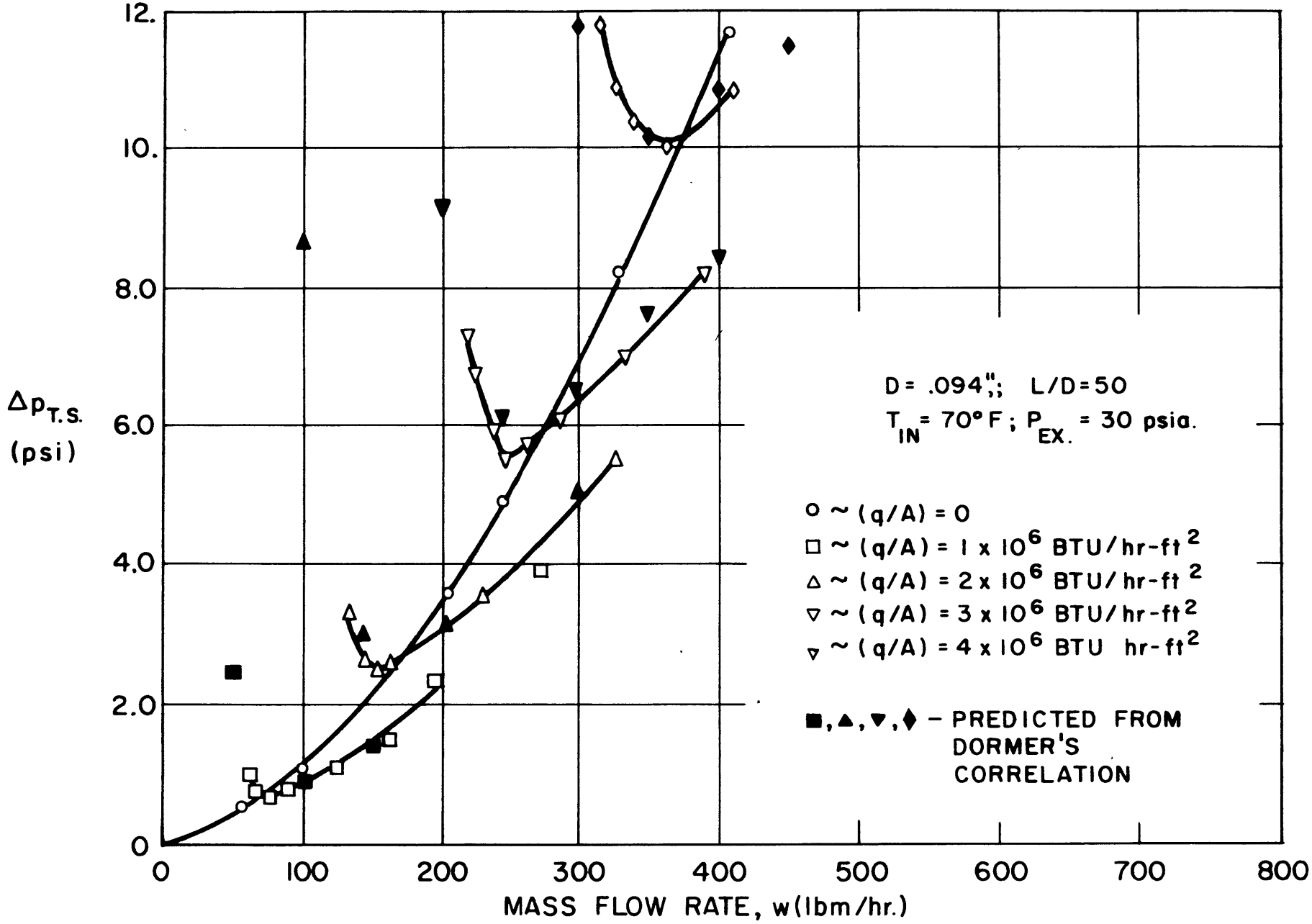

FIGURE 16: TEST SECTION PRESSURE DROP VS. MASS FLOW RATE

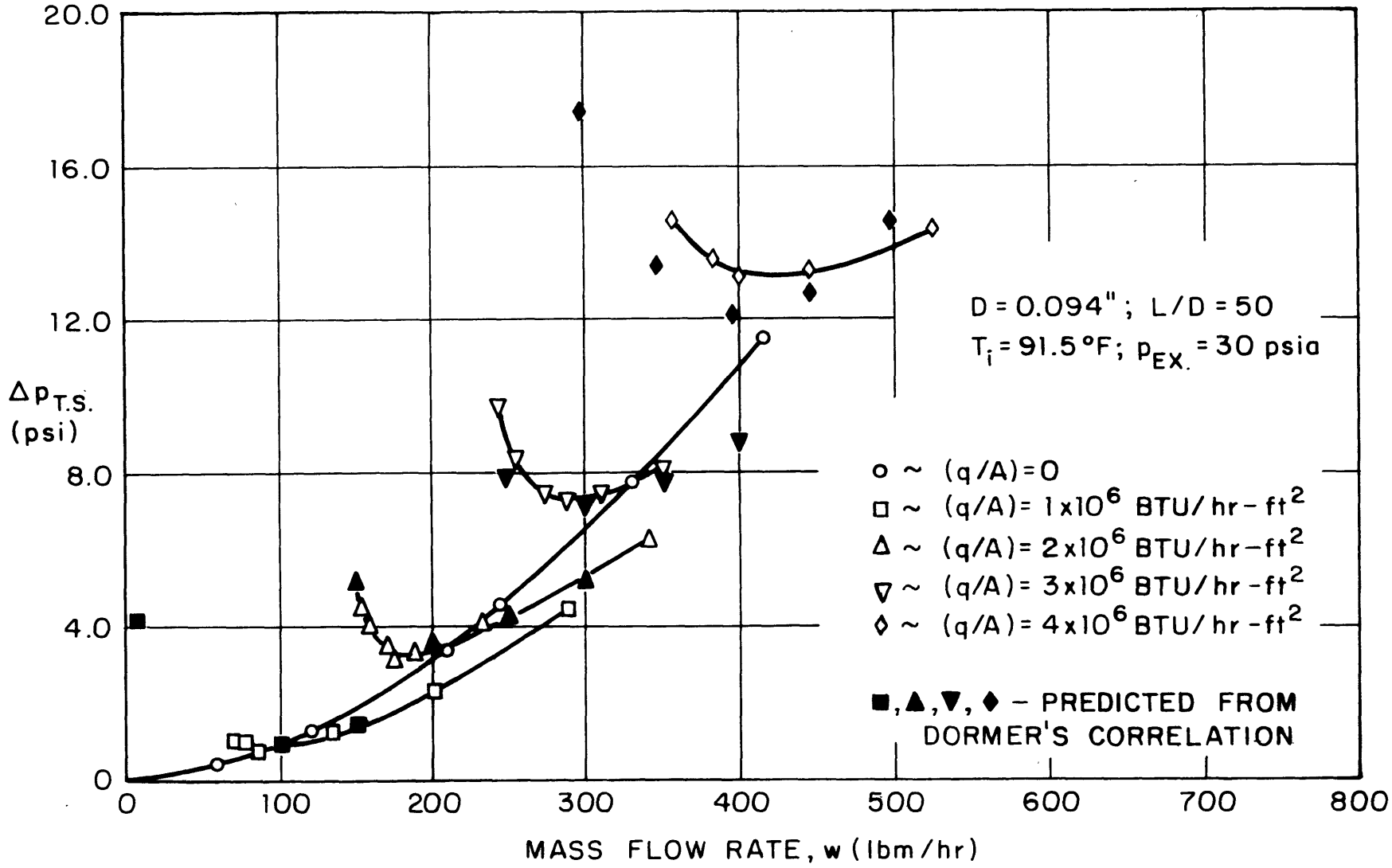

FIGURE 17: TEST SECTION PRESSURE DROP VS. MASS FLOW RATE

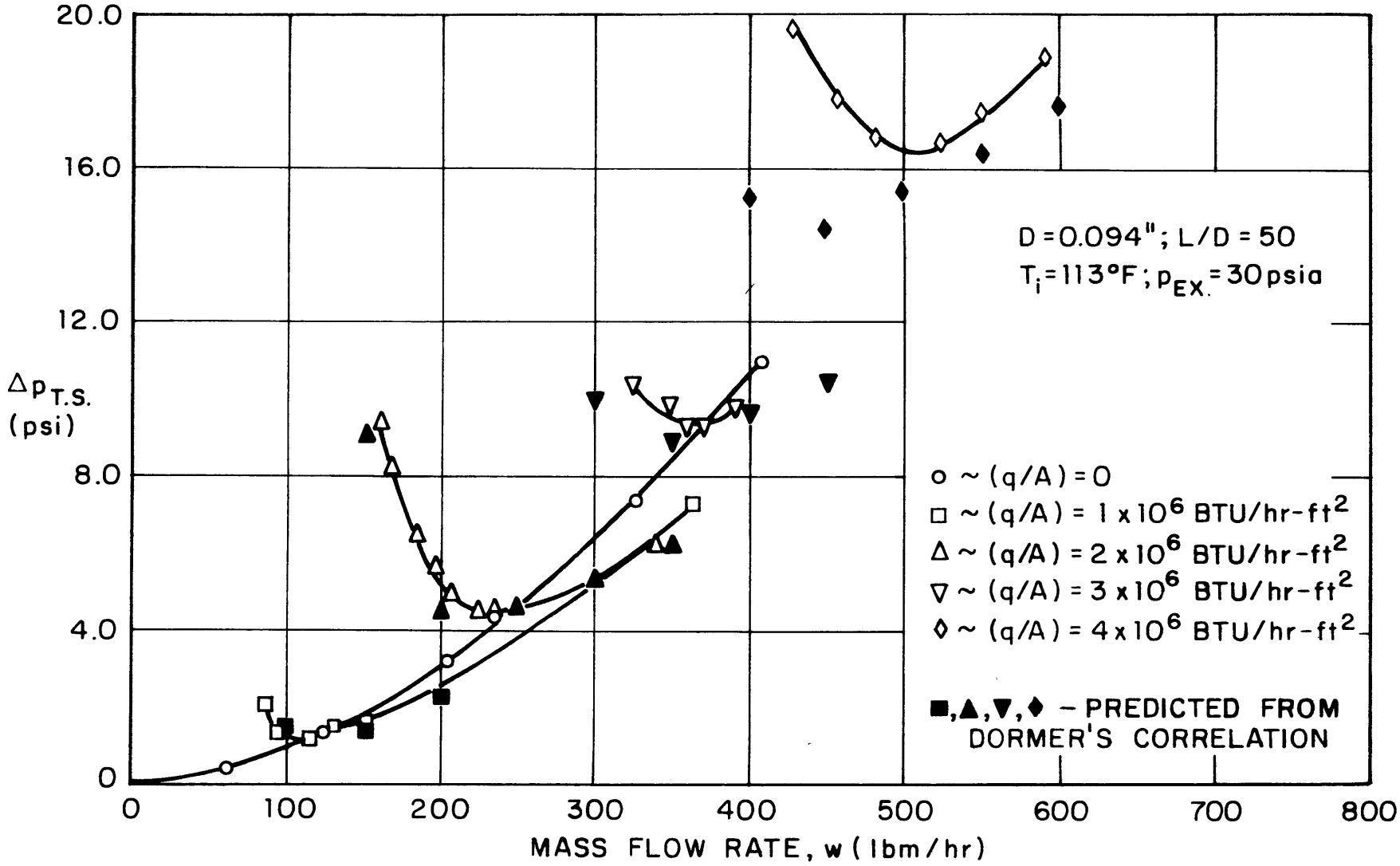

FIGURE 18: TEST SECTION PRESSURE DROP VS. MASS FLOW RATE

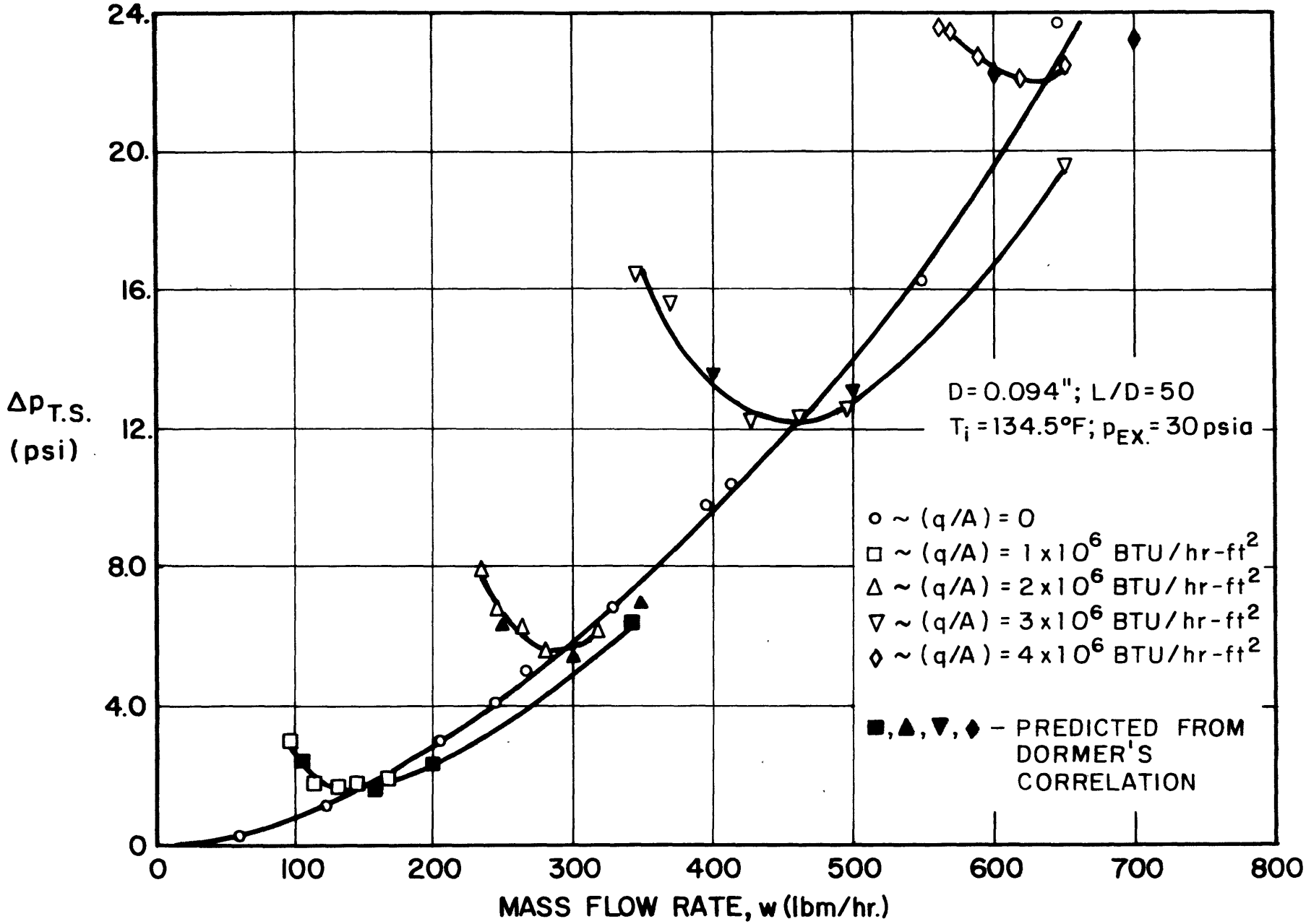

FIGURE 19: TEST SECTION PRESSURE DROP VS. MASS FLOW RATE

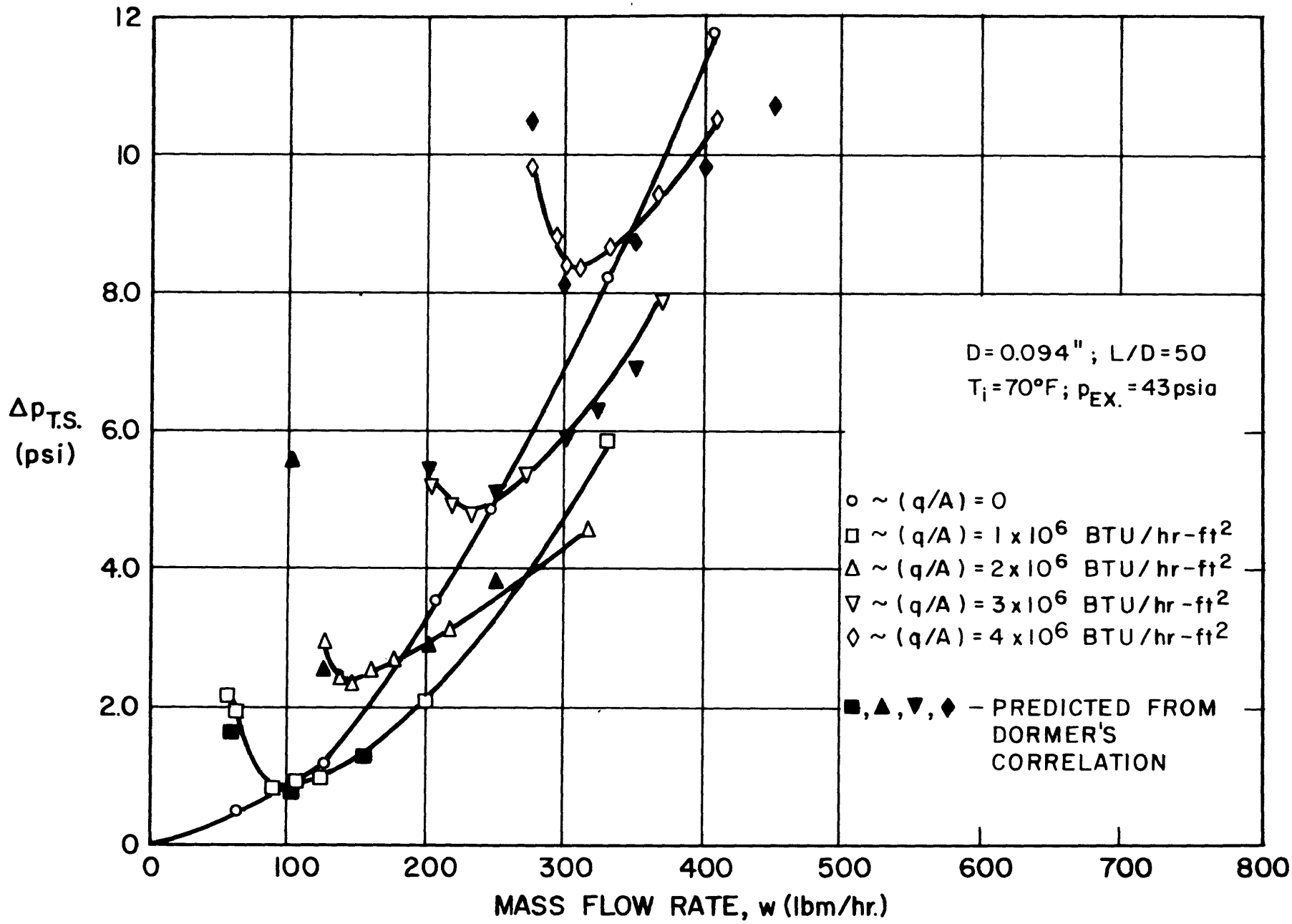

FIGURE 20: TEST SECTION PRESSURE DROP VS. MASS FLOW RATE

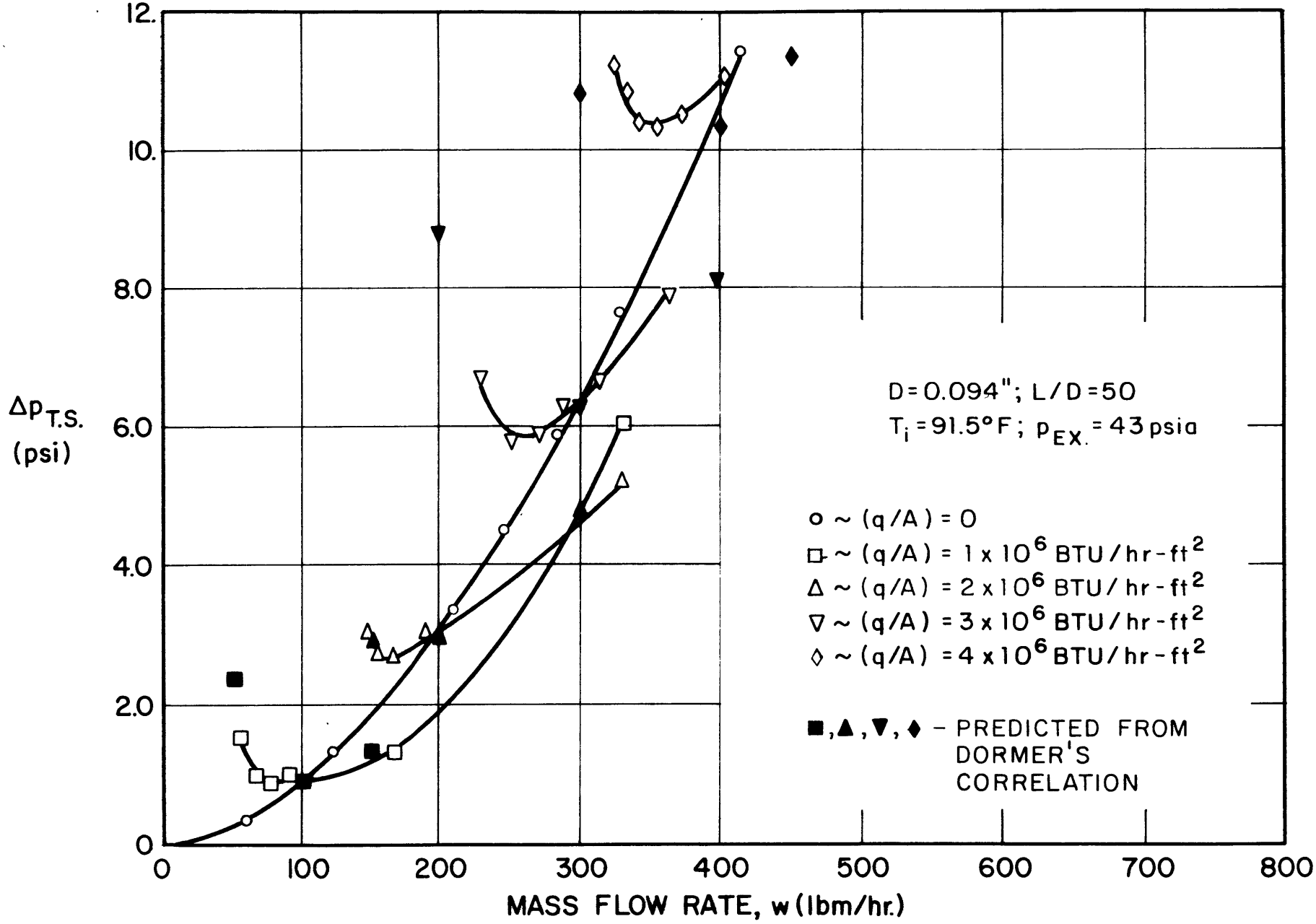

FIGURE 21: TEST SECTION PRESSURE DROP VS. MASS FLOW RATE

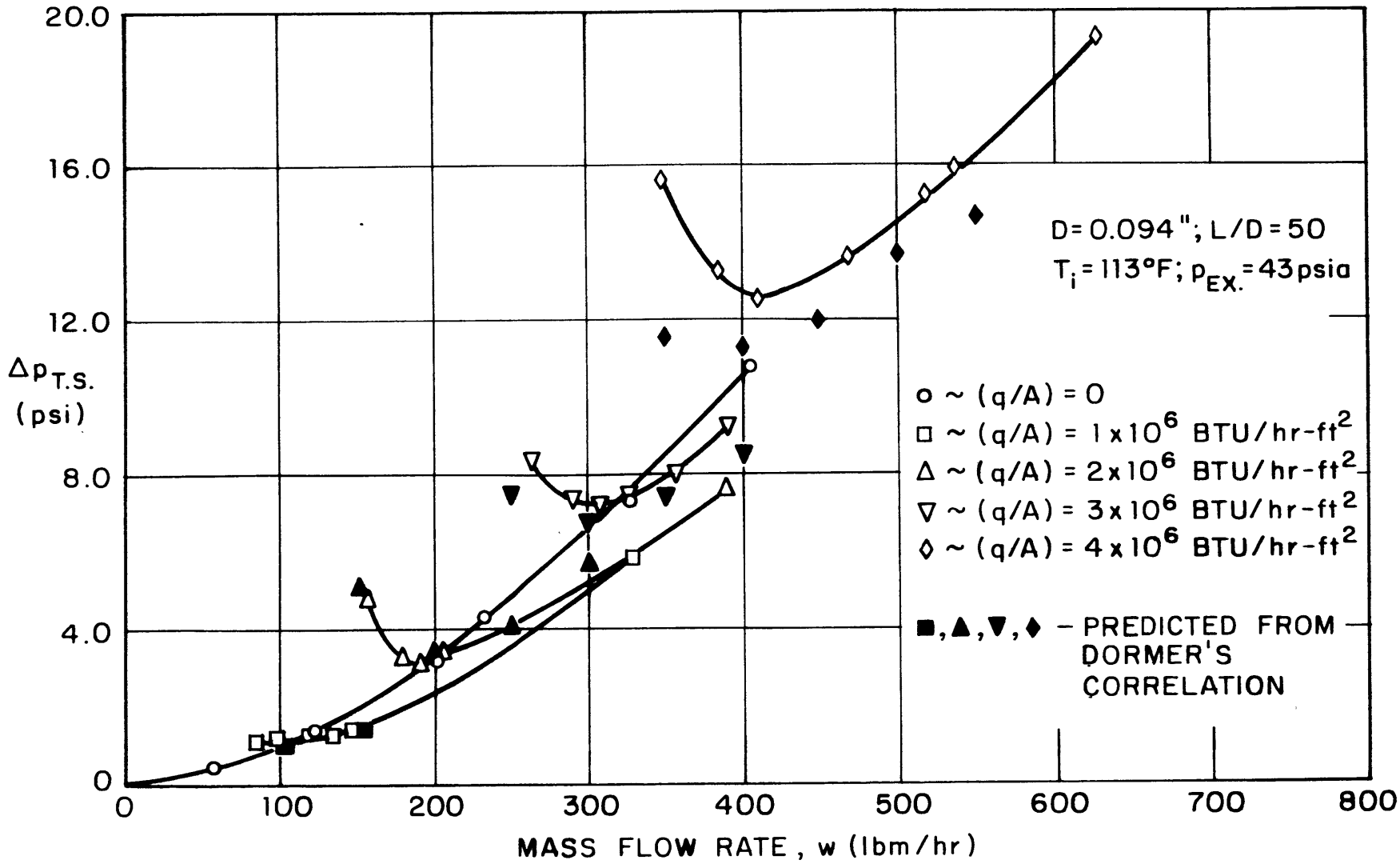

FIGURE 22: TEST SECTION PRESSURE DROP VS. MASS FLOW RATE

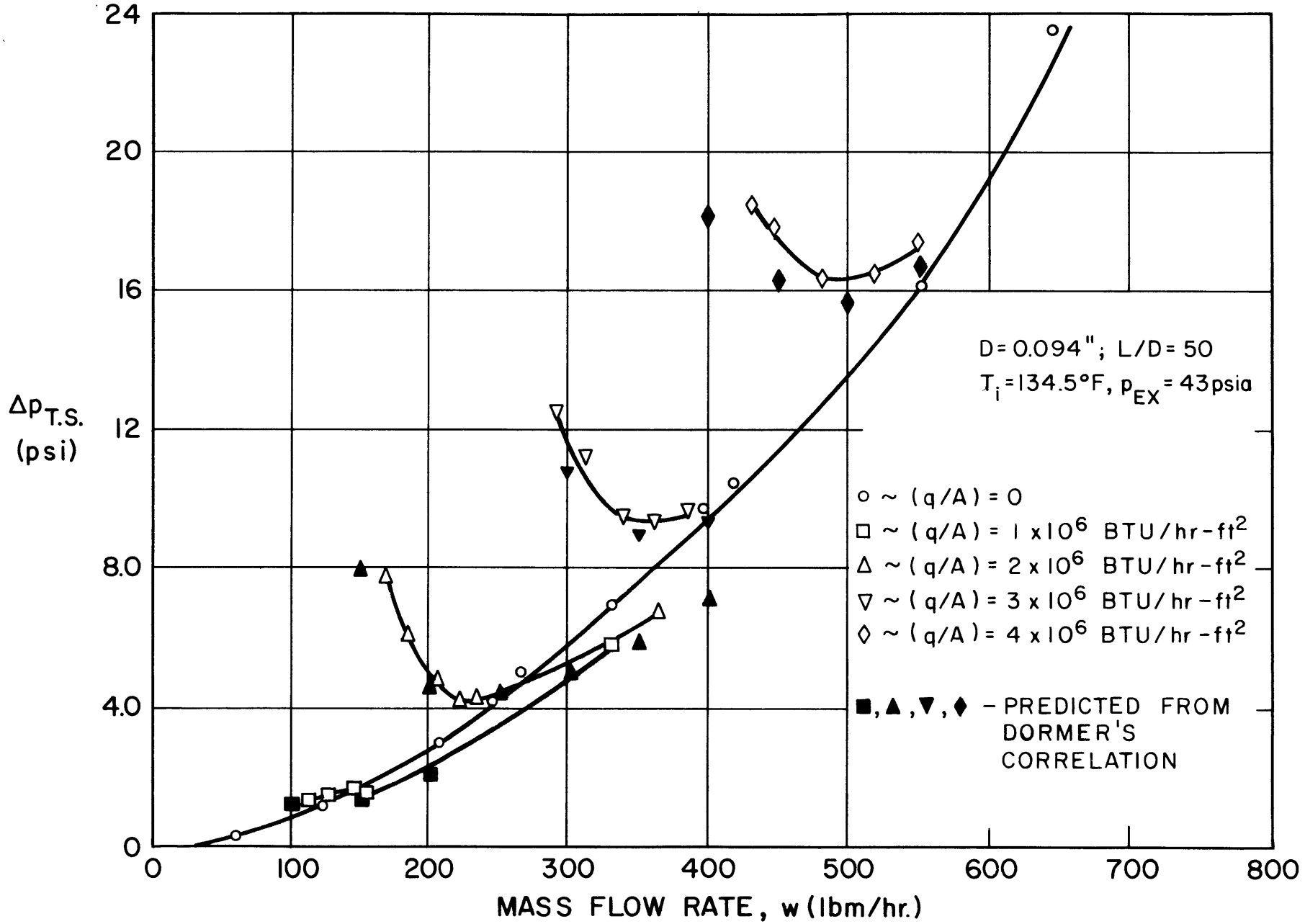

FIGURE 23: TEST SECTION PRESSURE DROP VS. MASS FLOW RATE

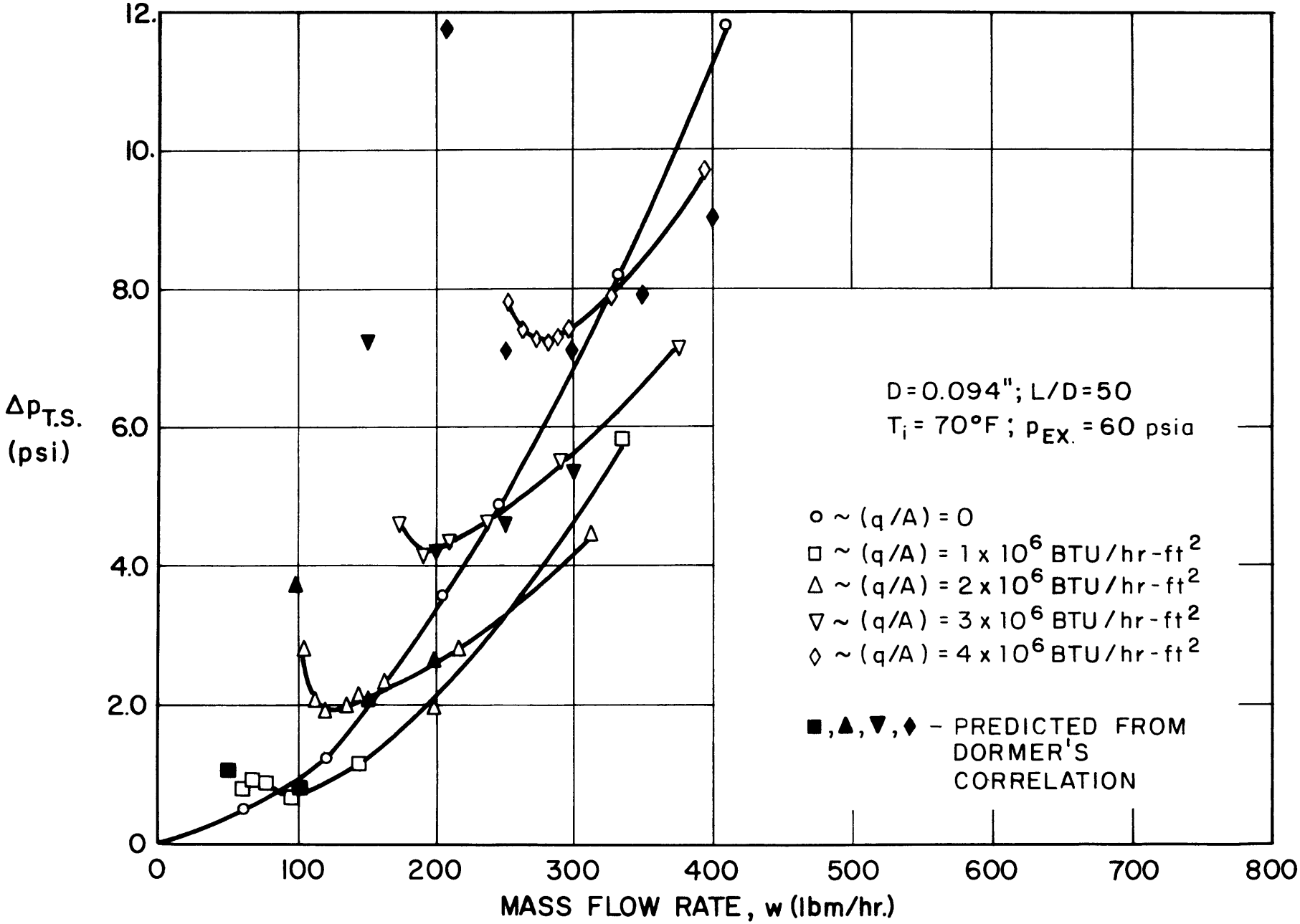

FIGURE 24: TEST SECTION PRESSURE DROP VS. MASS FLOW RATE

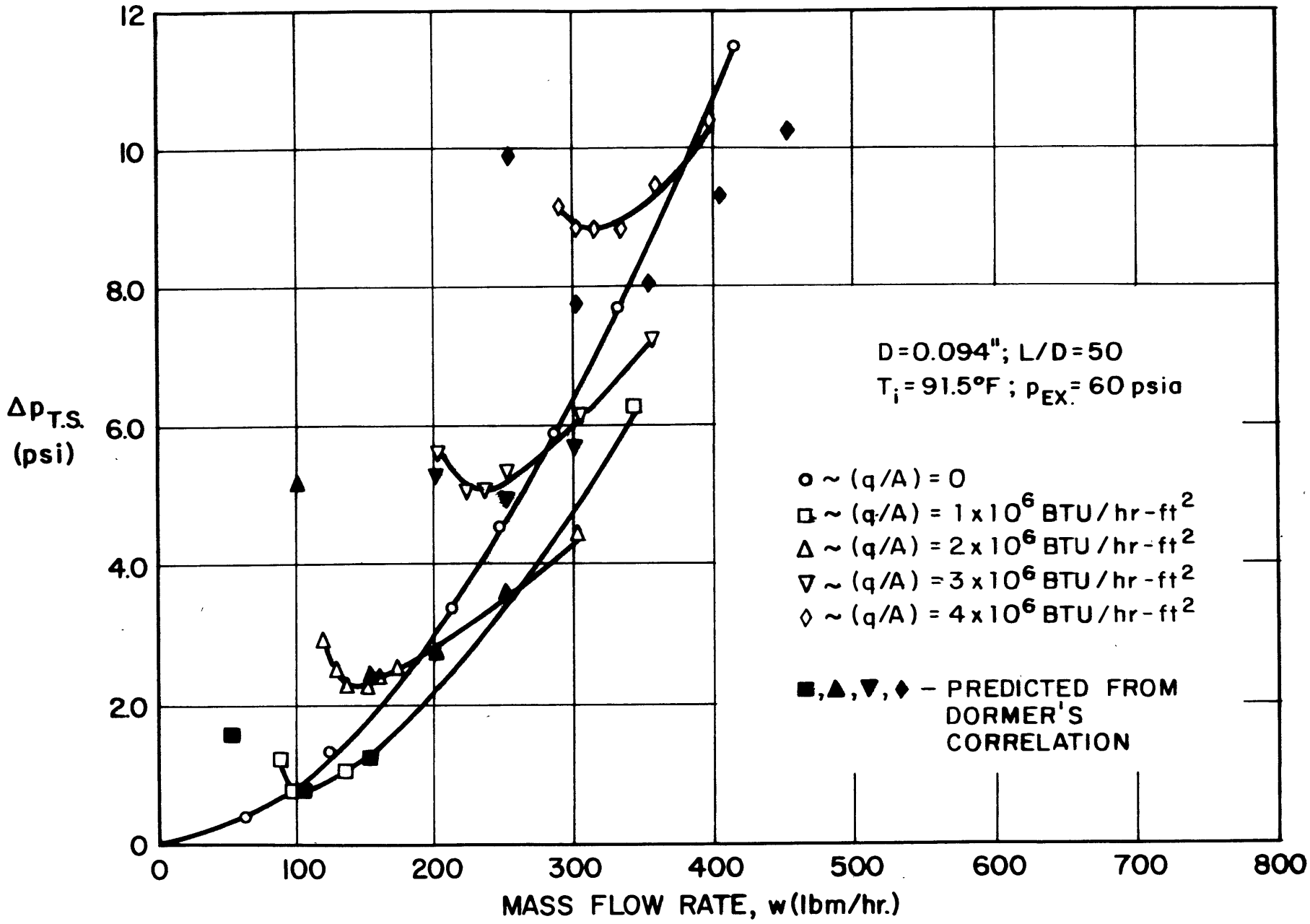

FIGURE 25: TEST SECTION PRESSURE DROP VS. MASS FLOW RATE

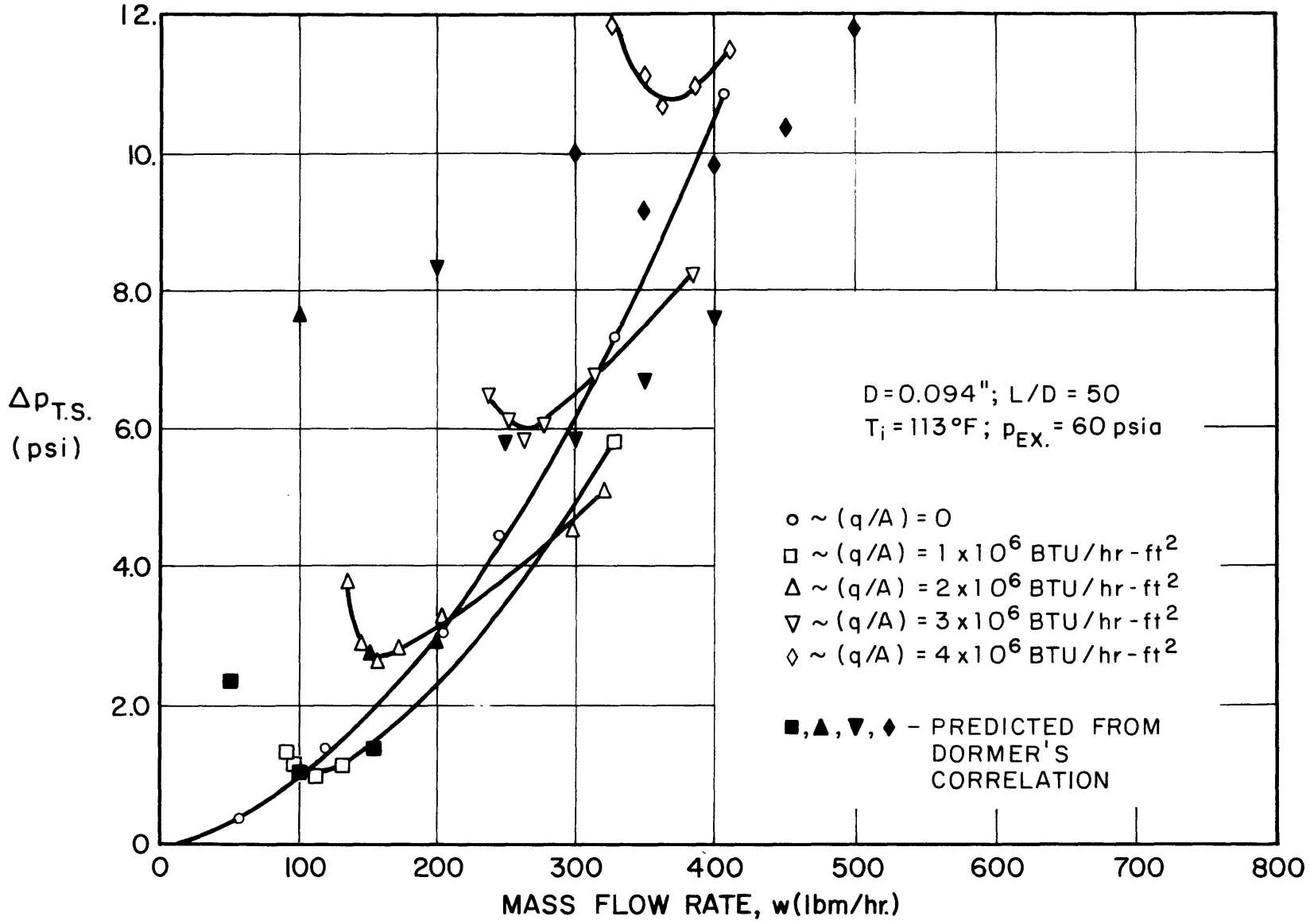

FIGURE 26. TEST SECTION PRESSURE DROP VS. MASS FLOW RATE

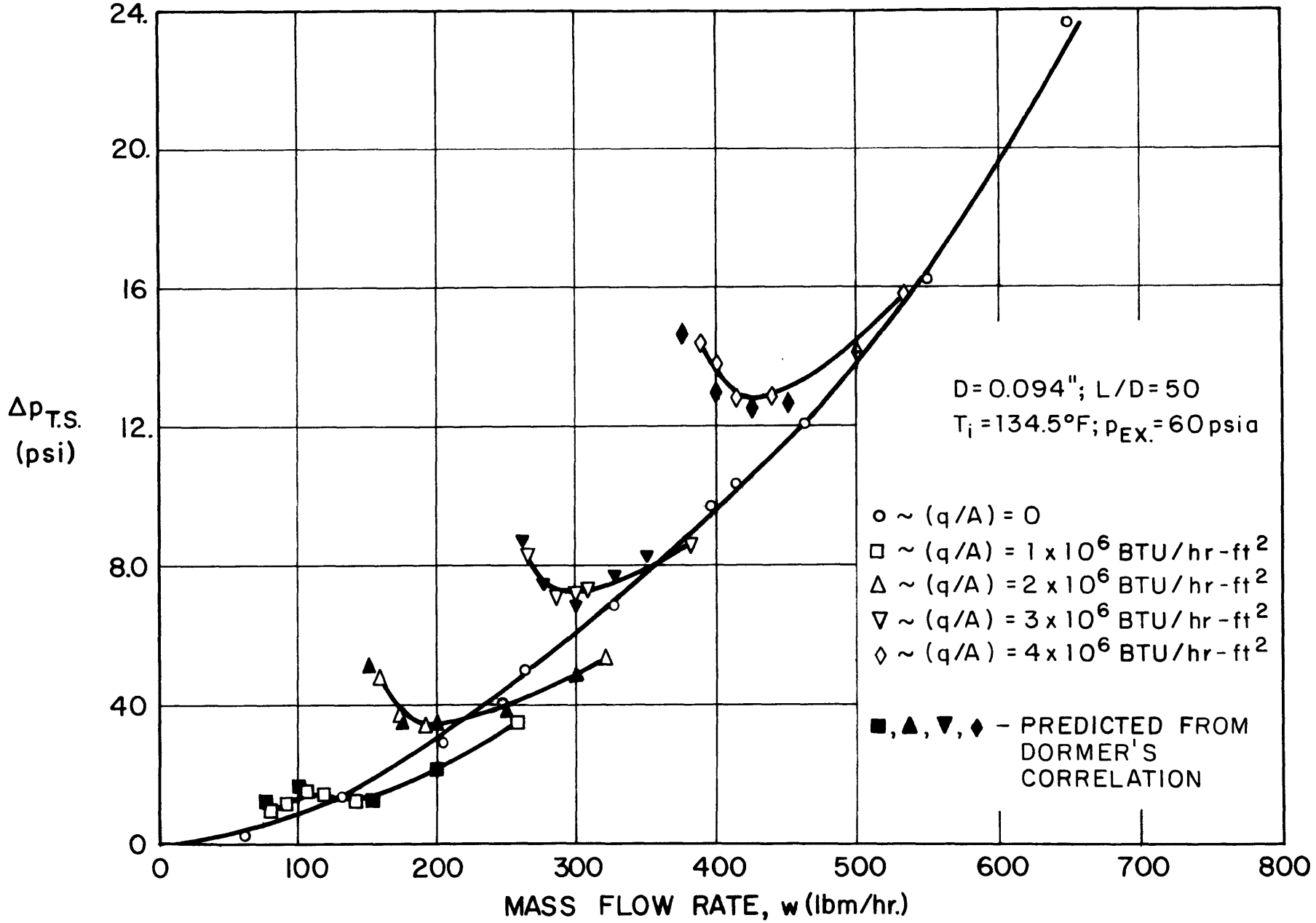

FIGURE 27: TEST SECTION PRESSURE DROP VS. MASS FLOW RATE

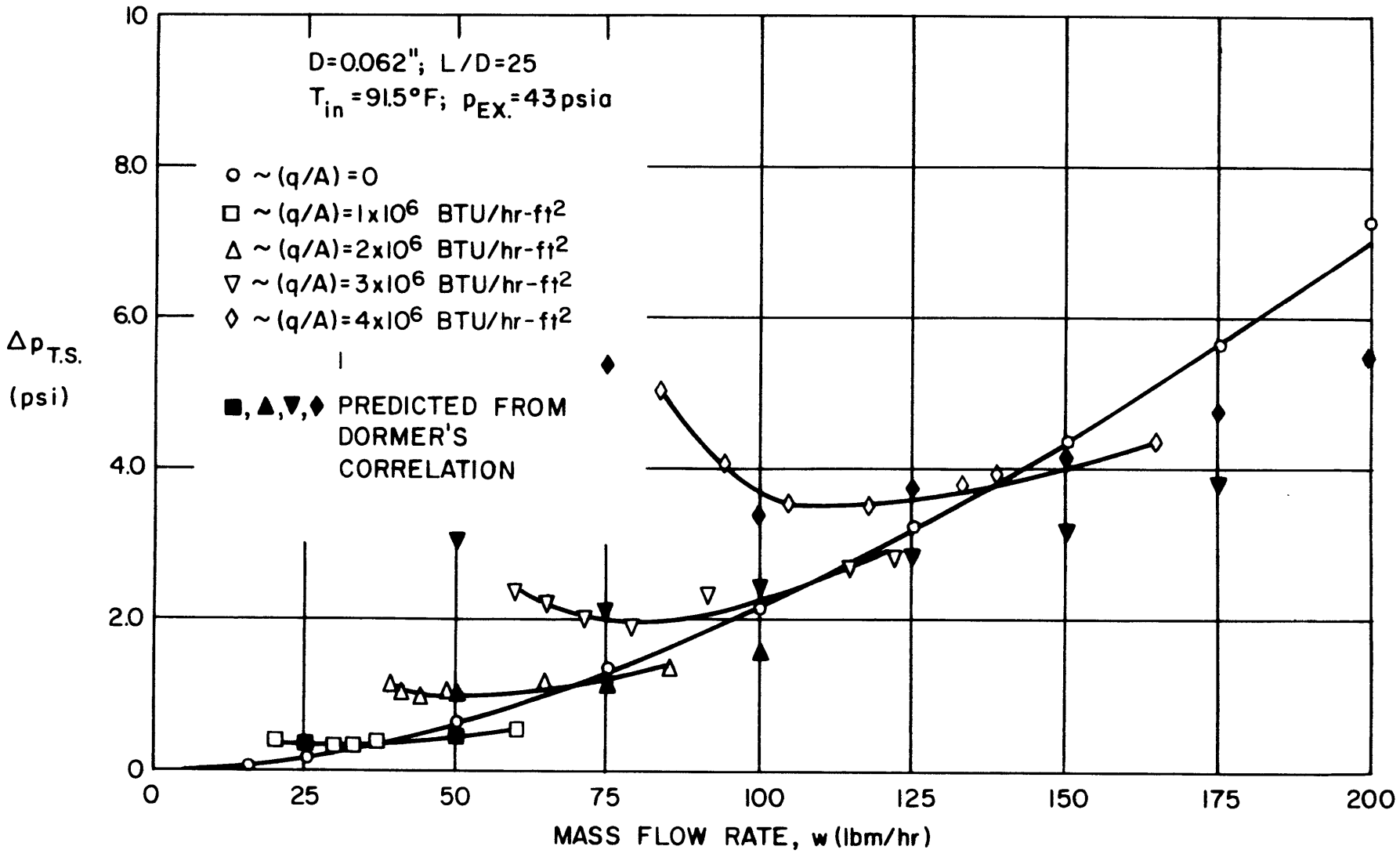

FIGURE 28. TEST SECTION PRESSURE DROP VS. MASS FLOW RATE

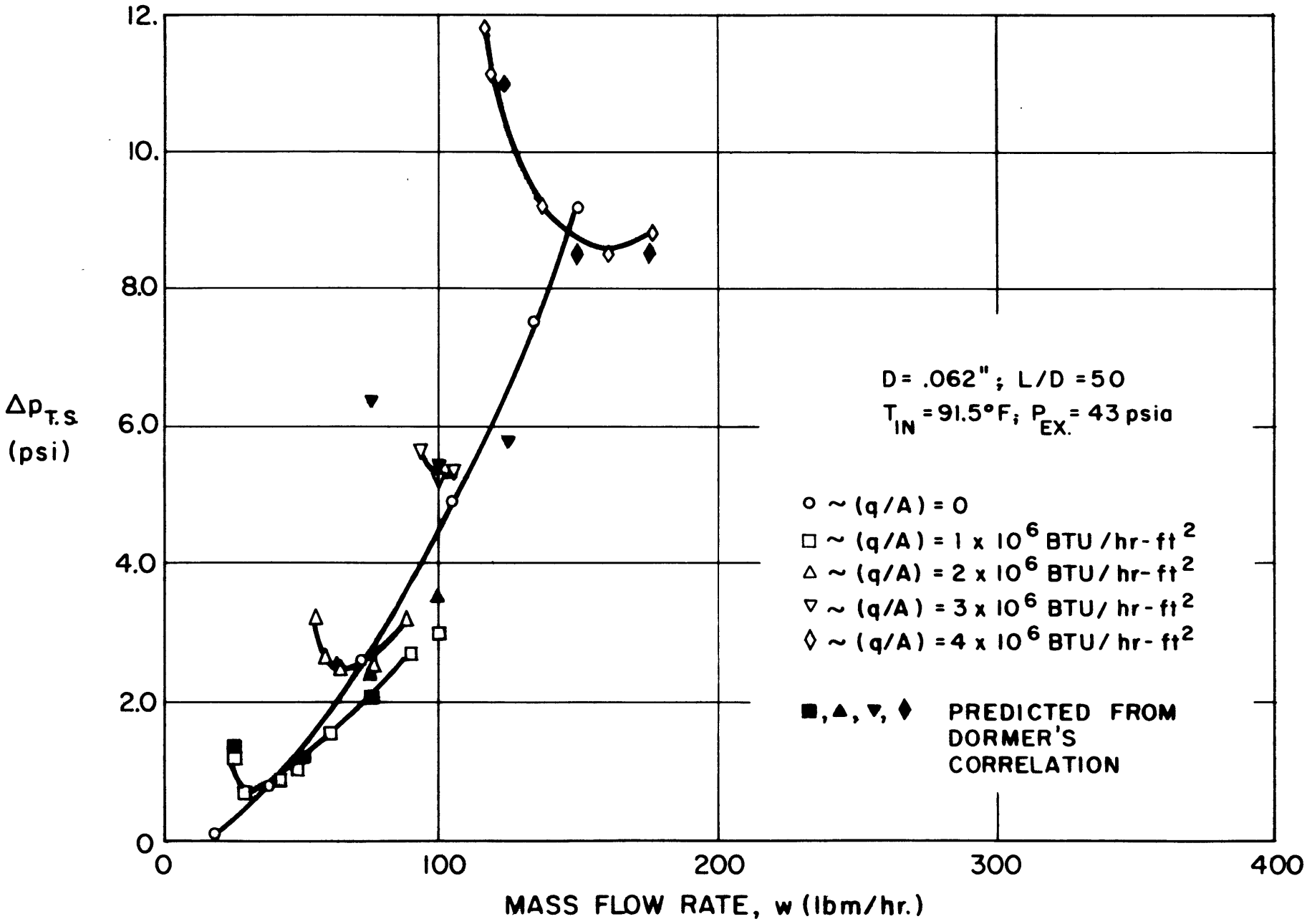

FIGURE 29: TEST SECTION PRESSURE DROP VS. MASS FLOW RATE

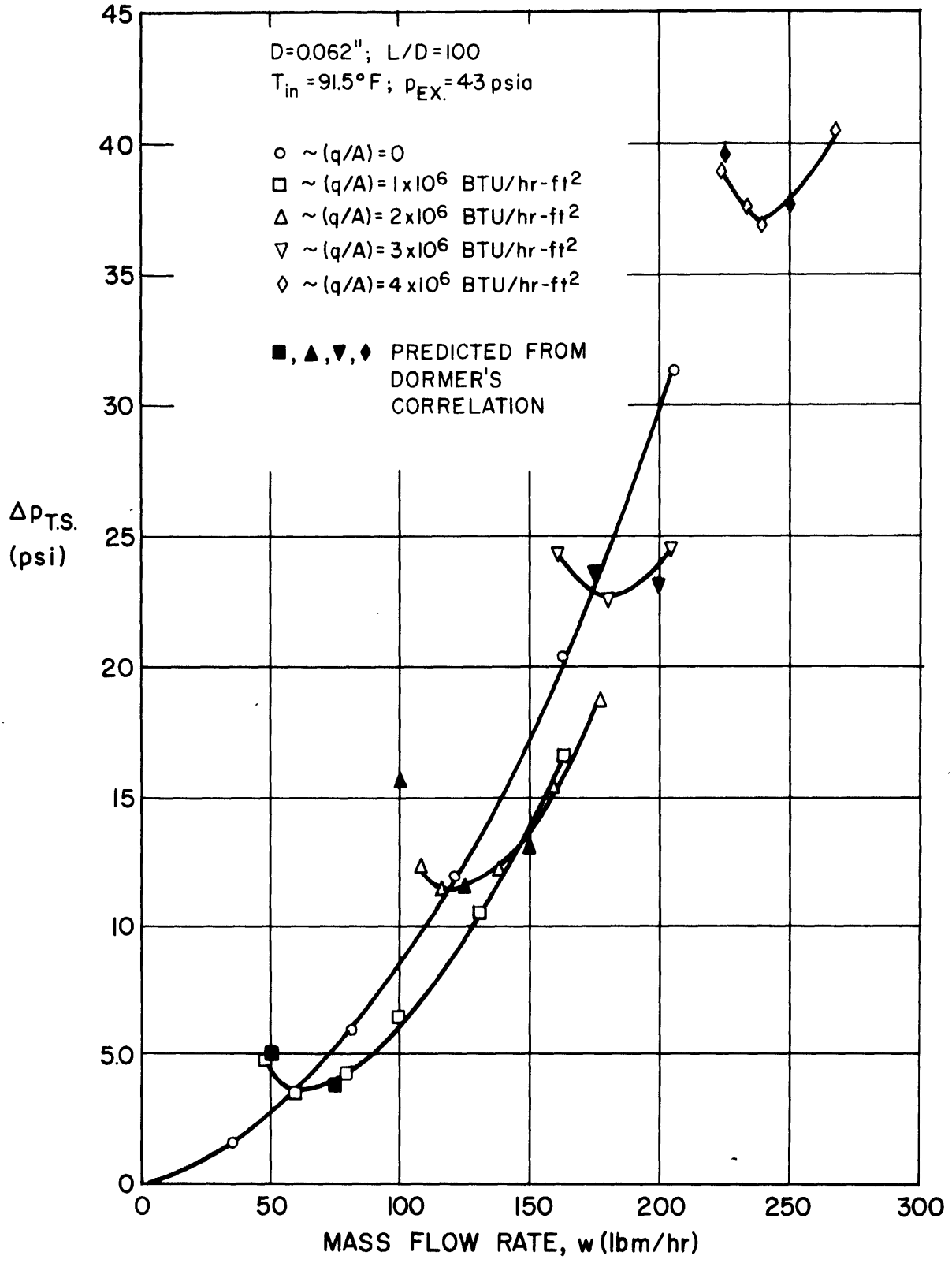

FIGURE 30. TEST SECTION PRESSURE DROP VS. MASS FLOW RATE

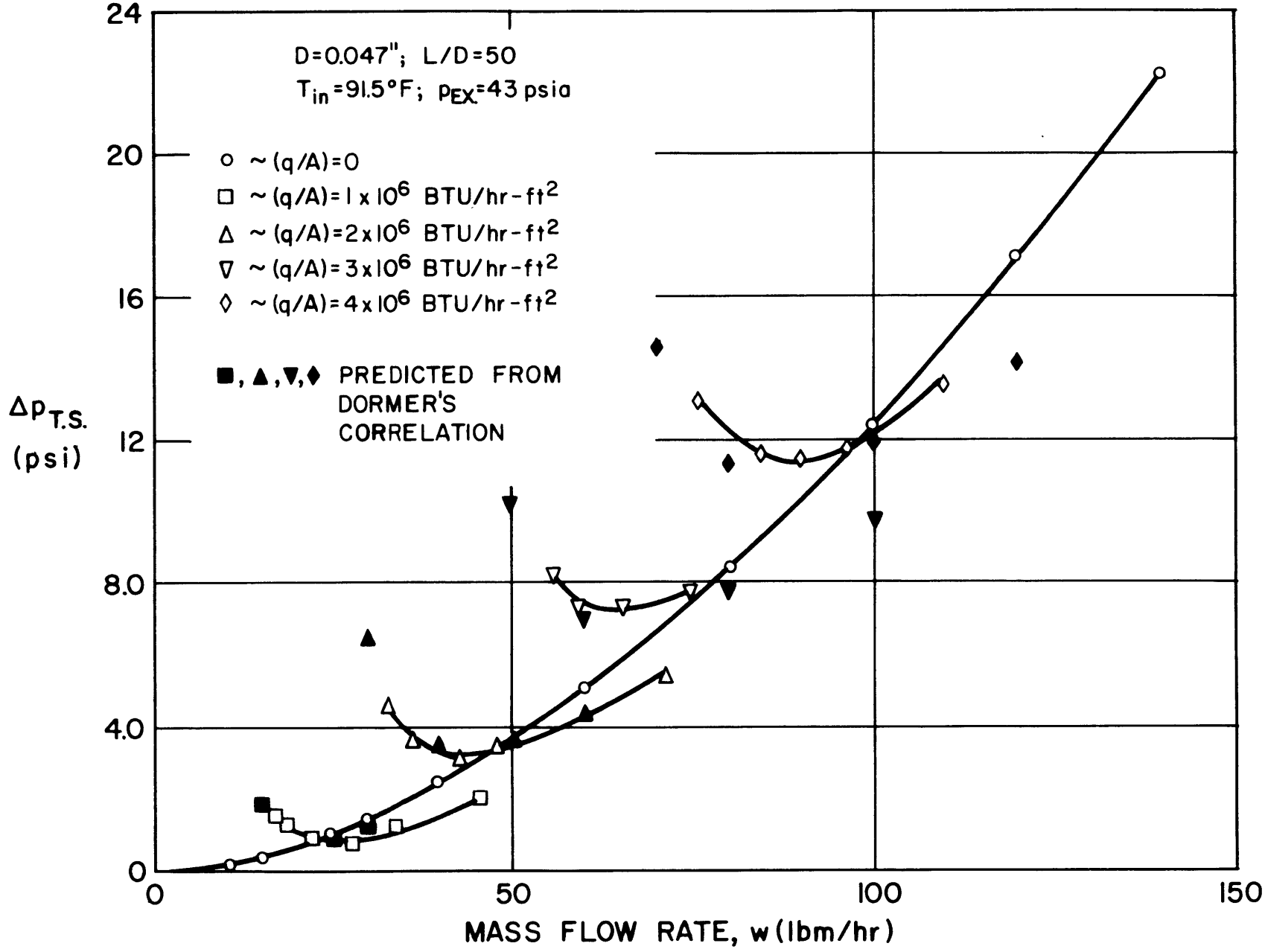

FIGURE 31: TEST SECTION PRESSURE DROP VS. MASS FLOW RATE

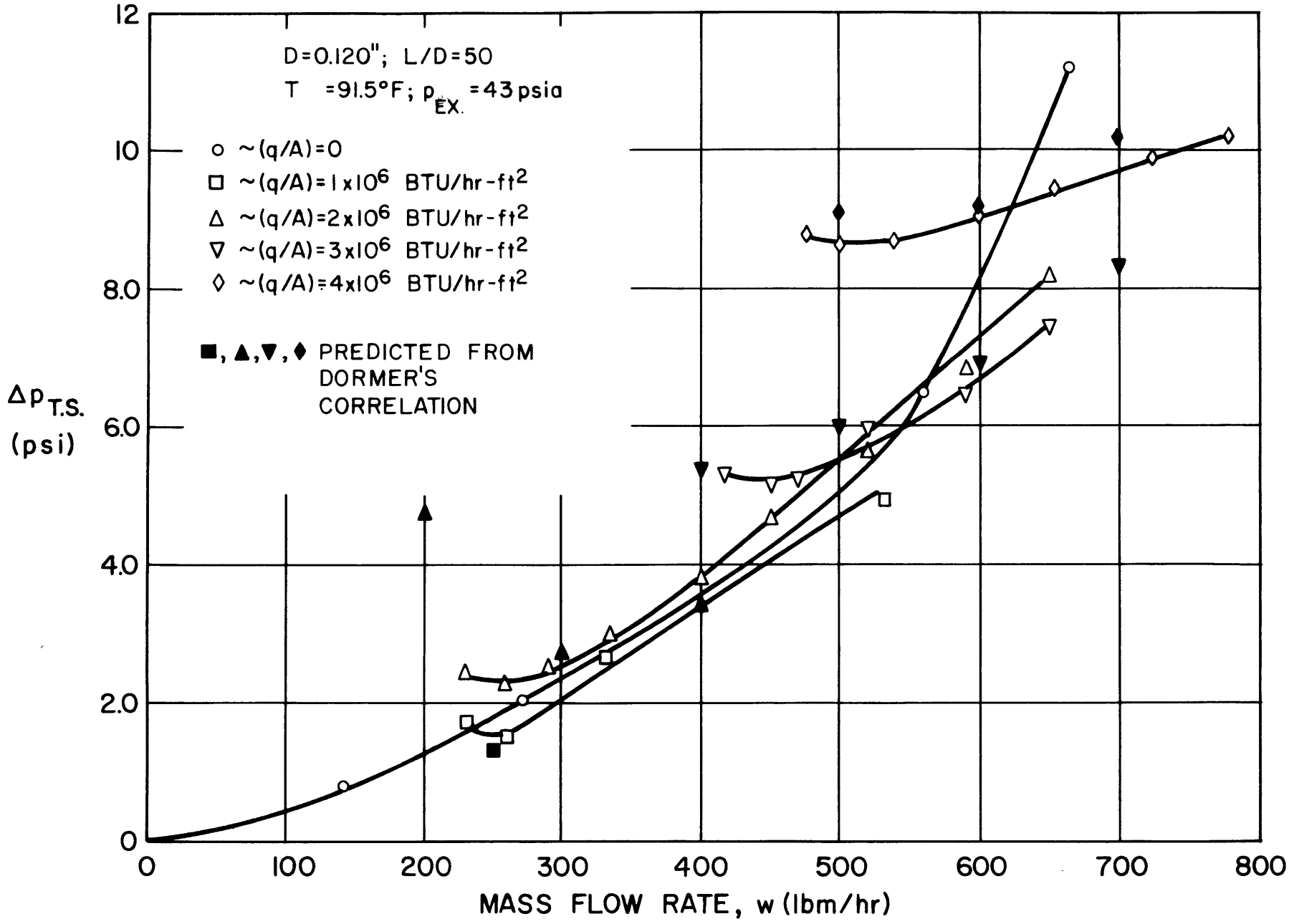

FIGURE 32. TEST SECTION PRESSURE DROP VS. MASS FLOW RATE

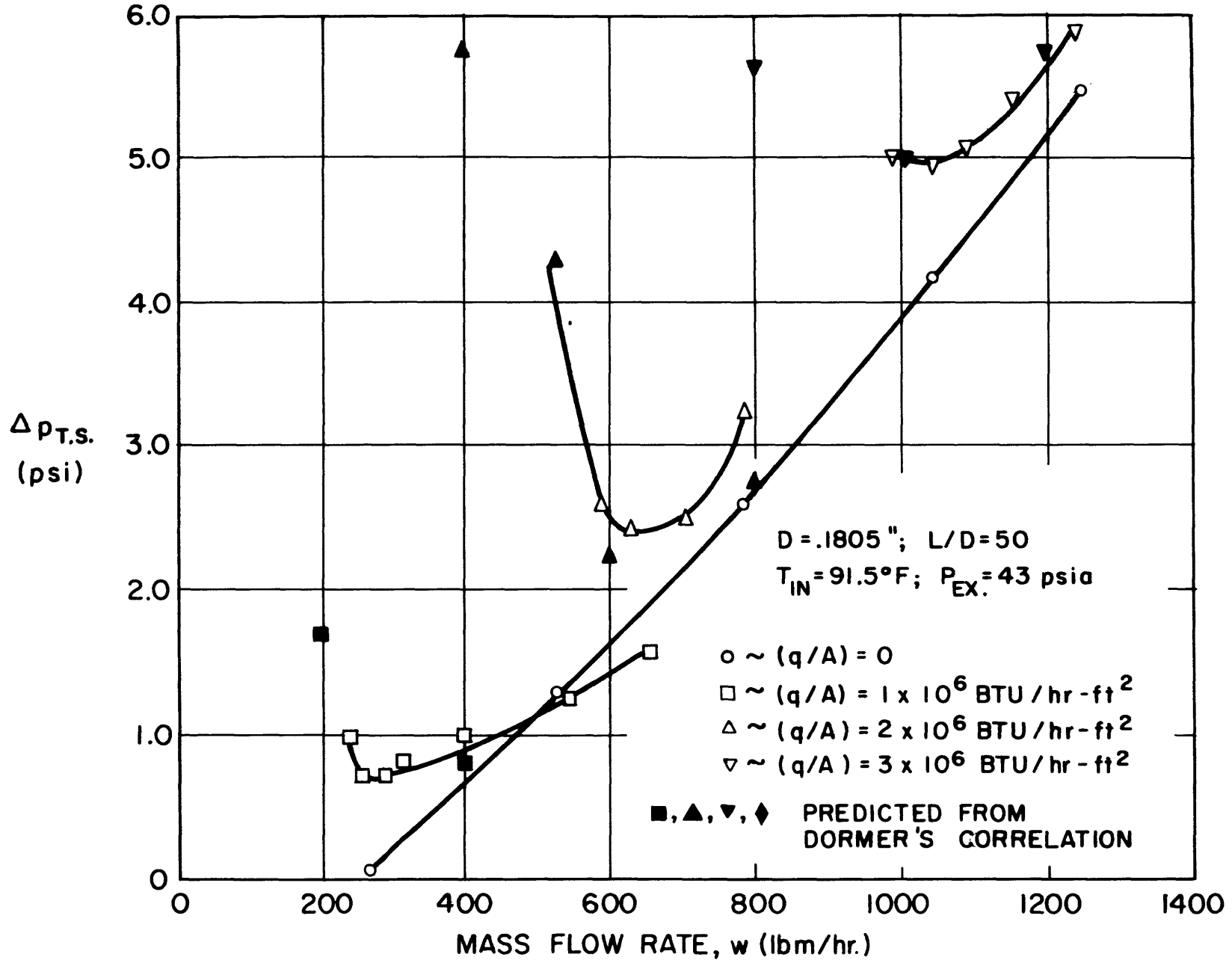

FIGURE 33: TEST SECTION PRESSURE DROP VS. MASS FLOW RATE

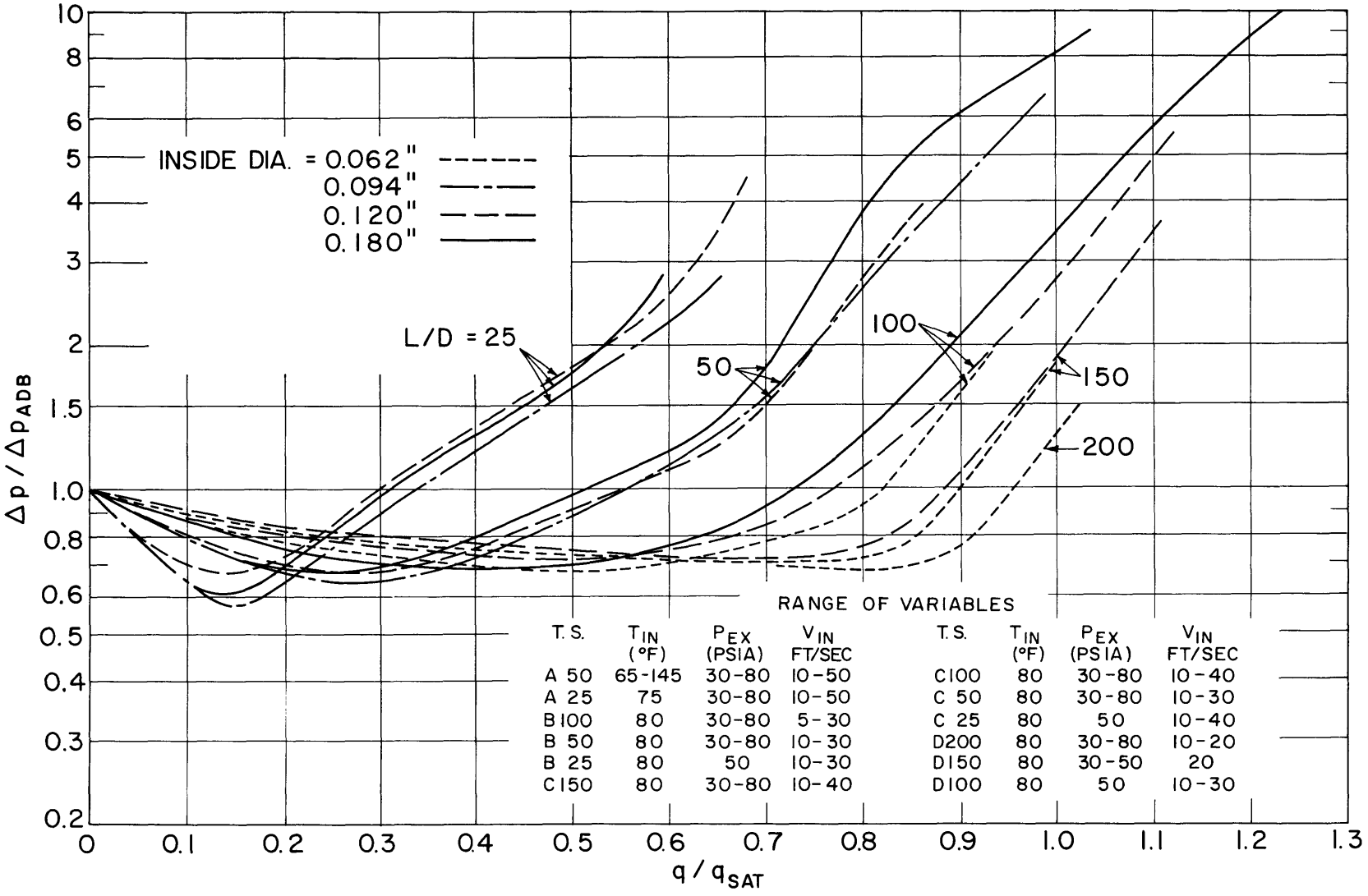

FIGURE 34: CORRELATED PRESSURE DROP DATA

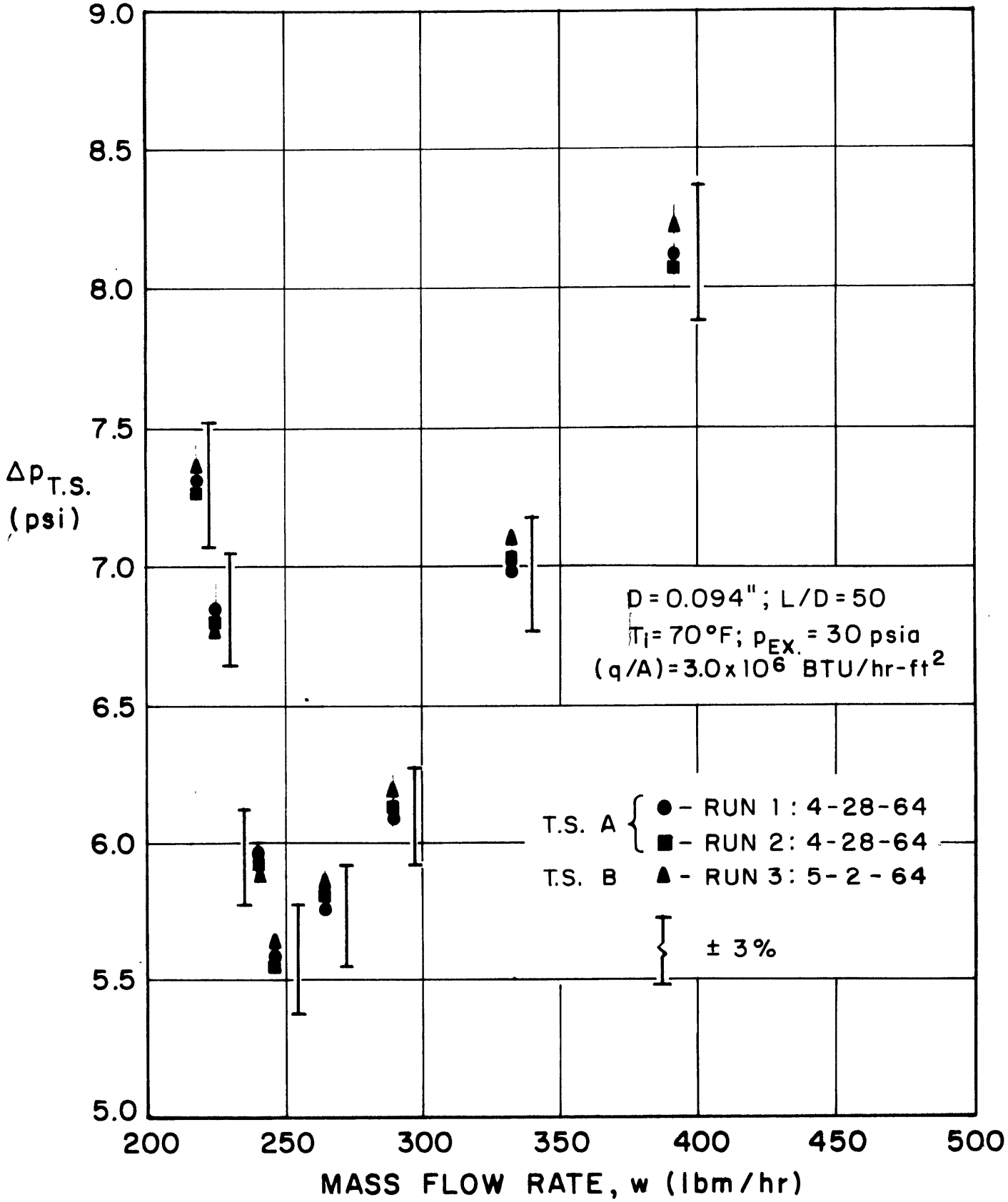

FIGURE 35: CHECK ON REPRODUCIBILITY OF DATA

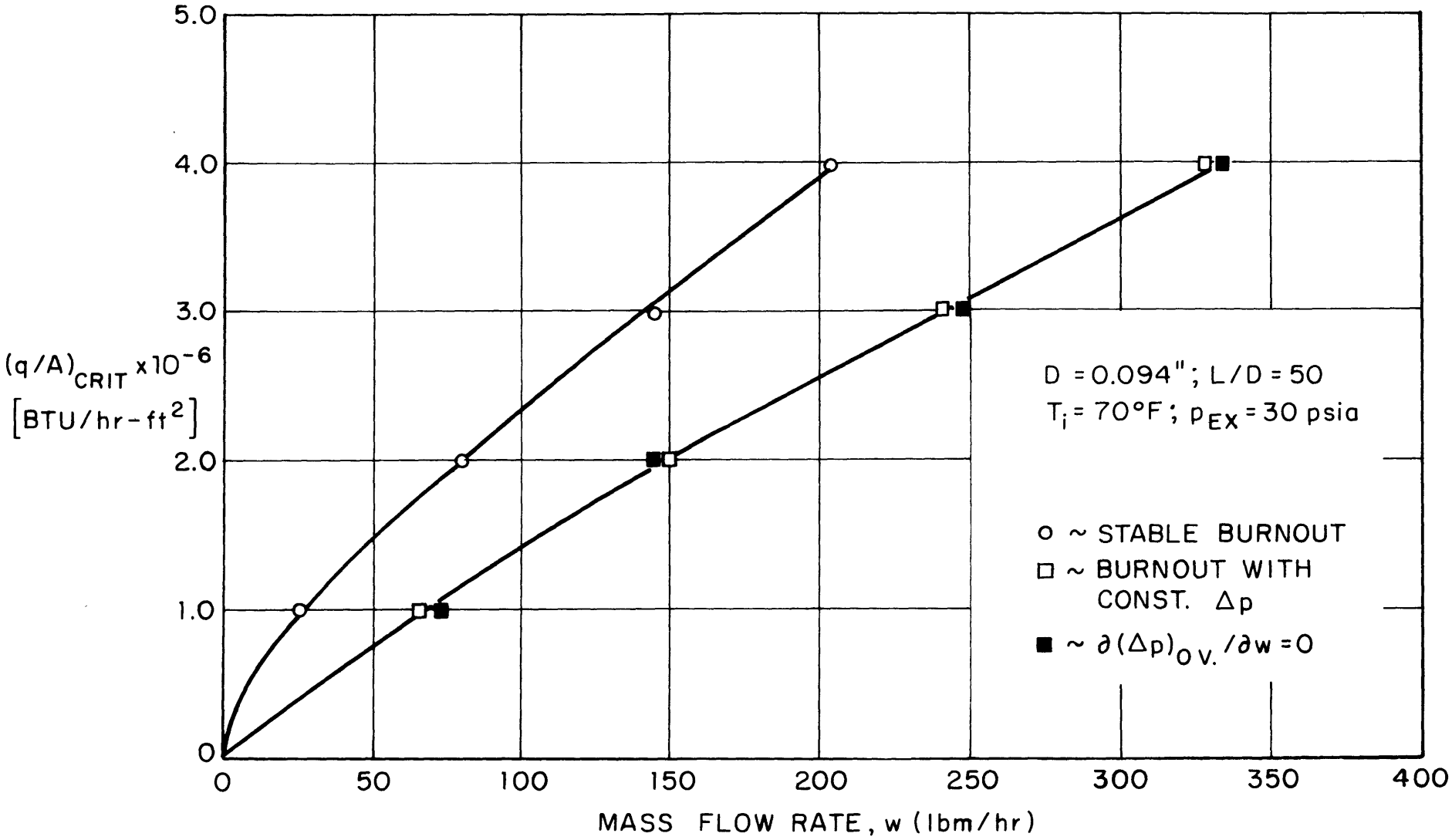

FIGURE 36: CRITICAL HEAT FLUX VS. MASS FLOW RATE FOR CONSTANT PRESSURE DROP

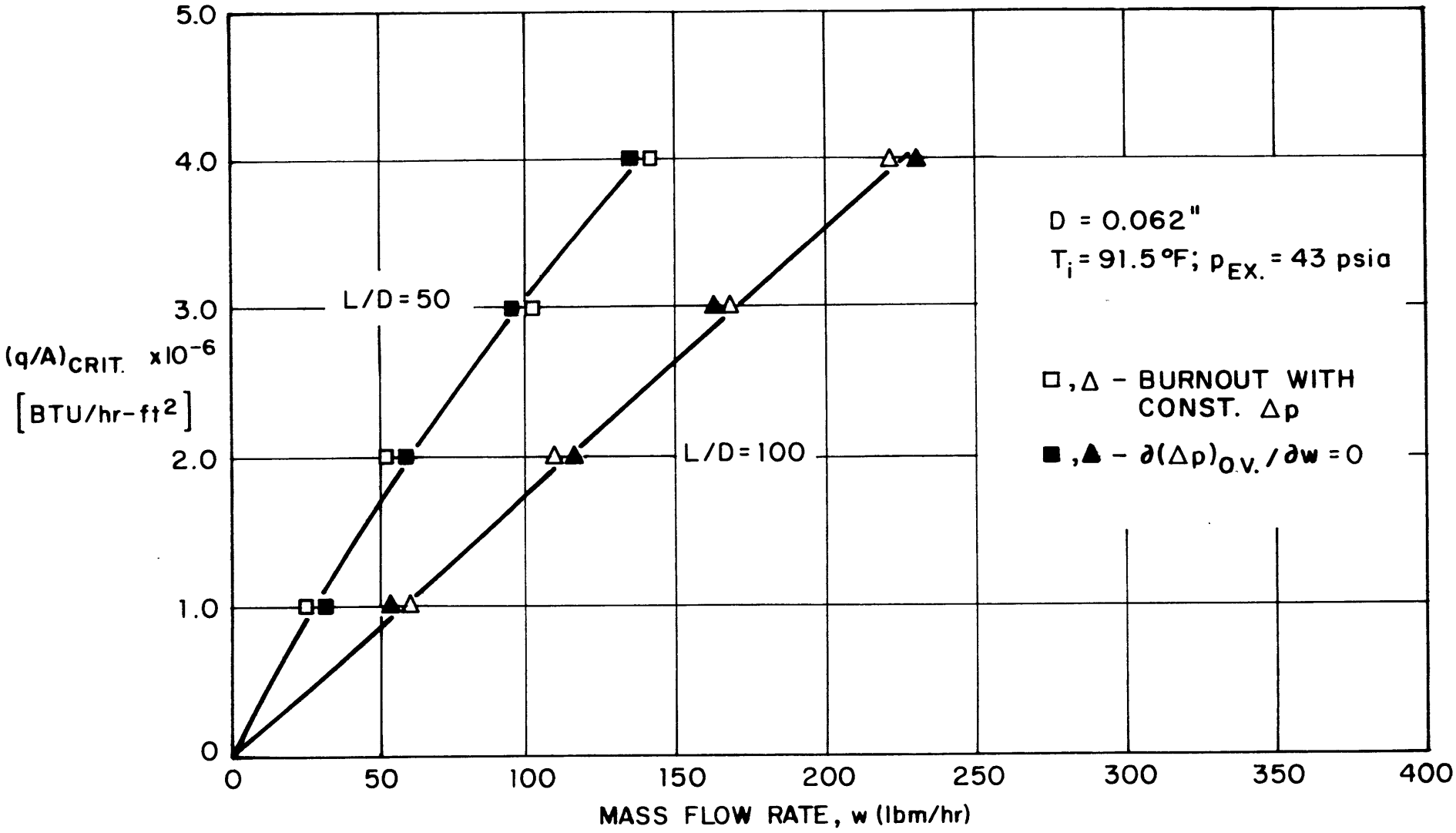

FIGURE 37: CRITICAL HEAT FLUX VS. MASS FLOW RATE FOR CONSTANT PRESSURE DROP

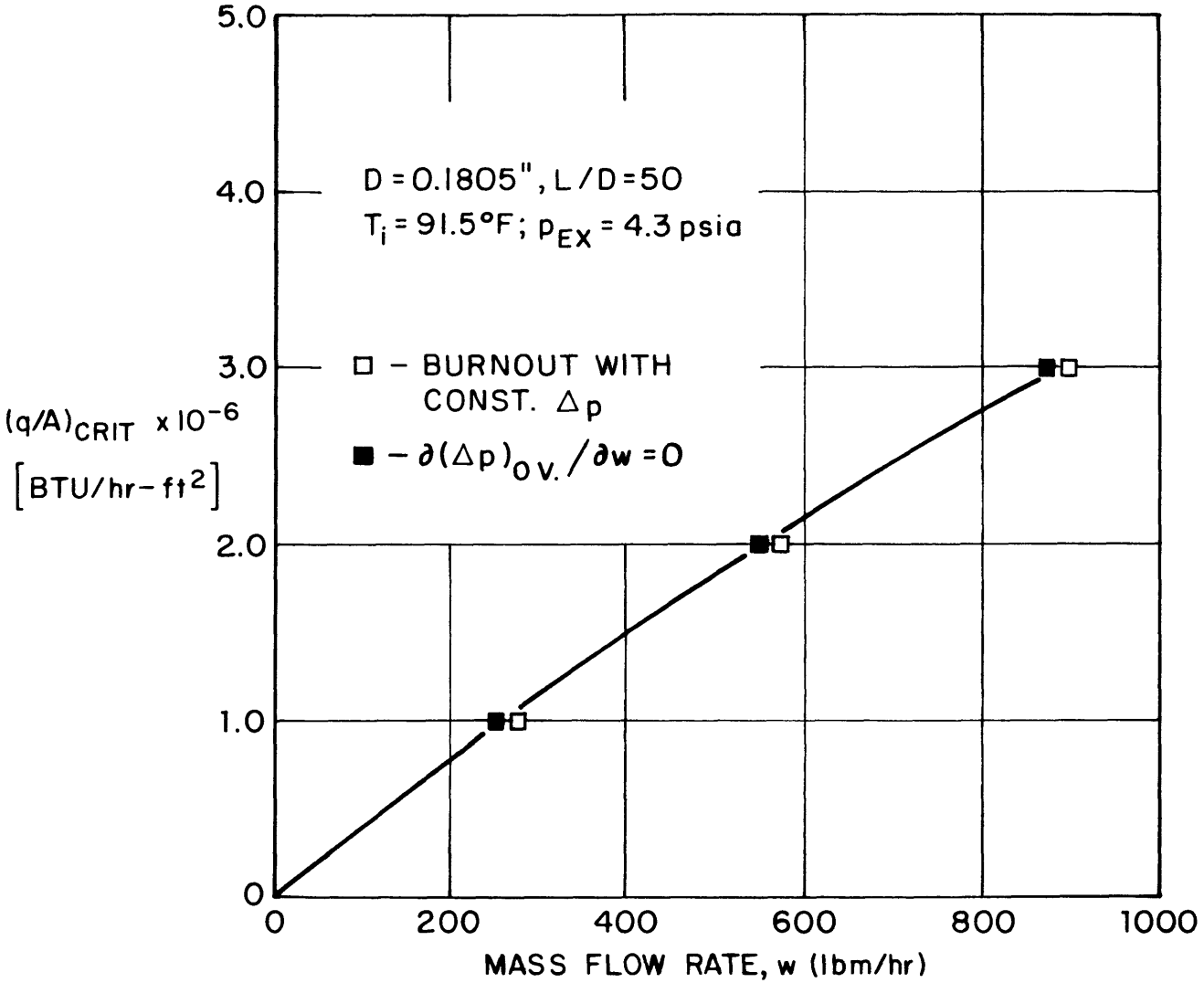

FIGURE 38: CRITICAL HEAT FLUX VS. MASS FLOW RATE FOR CONSTANT PRESSURE DROP

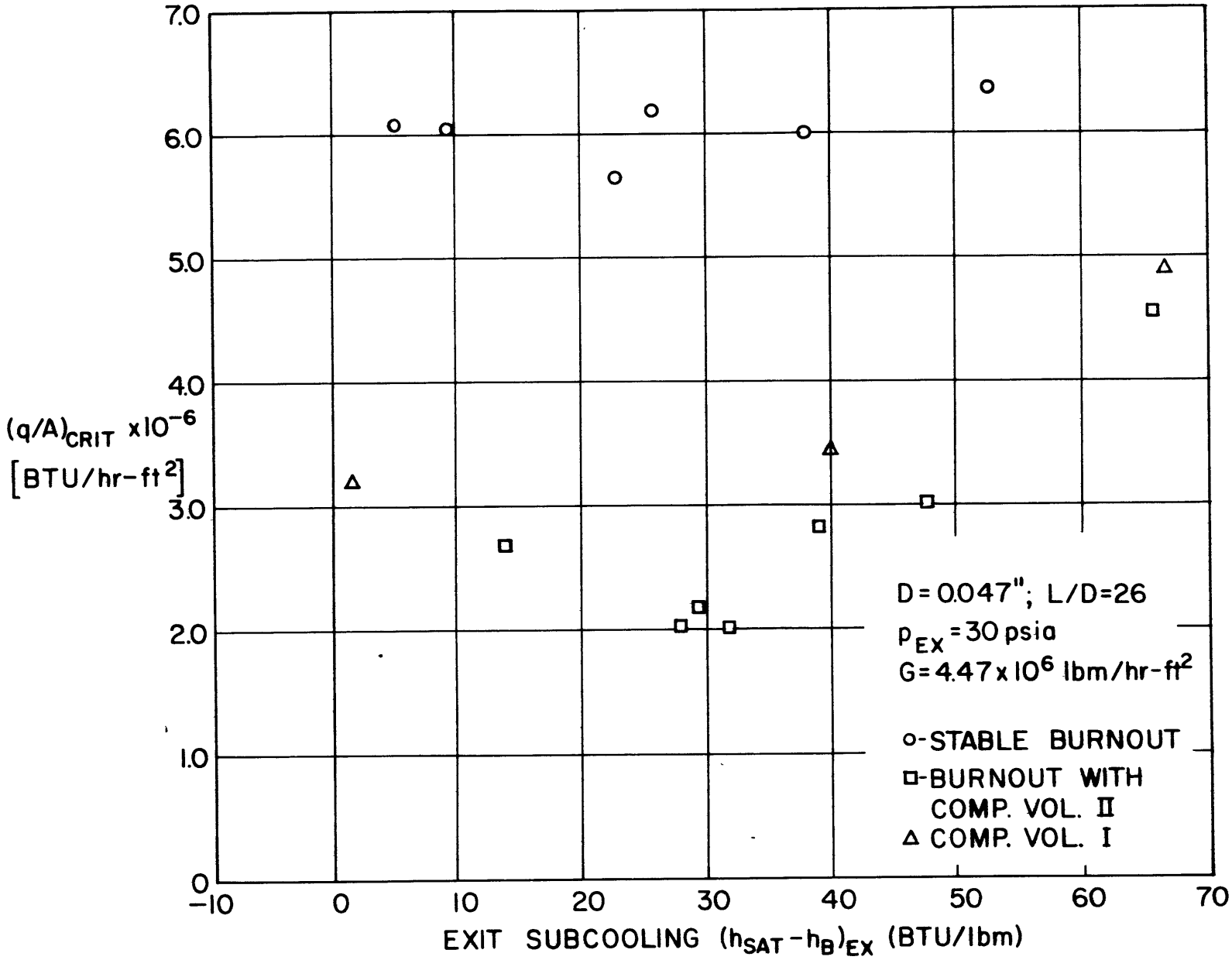

FIGURE 39: CRITICAL HEAT FLUX VS. EXIT SUBCOOLING

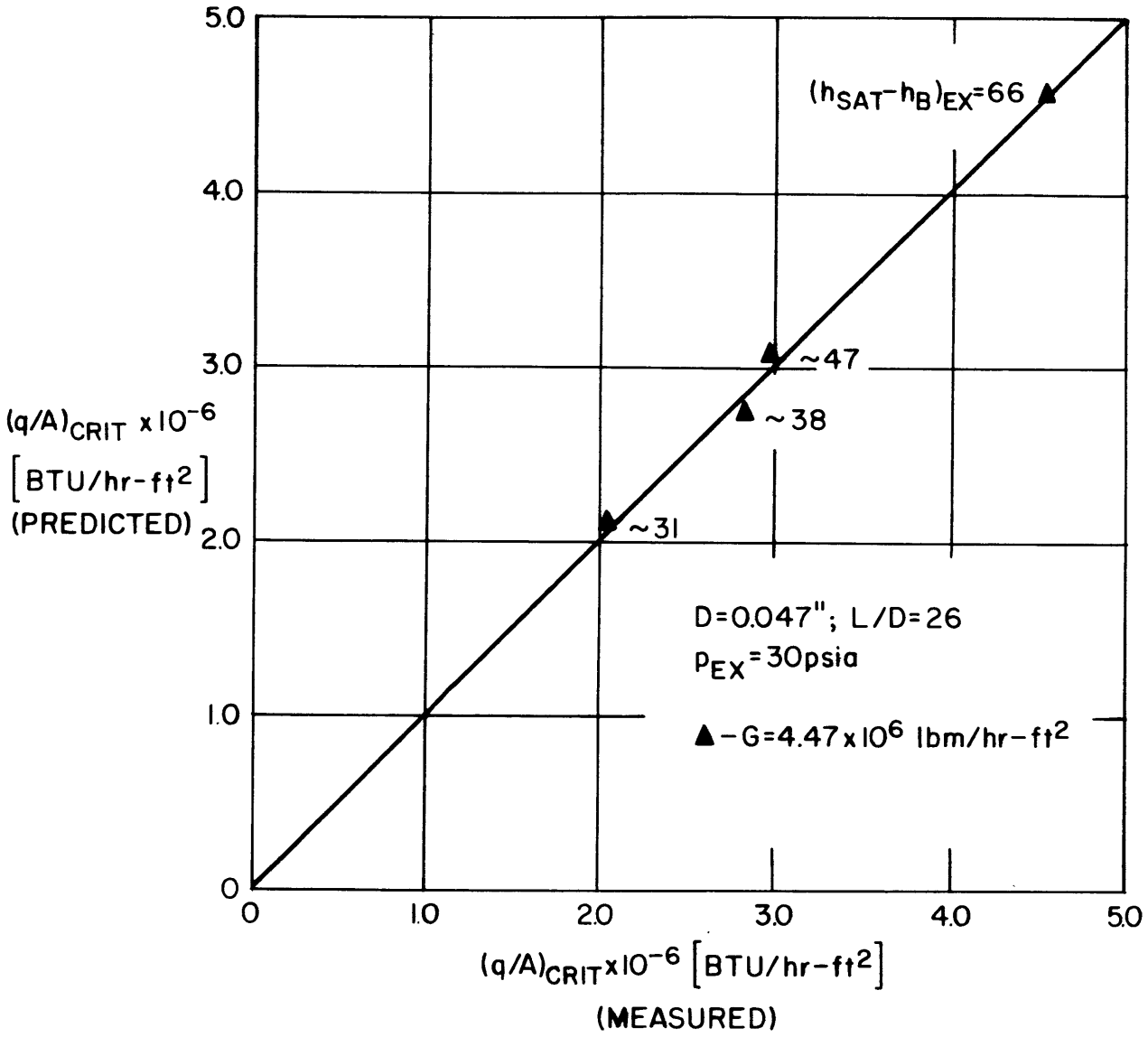

FIGURE 40: COMPARISON OF PREDICTED ONSET OF INSTABILITY WITH MEASURED CRITICAL HEAT FLUX

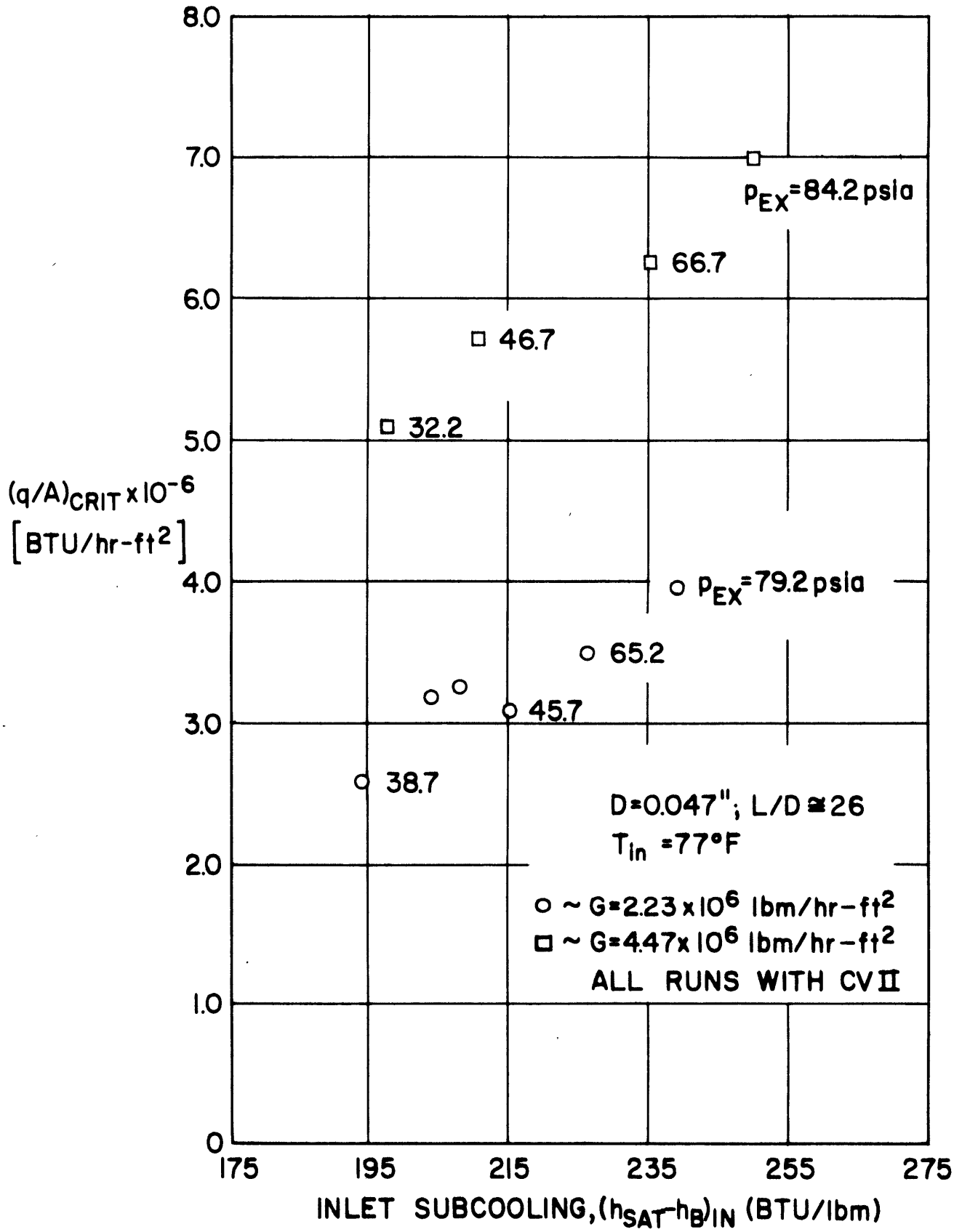

FIGURE 41: EFFECT OF PRESSURE LEVEL; CRITICAL HEAT FLUX VS. INLET SUBCOOLING

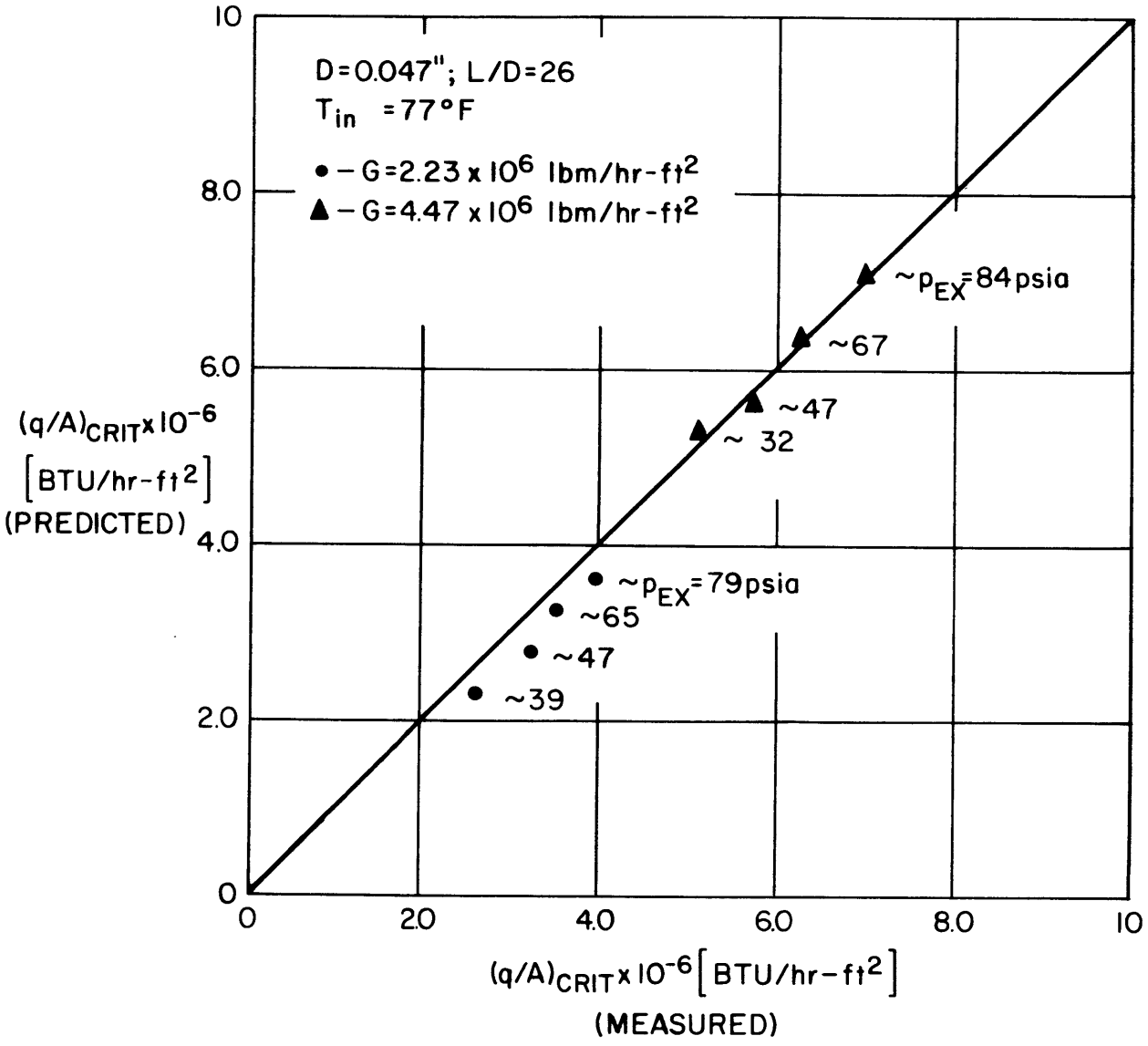

FIGURE 42: COMPARISON OF PREDICTED ONSET OF INSTABILITY WITH MEASURED CRITICAL HEAT FLUX

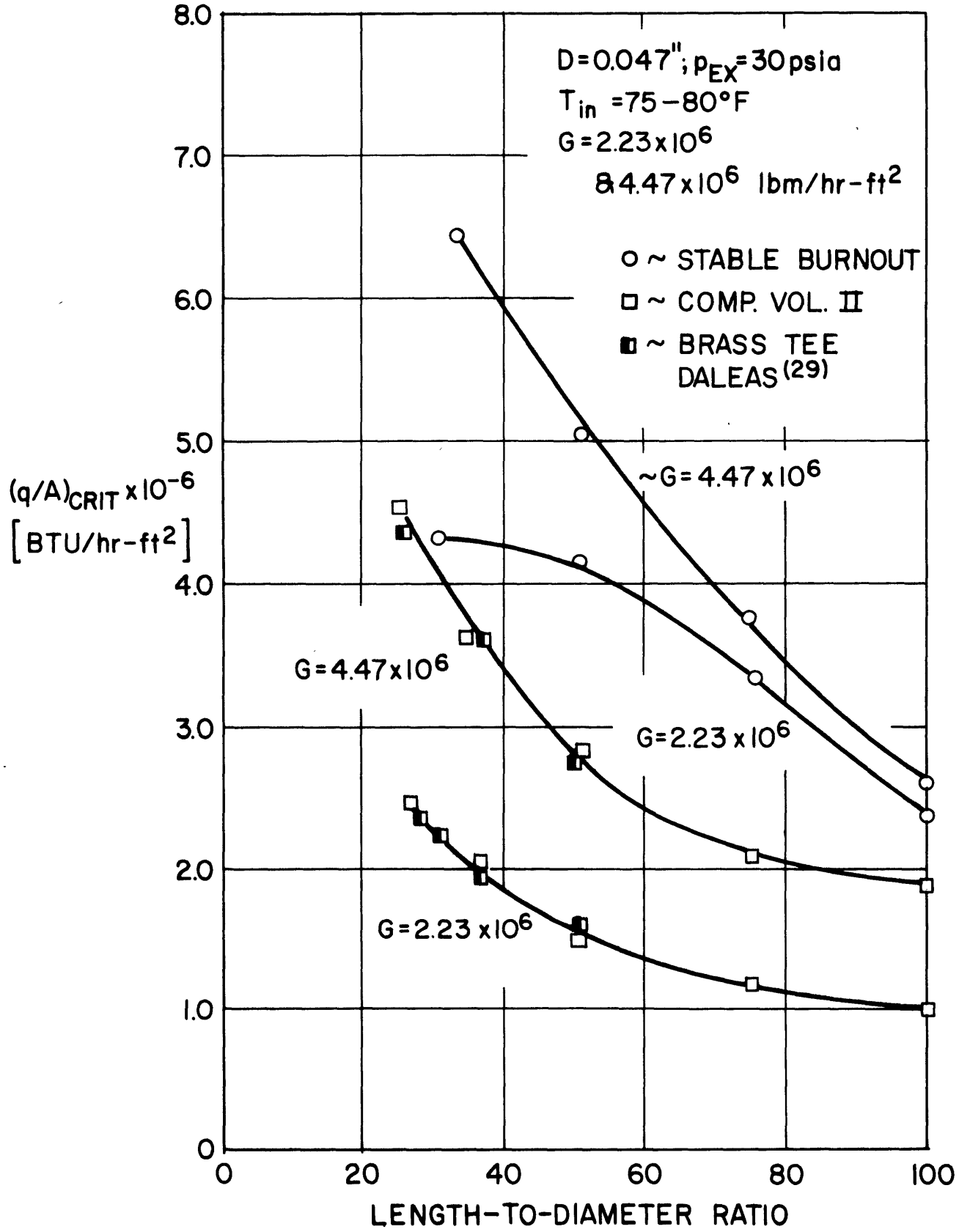

FIGURE 43 - CRITICAL HEAT FLUX VS. LENGTH TO DIAMETER RATIO

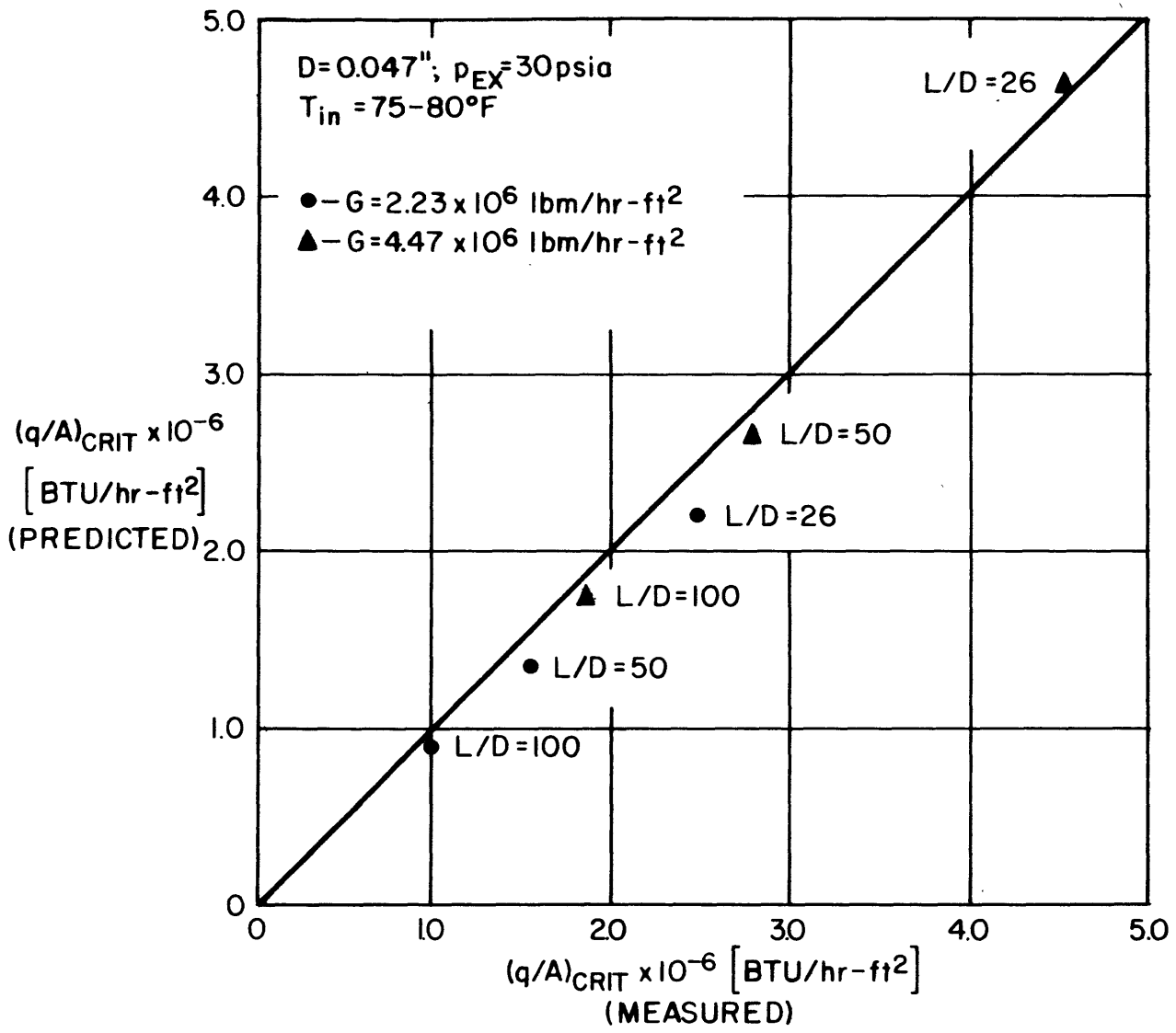

FIGURE 44: COMPARISON OF PREDICTED ONSET OF INSTABILITY WITH MEASURED CRITICAL HEAT FLUX

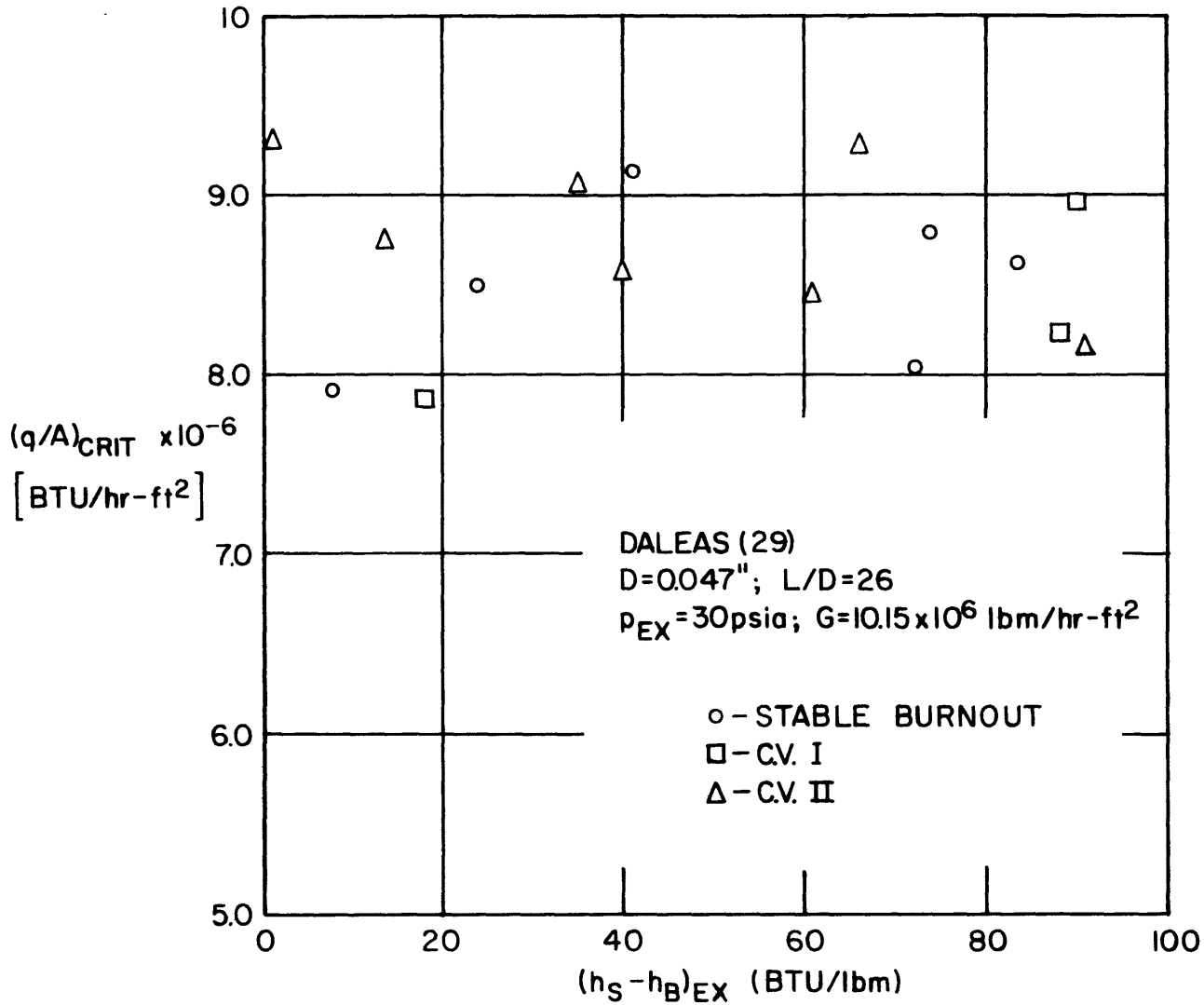

FIGURE 45: CRITICAL HEAT FLUX VS. EXIT SUBCOOLING

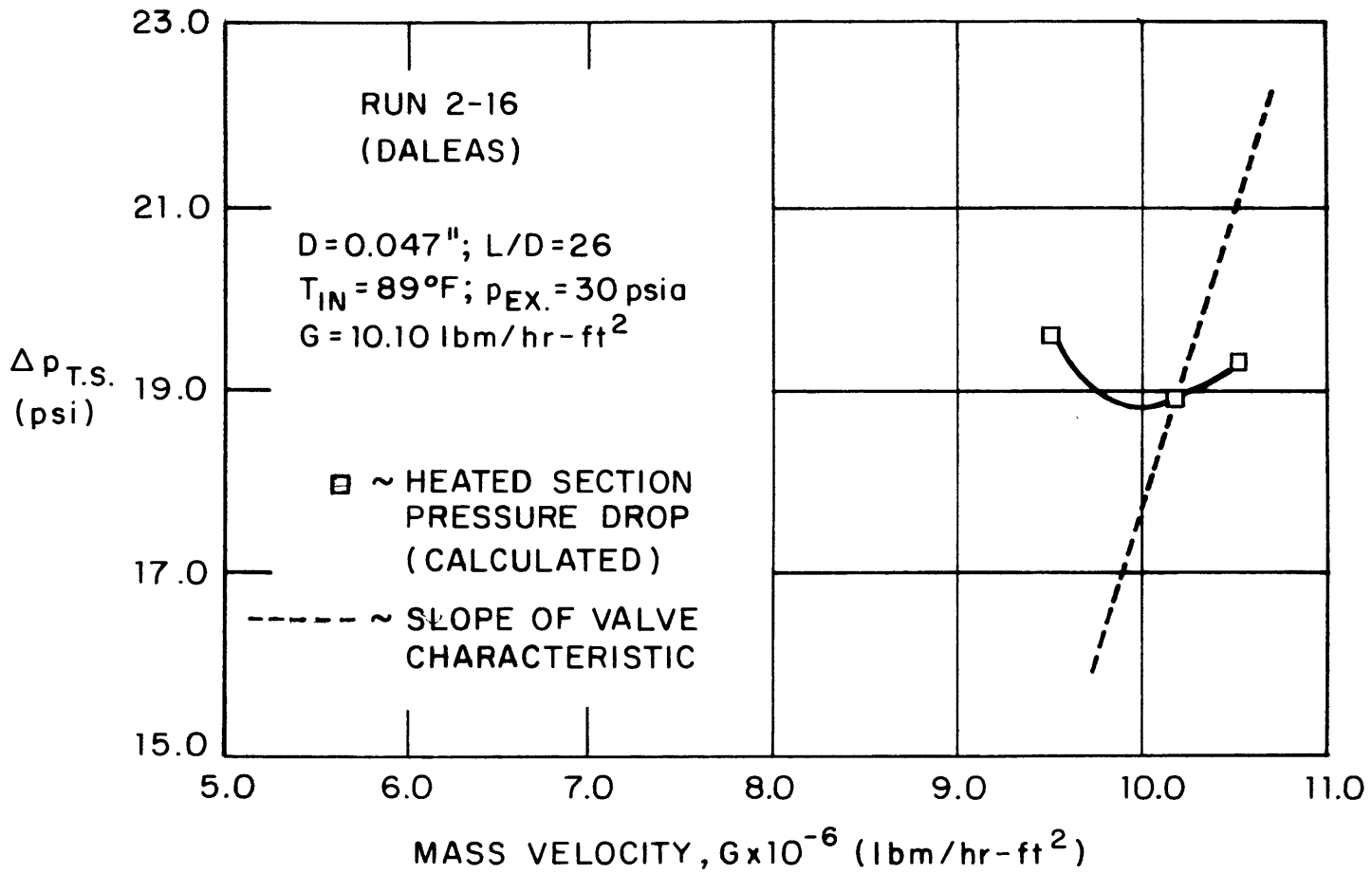

FIGURE 46: COMPARISON OF SLOPES IN STABLE OPERATION

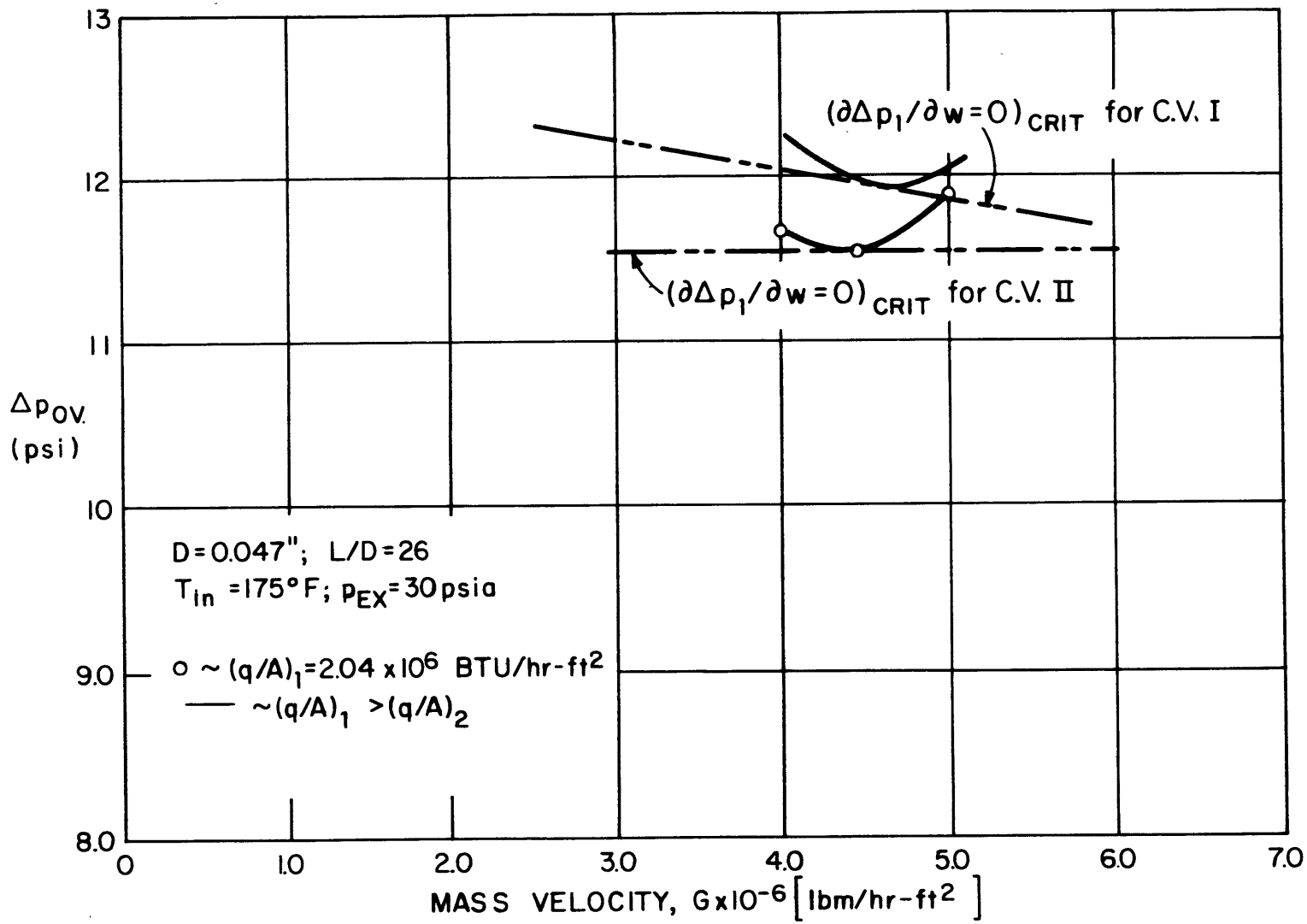

FIGURE 47 COMPARISON OF CRITICAL SLOPES FOR C.V. I & C.V. II

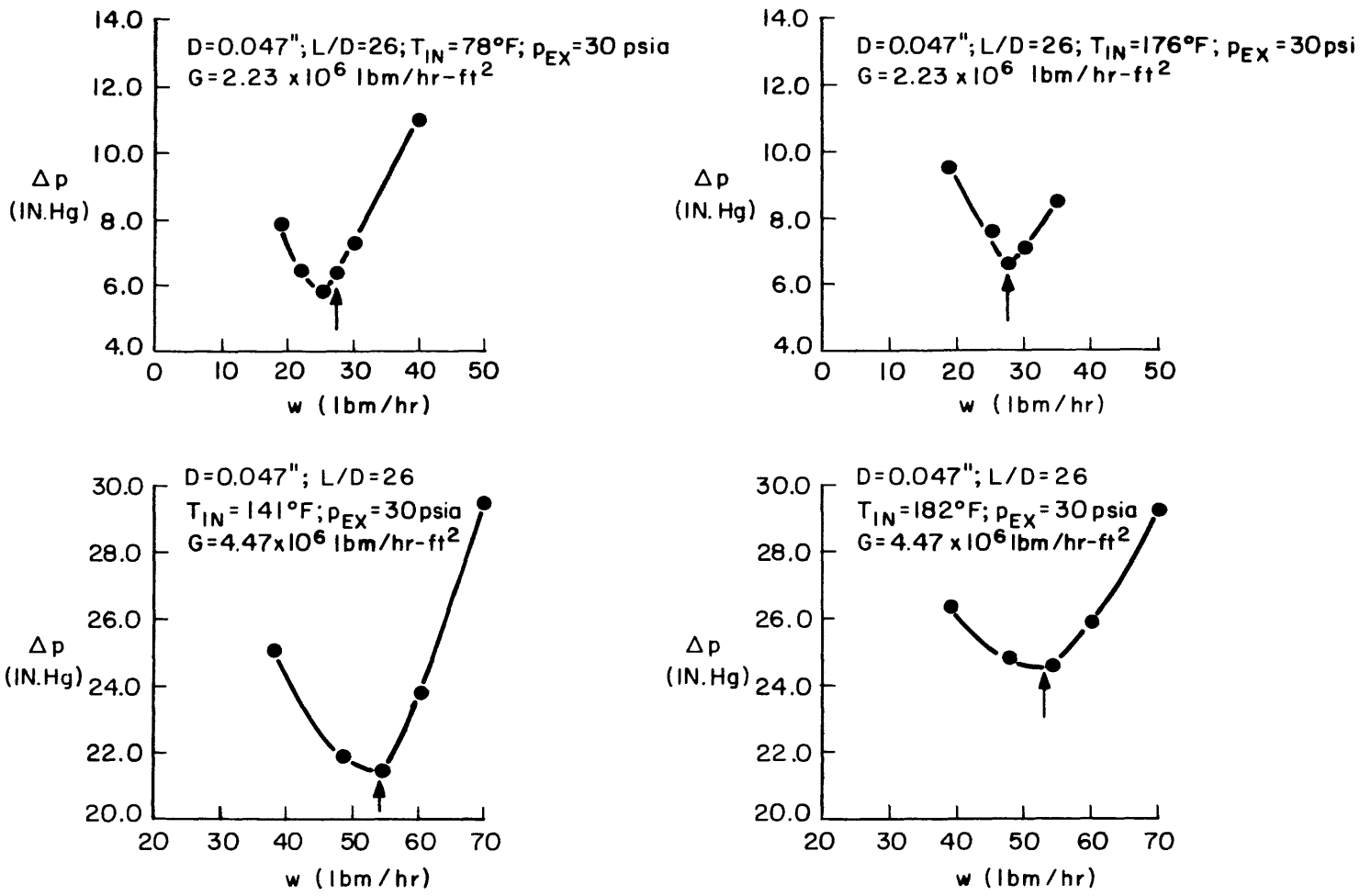

FIGURE 48: EXPERIMENTAL VERIFICATION OF LOCATION OF MINIMUM

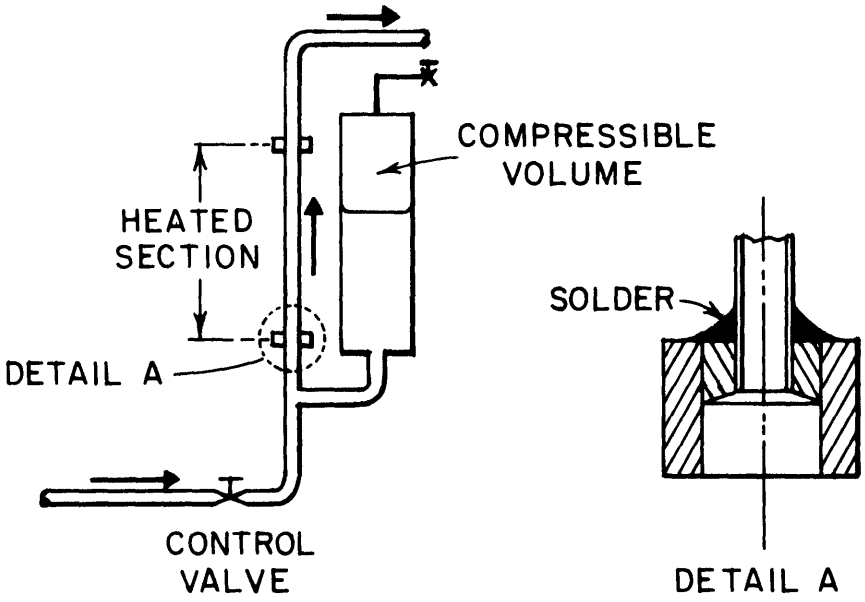

FIGURE 49: SKETCH OF LOWDERMILK'S[25] COMPRESSIBLE VOLUME CONFIGURATION WITH DETAIL OF TEST SECTION INLET

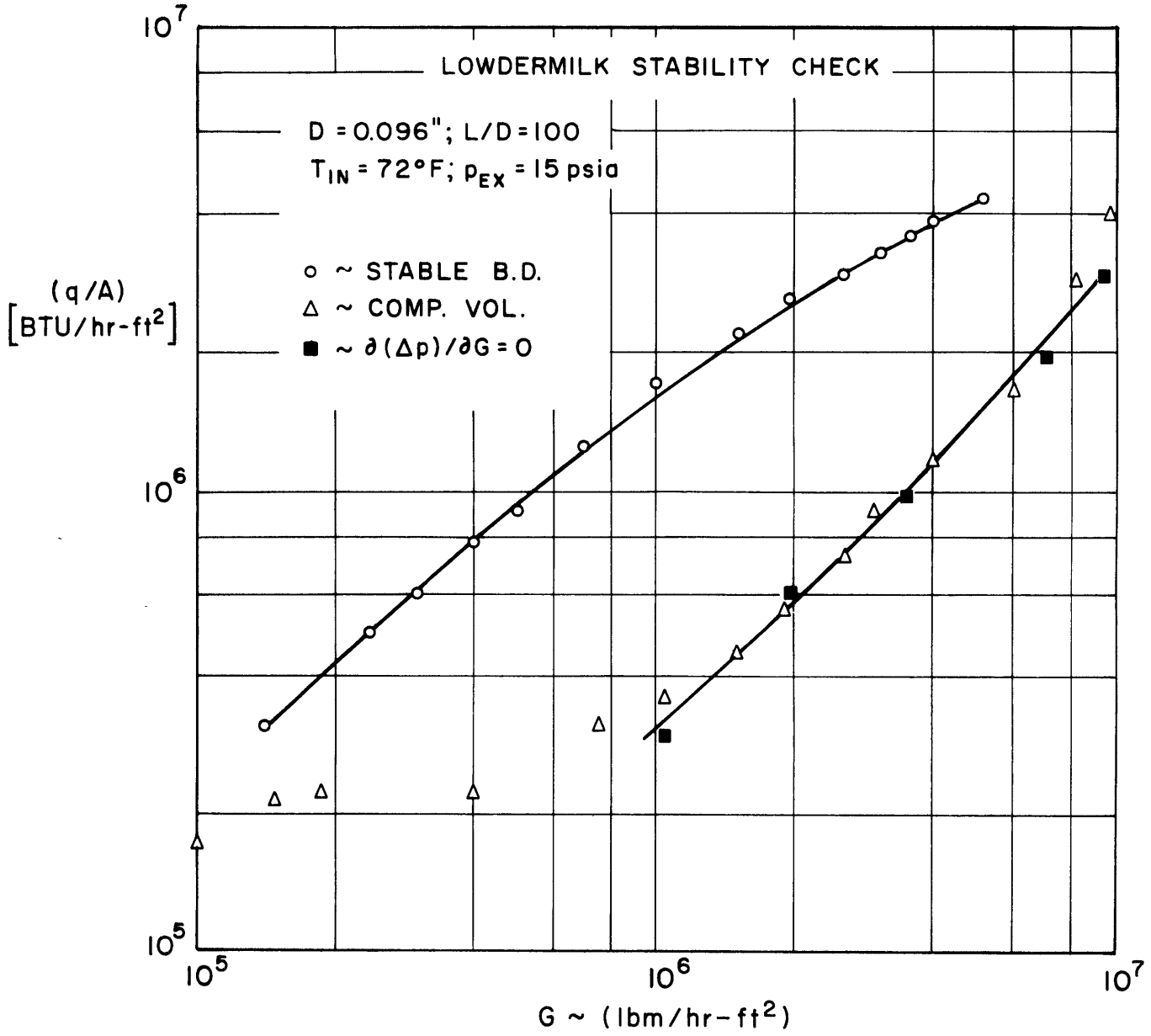

FIGURE 50: COMPARISON OF STABLE AND UNSTABLE CONDITIONS FROM LOWDERMILK ET AL.[25]

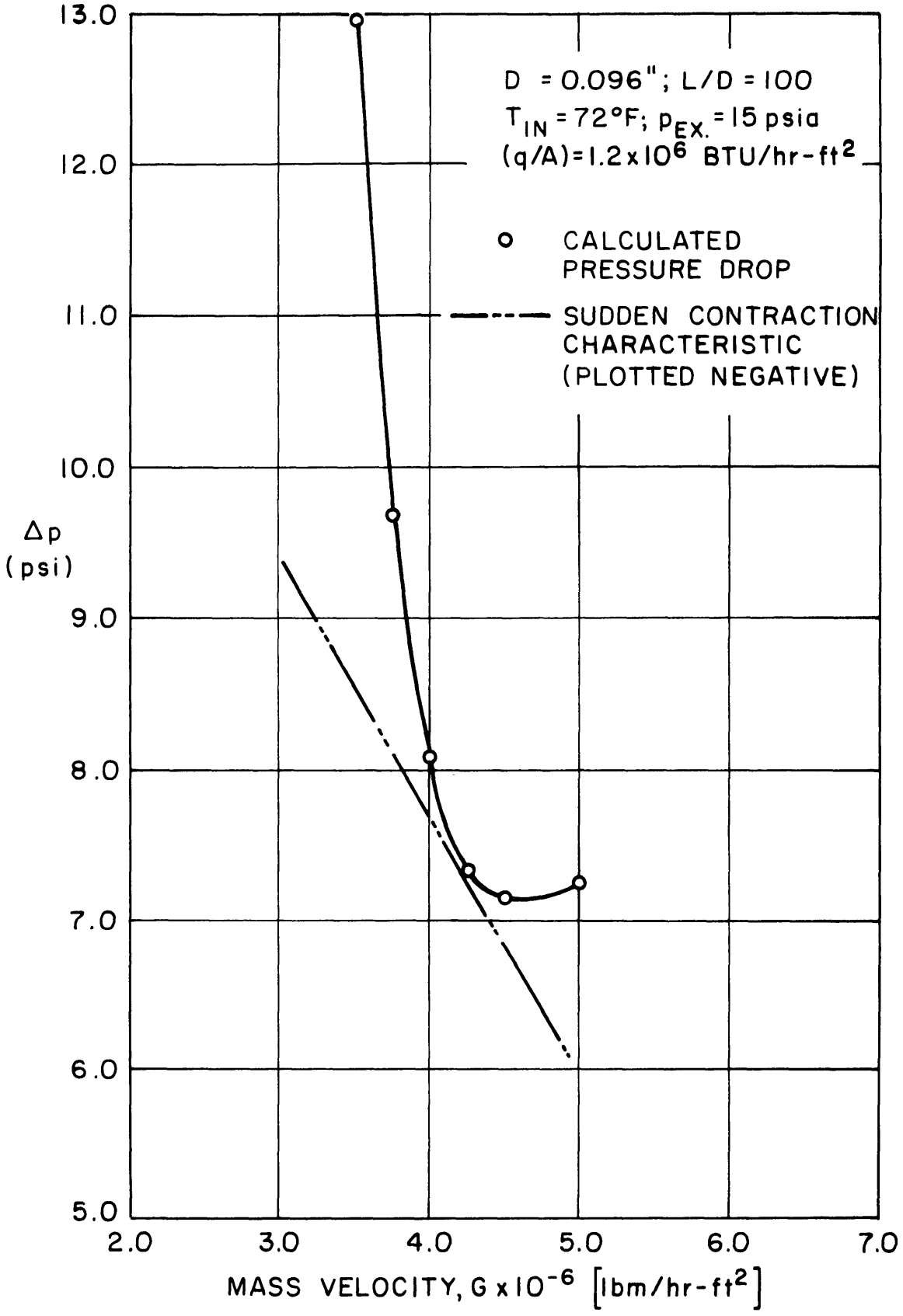

FIGURE 51 DETERMINATION OF MINIMUM LOCATION (LOWDERMILK ET. AL.[25])

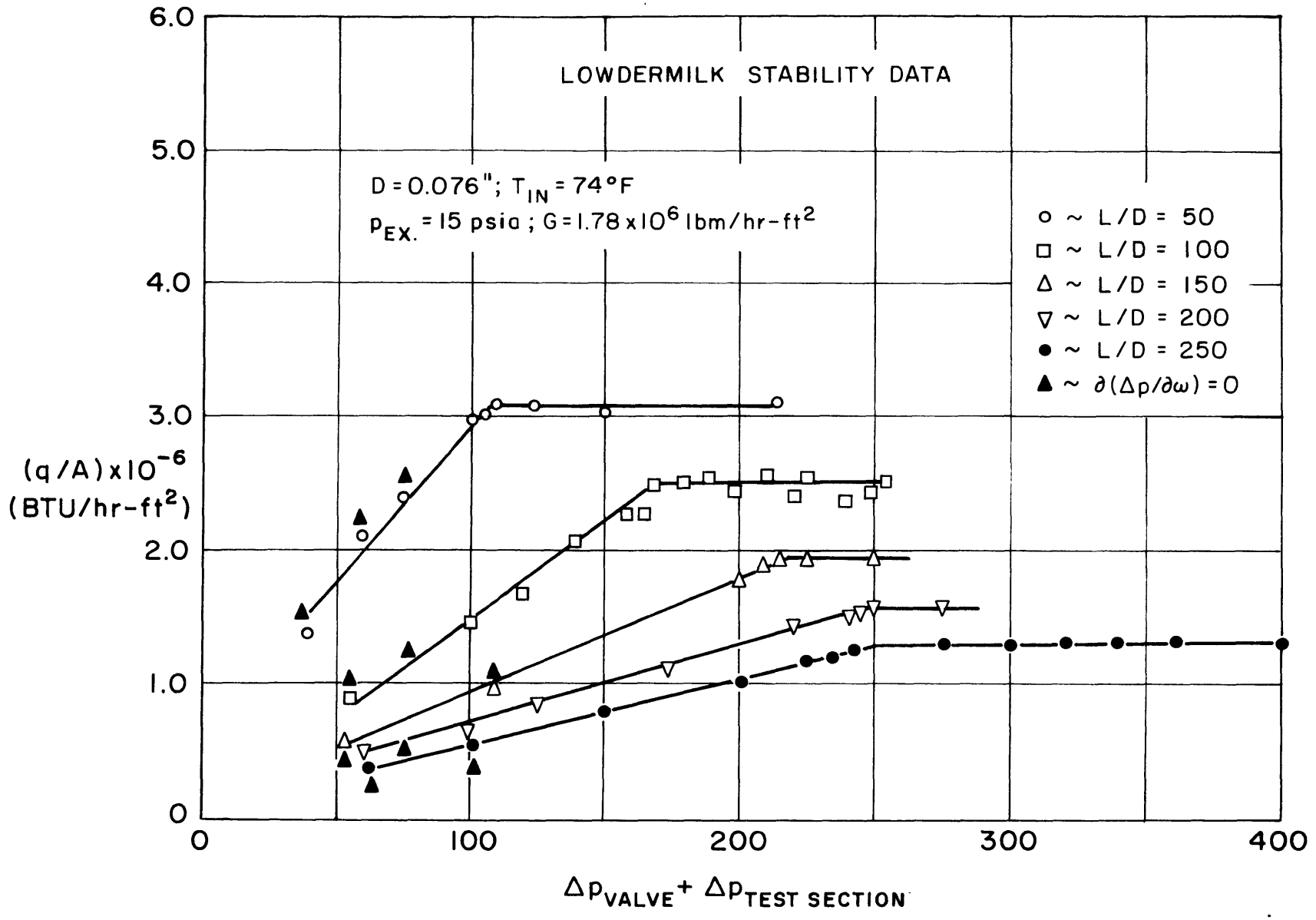

FIGURE 52 DATA OF LOWDERMILK ON EFFECT OF UPSTREAM THROTTLING

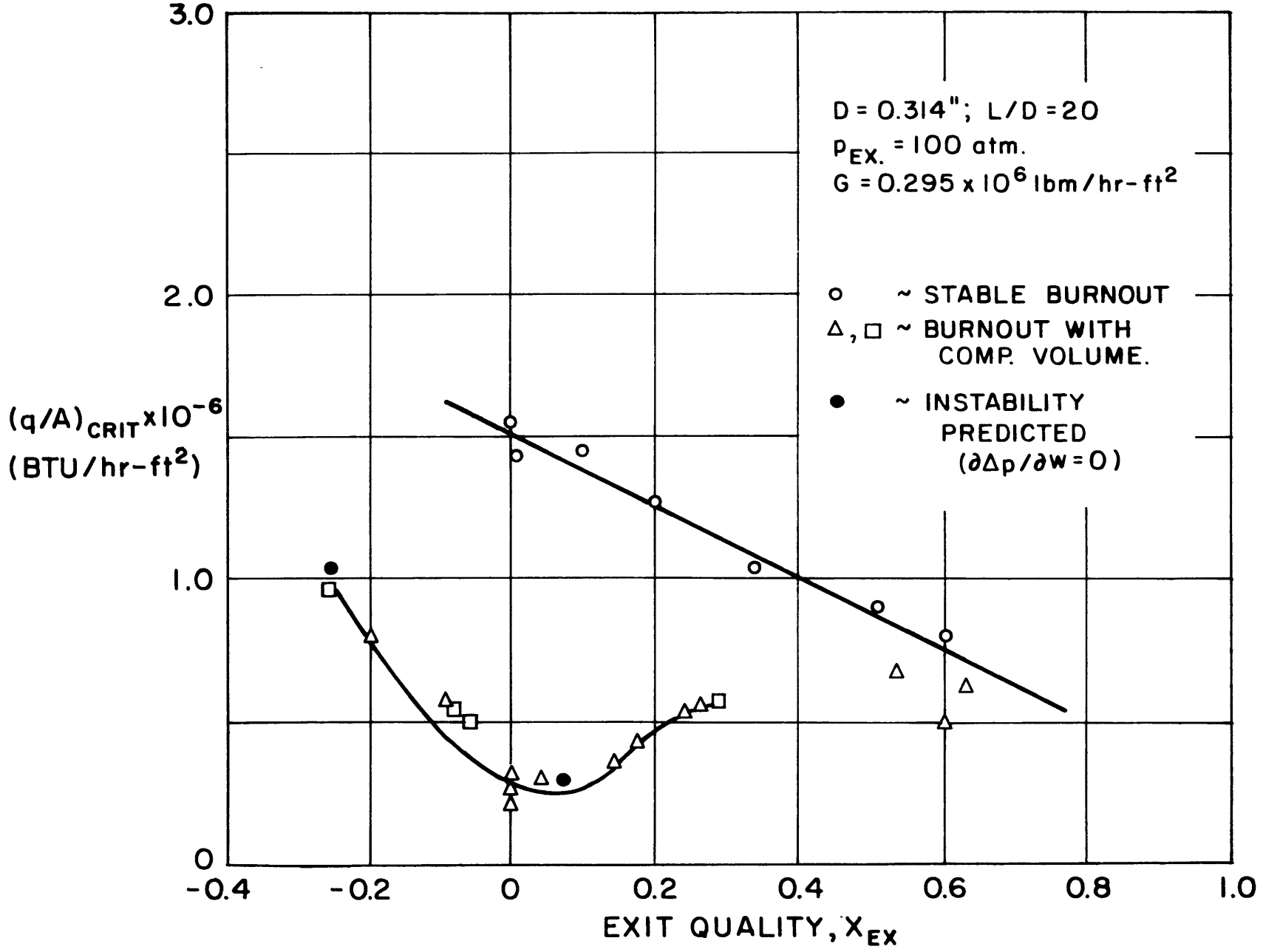

FIGURE 53 COMPARISON WITH DATA OF ALADIEV ET AL.[26]

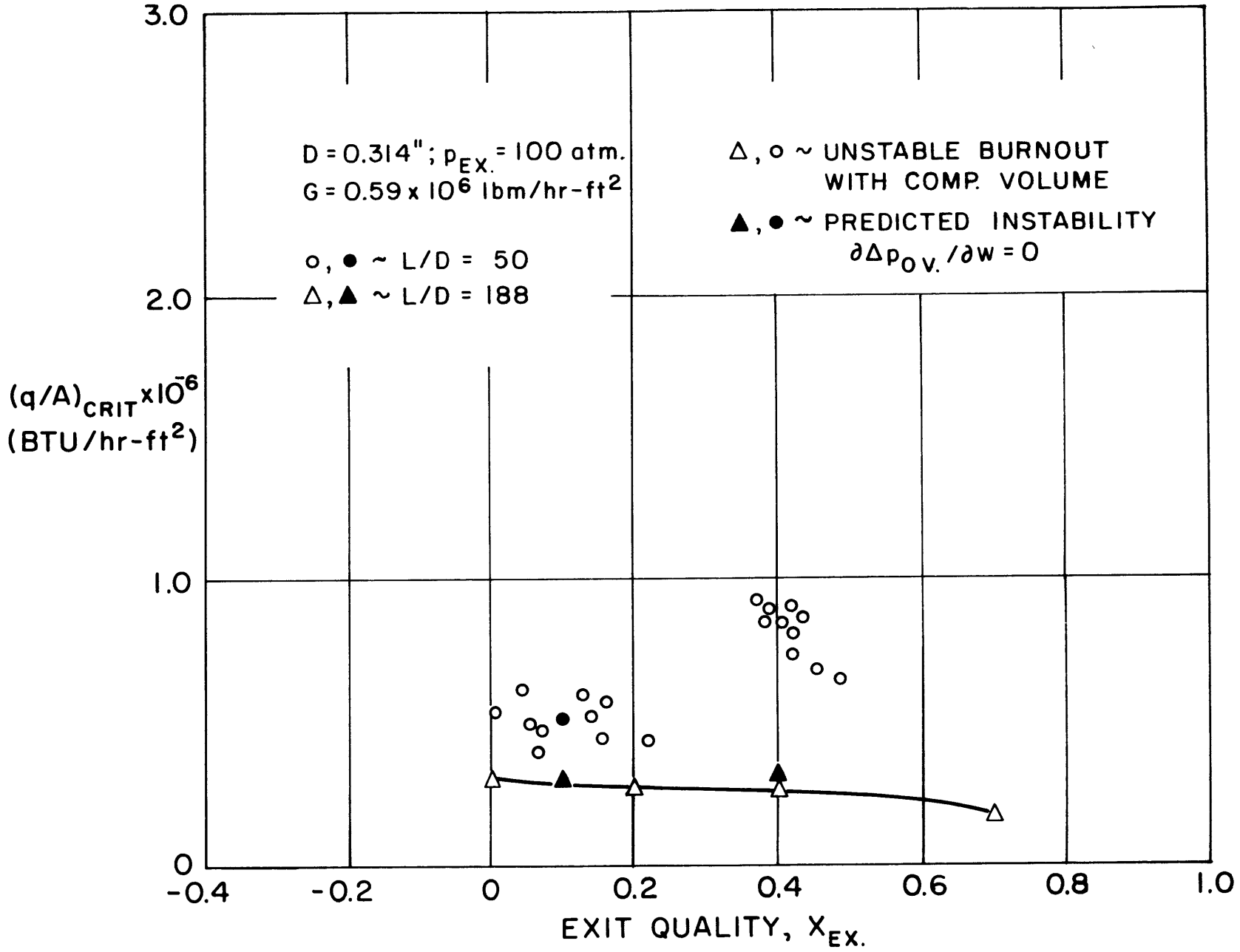

FIGURE 54 COMPARISON WITH DATA OF ALADIEV ET AL.[26]

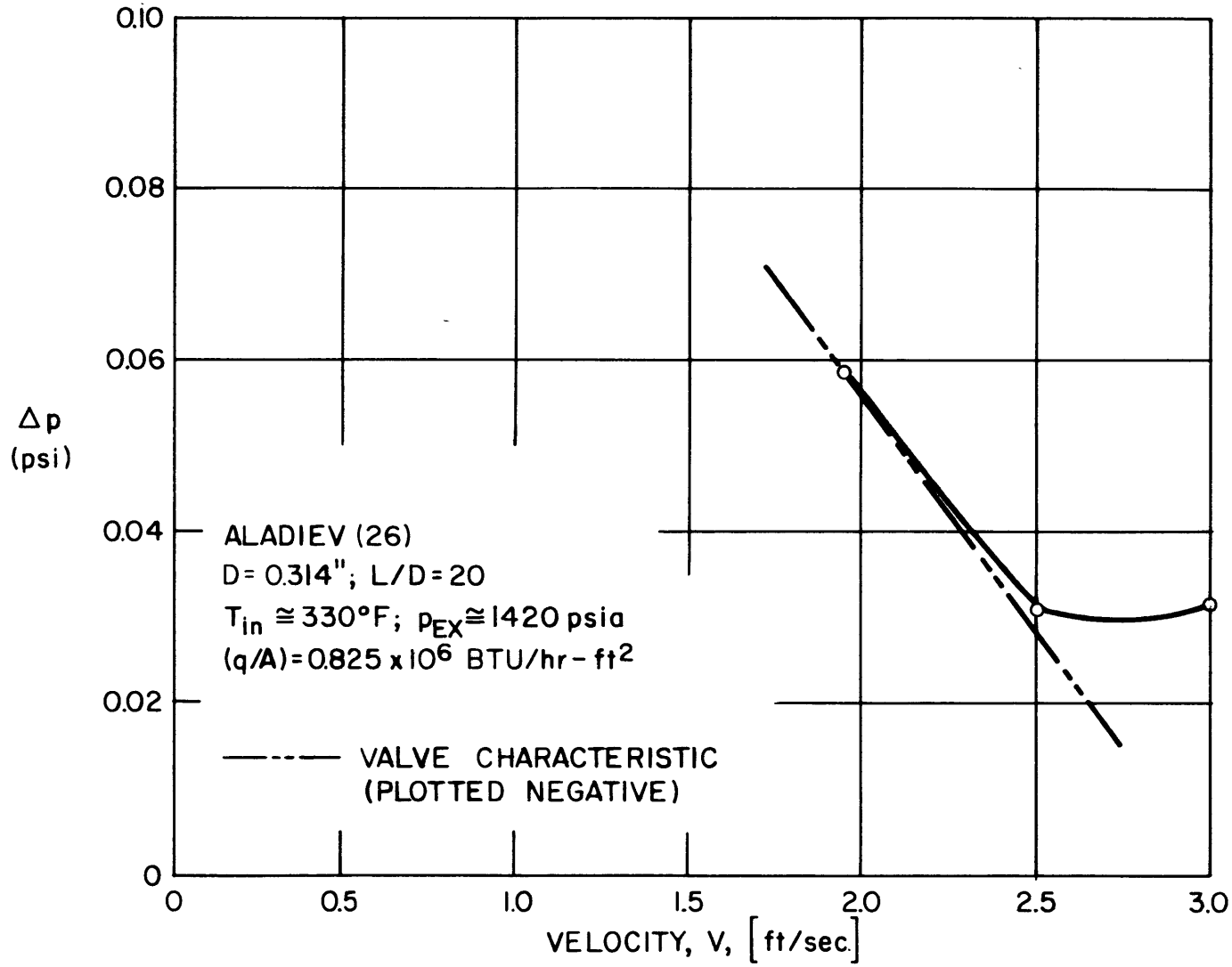

FIGURE 55: COMPARISON OF CRITICAL SLOPES AT CRITICAL HEAT FLUX

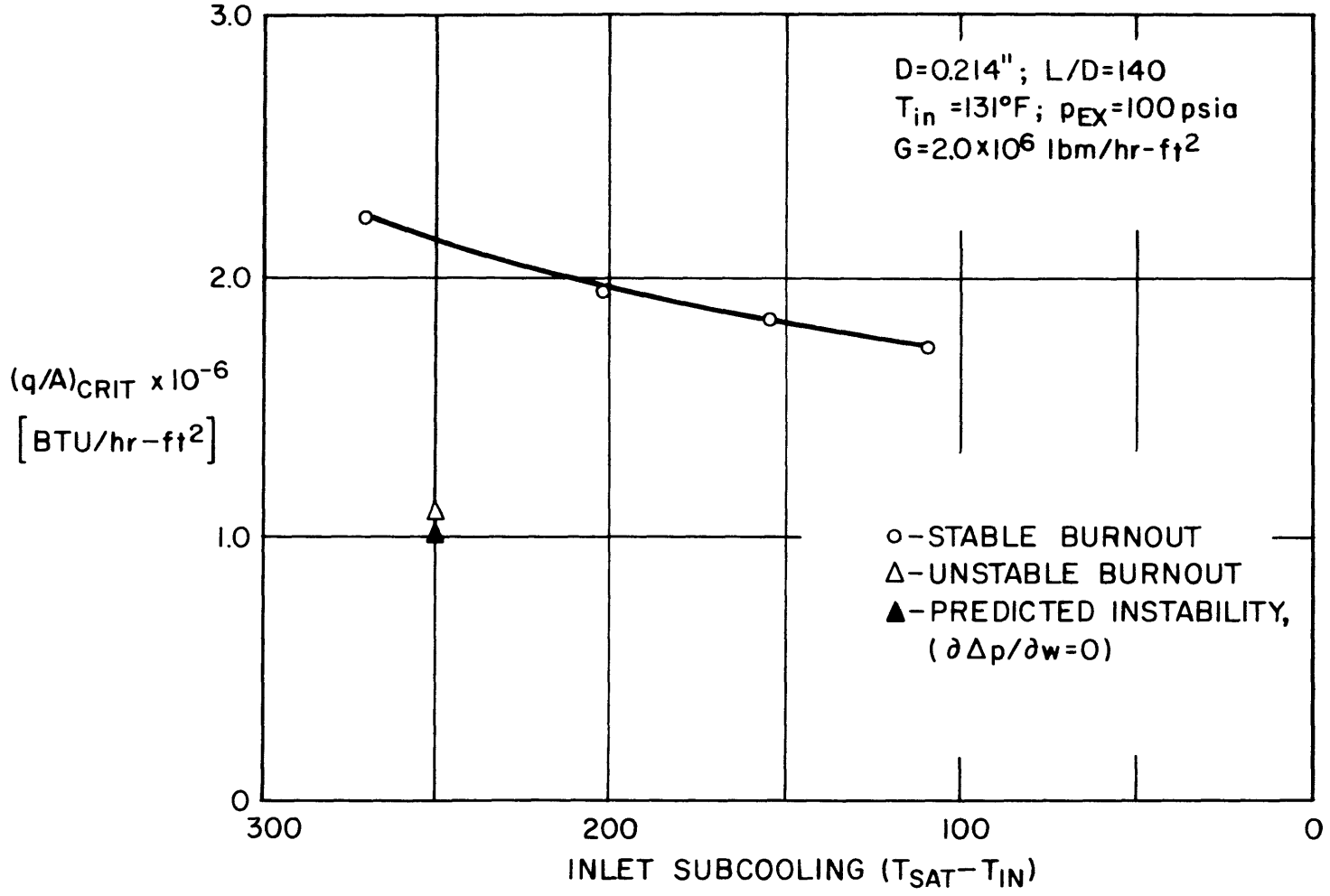

FIGURE 56: COMPARISON WITH DATA OF TODREAS (39)

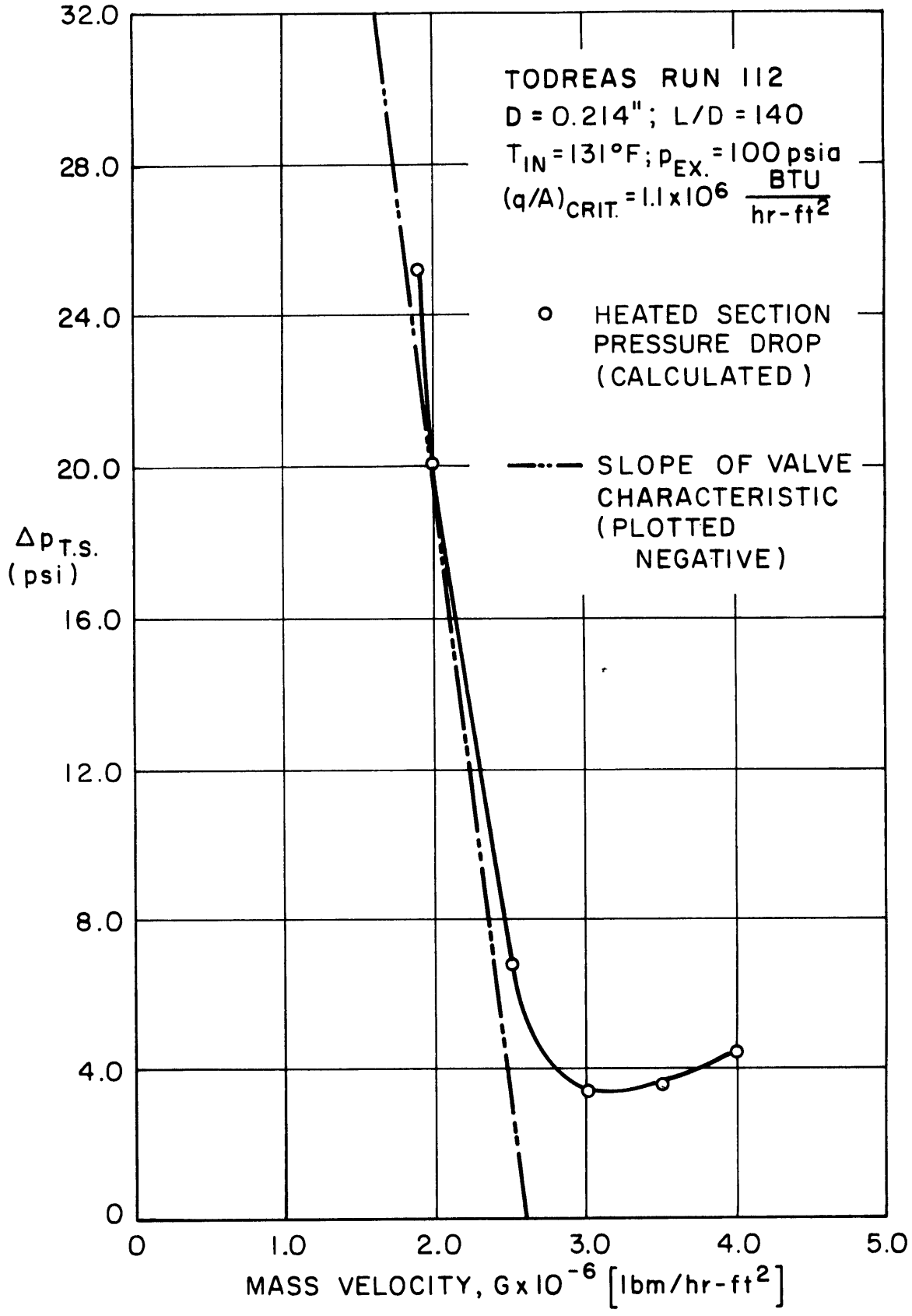

FIGURE 57: DETERMINATION OF LOCATION OF MINIMUM

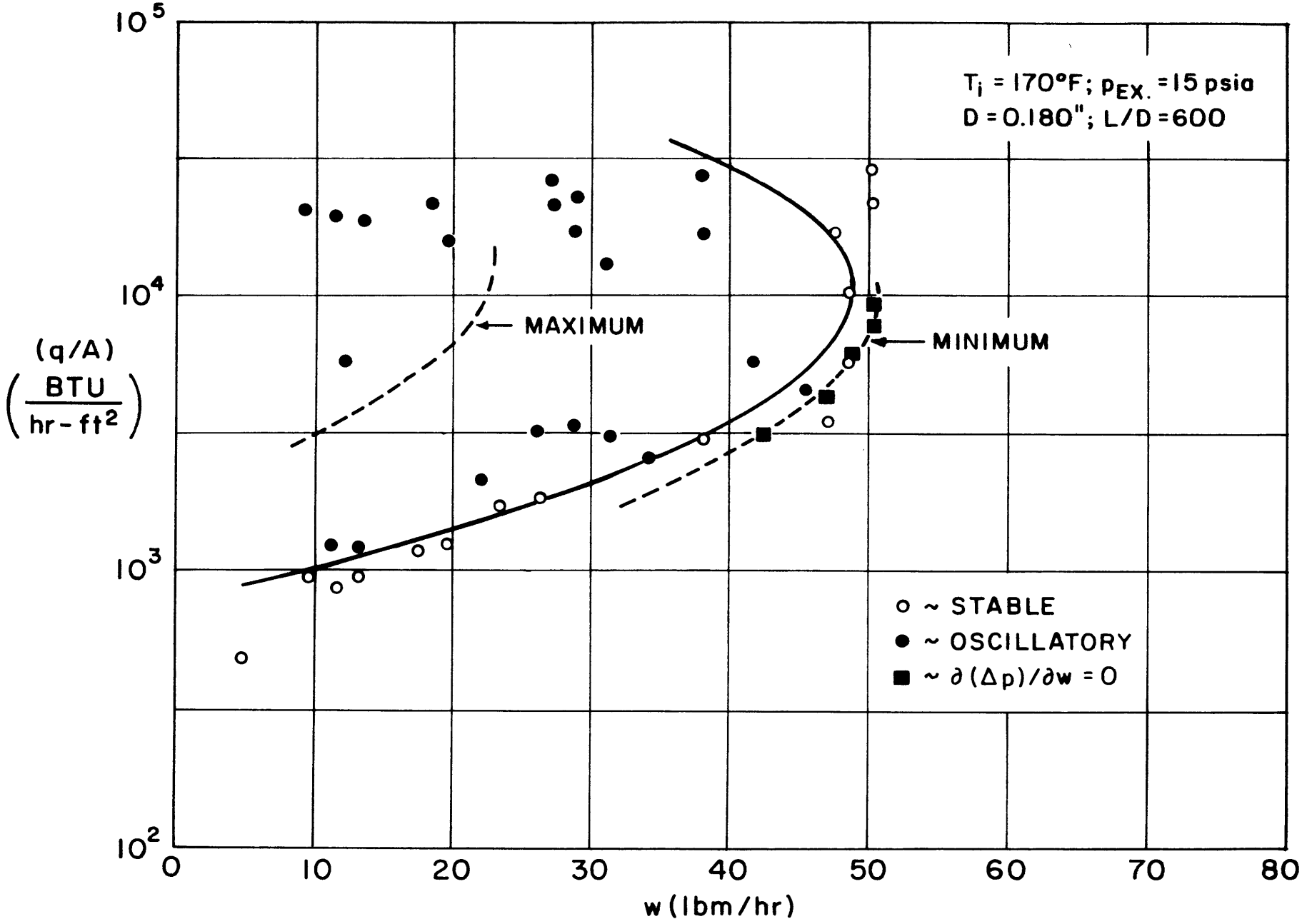

FIGURE 58 COMPARISON OF CRITERION WITH ANDOH'S [40] STABILITY MAP

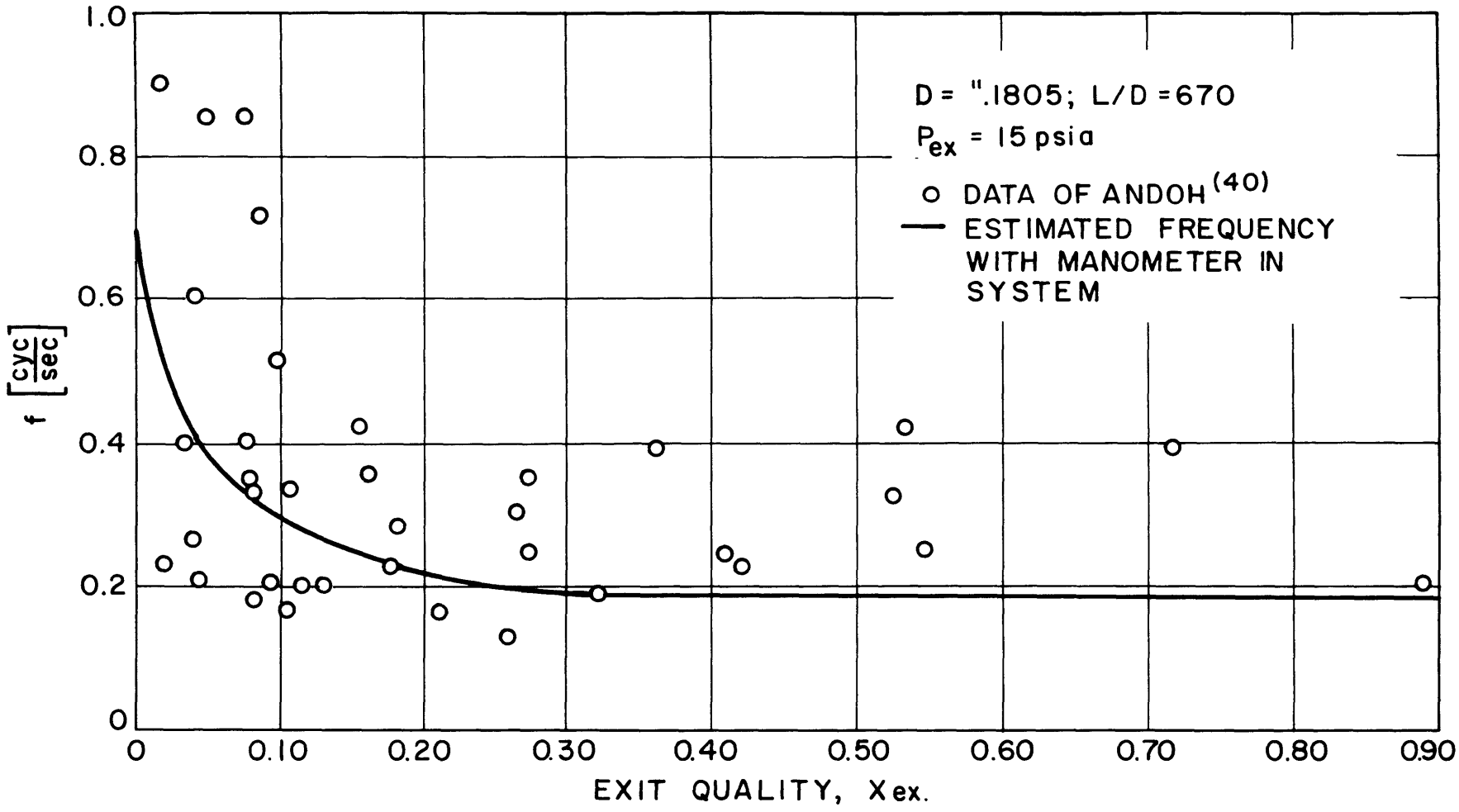

FIGURE 59: FREQUENCY MEASUREMENTS OF OSCILLATORY INSTABILITY

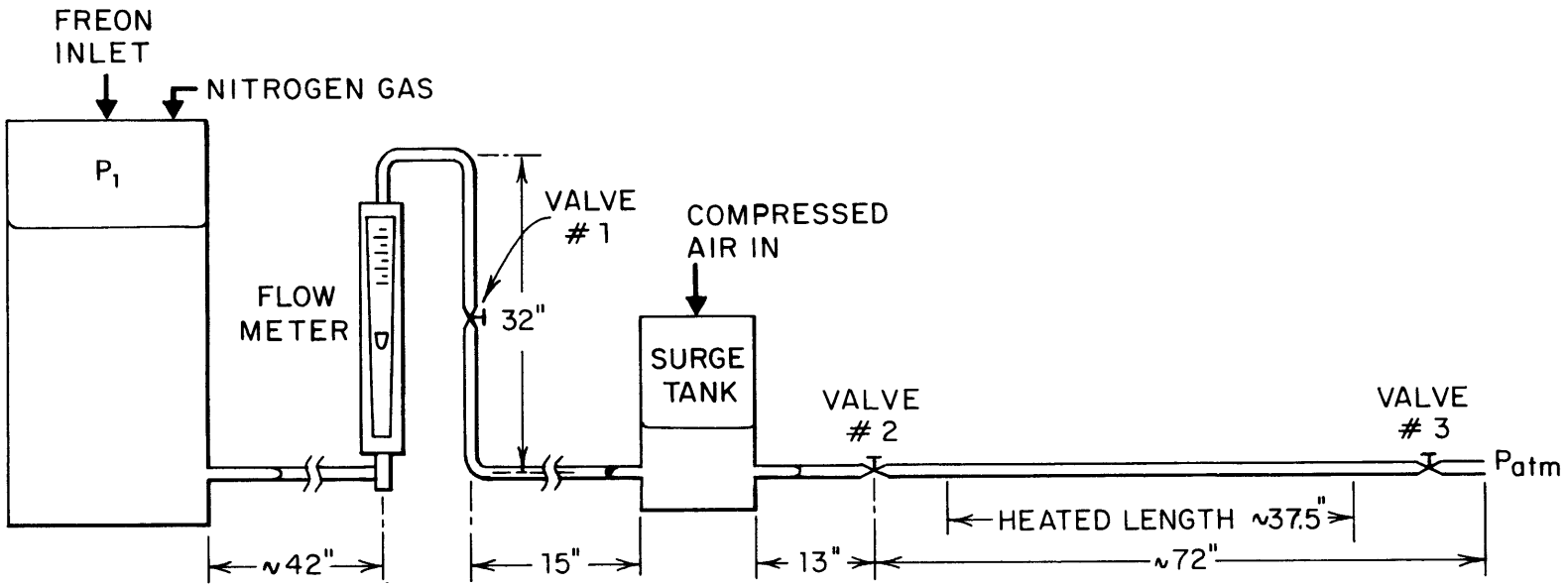

FIGURE 60: SCHEMATIC OF STENNING AND VEZIROGLU[28] FLOW LOOP

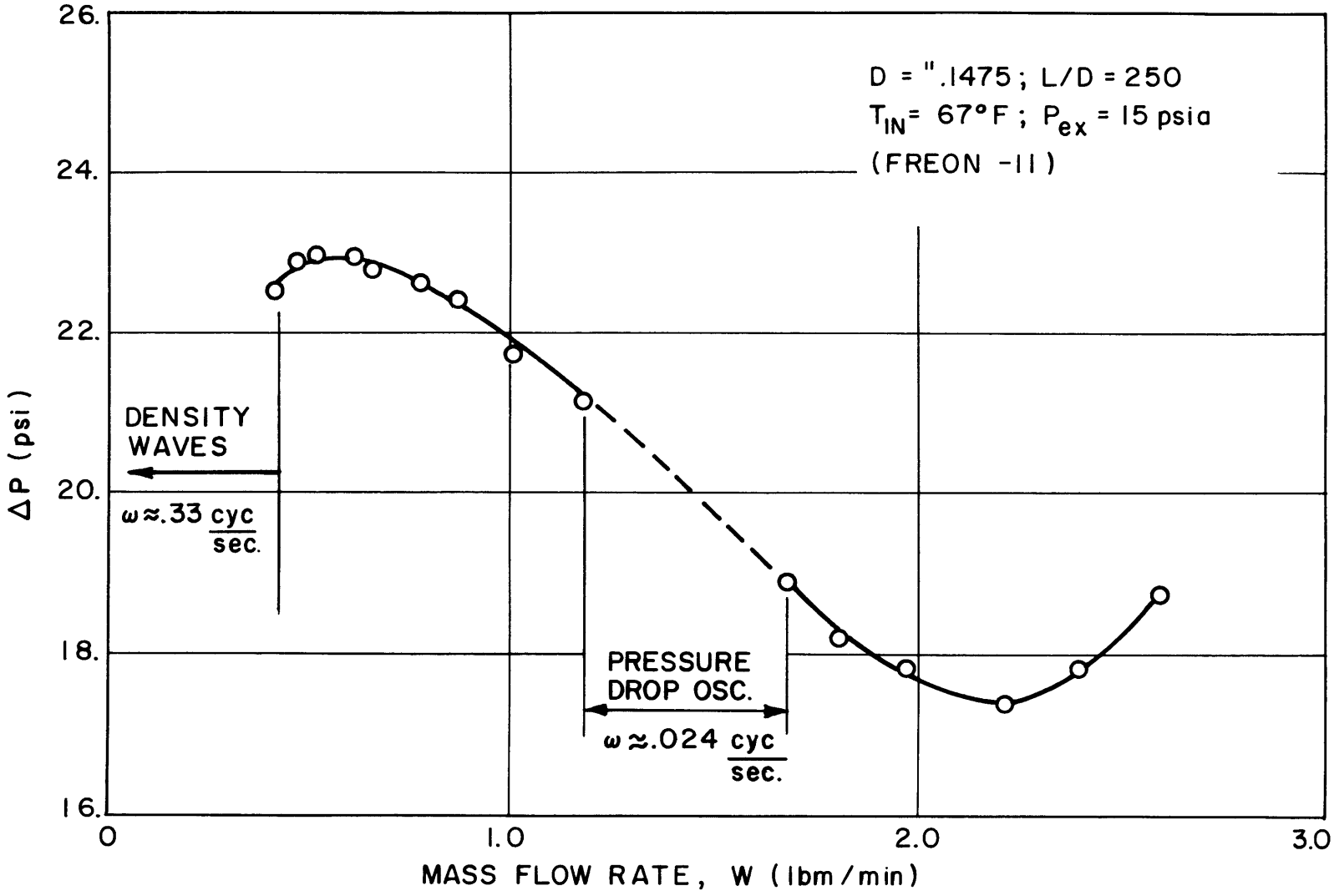

FIGURE 61: DATA OF STENNING AND VEZIROGLU [28]

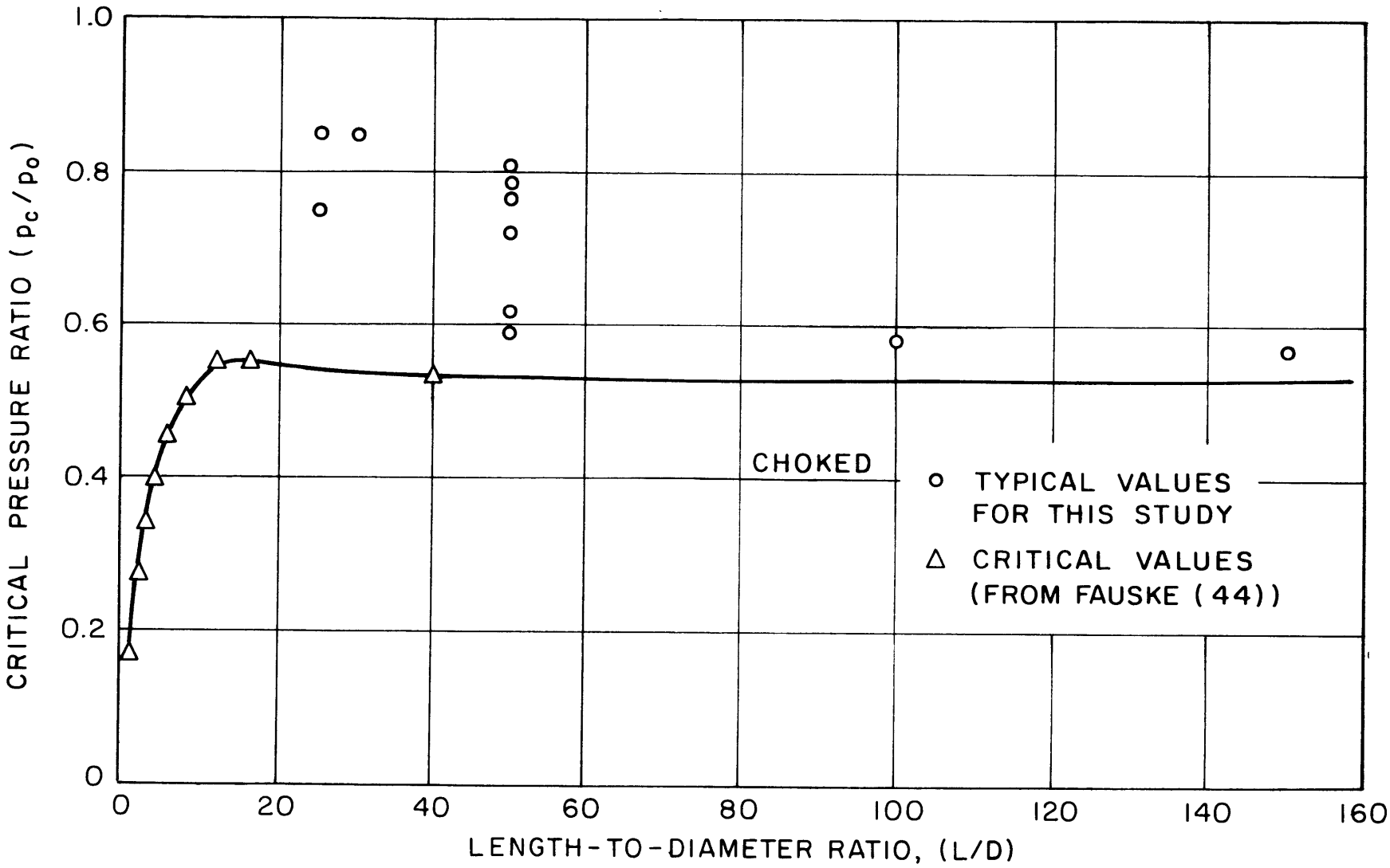

FIGURE 62 COMPARISON OF MEASURED PRESSURE RATIOS TO CRITICAL VALUES